



universität
wien

MASTERARBEIT

Titel der Masterarbeit

„Chlorophyllin and Friedreich’s Ataxia: Biological activity
of chlorophyllin in intestinal enterocytes
and neuronal cells“

verfasst von

Barbara Schwaiger, Bakk. rer. nat.

angestrebter akademischer Grad

Master of Science (MSc)

Wien, 2013

Studienkennzahl lt. Studienblatt: A 066 838

Studienrichtung lt. Studienblatt: Masterstudium Ernährungswissenschaften

Betreut von: o. Univ.-Prof. i.R. Dr. Hans Goldenberg

Danksagung

Vorab bedanke ich mich bei Herrn Prof. Dr. Goldenberg Hans, der mir durch die Aufnahme in seine Arbeitsgruppe die praktische Erstellung dieser Arbeit grundsätzlich ermöglicht hat.

Für die stets sehr hilfreiche und verständnisvolle Betreuung während der Erstellung dieser Masterarbeit möchte ich mich bei meiner Betreuerin, Frau Prof. Dr. Scheiber-Mojdehkar Barbara herzlichst bedanken. Weiters bedanke ich mich bei ihr, für das Ermöglichen der Teilnahme an den „Days of Molecular Medicine 2012“ in Wien, sowie an der „Ataxia Research Conference 2012“ in London.

Eine angenehme und abwechslungsreiche Arbeitsatmosphäre im Labor wurde mir durch die Zusammenarbeit mit meinen Kolleginnen Monika und Nina ermöglicht, welche es schafften auch lange Tage im Labor kurzweilig zu gestalten.

Besonders bedanken möchte ich mich ebenfalls bei meinen Eltern, die mir durch die Realisierung meiner schulischen Ausbildung den Grundstein für das Studium legten und mich in meinen Entscheidungen immer unterstützten. Ebenso gebührt meiner Schwester Elisabeth großer Dank, die mir immer als großes Vorbild und Ansprechspartnerin in meinem Leben vorhanden ist.

Bei meinem Freund David bedanke ich mich besonders für seine stets geduldige, aufmunternde und liebenswerte Art, sowie seinem bedingungslosen Verständnis während zeitintensiven Phasen des Studiums. Weiters bedanke ich mich bei seiner Familie für die Unterstützungen jeglicher Art, wodurch das Studium wesentlich erleichtert wurde.

Und abschließend bedanke ich mich bei all meinen Freunden, die immer für die notwendige Abwechslung in meinem Leben sorgen.

„Und wenn du dich getröstet hast (man tröstet sich immer), wirst du froh sein, mich gekannt zu haben. Du wirst immer mein Freund sein. Du wirst Lust haben, mit mir zu lachen. Und deine Freunde werden sehr erstaunt sein, wenn sie sehen, dass du den Himmel anblickst und lachst.“

Antoine de Saint-Exupéry aus „Der Kleine Prinz“

Gewidmet an all meine Lieben, die ihr irdische Leben bereits verlassen mussten.

I. Table of content

I. Table of content.....	IV
II. List of figures	VI
III. List of tables	VIII
IV. List of abbreviations	IX
1. Aim of the study	1
2. Introduction.....	4
2.1. The history of Friedreich's Ataxia.....	4
2.2. Clinical features of FRDA	5
2.3. Pathophysiology	7
2.4. Genetic pathogenesis.....	11
2.4.1. FXN gene	11
2.4.2. FXN gene mutations.....	11
2.4.3. Gene silencing due to the expanded GAA repeats	13
2.5. Frataxin.....	16
2.5.1. Structure and mitochondrial maturation.....	16
2.5.2. Functions of frataxin	17
2.6. Treatment of Friedreich's ataxia patients	22
2.6.1. Therapeutic approaches	22
2.7. Chlorophyllin	30
2.7.1. Bioavailability and metabolism	32
2.7.2. Biological effects and disease prevention.....	33
3. Materials and Methods.....	34
3.1. Cell Culture	34
3.2. Cell lines.....	35
3.2.1. Caco-2 cells.....	35
3.2.2. P19 cells	39

3.3.	Cytotoxicity Assays	44
3.3.1.	Preparation of the cells	44
3.3.2.	Preparation of the incubation solutions.....	44
3.3.3.	Incubation of the cells	45
3.4.	Permeability measurement of Caco-2 cells	50
3.4.1.	Preparation of the cells	50
3.5.	Cultivation of Caco-2 cells and differentiated neuronal cells	53
3.5.1.	Incubation of the cells with different compounds	54
3.5.2.	<i>In vitro</i> model to study intestinal drug uptake and bioactivity	55
3.6.	Statistics.....	65
4.	Results and Discussion	66
4.1.	Cytotoxicity of porphyrin compounds.....	67
4.1.1.	Metabolic activity of cells following incubation with CHL compounds.....	67
4.1.2.	Metabolic activity of cells following incubation with hemin.....	72
4.2.	Effect of exogenous substances on frataxin expression	76
4.2.1.	Effect of chlorophyllin compounds on frataxin expression.....	76
4.2.2.	Effect of hemin on frataxin expression.....	79
4.2.3.	Effect of other exogenous substances on frataxin expression.....	82
4.3.	Permeability measurement of Caco-2 cells	85
4.3.1.	Phenol Red Exclusion.....	85
4.3.2.	TEER-Measurement.....	86
4.3.3.	Bioactivity of CHL compounds in a Caco-2 cell/recipient cell co-culture model with P19 neuronal cells	87
5.	Conclusion	90
6.	Summary	94
7.	Zusammenfassung	95
8.	List of references.....	96

II. List of figures

Figure 1: Nikolaus Friedreich	4
Figure 2: Clinical features of FRDA	6
Figure 3: Degeneration of the thoracic spinal cord and the dentate nucleus	8
Figure 4: Hypertrophic cardiomyopathy in FRDA	10
Figure 5: Influence of GAA trinucleotide repeats in FRDA	12
Figure 6: Models of an intramolecular DNA triplex and sticky DNA structures	13
Figure 7: A model for heterochromatin formation in FRDA	14
Figure 8: Mechanisms of FXN silencing by the expanded GAA repeat	15
Figure 9: Structure of human frataxin	16
Figure 10: Representation of different frataxin forms	17
Figure 11: Iron homeostasis and possible function of frataxin	21
Figure 12: Therapeutic strategies in FRDA	22
Figure 13: Gene-based strategy as possible treatment in FRDA	28
Figure 14: Photosynthesis and the critical role of chlorophyll	30
Figure 15: Manufacturing process of chlorophyllin derivatives from chlorophyll a	31
Figure 16: Possible scheme of digestion and absorption of SCC	32
Figure 17: Differentiation of embryonic P19 cells to neuronal cells	43
Figure 18: Reduction of MTT to formazan	46
Figure 19: Structure of neutral red	47
Figure 20: Reduction of resazurin to resorufin	48
Figure 21: Microscopic images of Caco-2 cells on several days of cultivation	50
Figure 22: Caco-2/recipient co-culture model with P19 neuronal cells	55
Figure 23: Standard curve for BioRad protein quantification assay	58
Figure 24: MSD SULFO-TAG label	59
Figure 25: Carbon surface of a MULTI-ARRAY™ plate	59
Figure 26: Scheme of frataxin-ECLIA measurement	60
Figure 27: Standard curve for frataxin-ECLIA measurement	65
Figure 28: ECL signal of the frataxin standards	65

Figure 29: Influence of CHL compounds on metabolic activity of non-differentiated Caco-2 cells	68
Figure 30: Influence of CHL compounds on metabolic activity of differentiated Caco-2 cells.....	69
Figure 31: Influence of CHL compounds on P19 neuronal cell metabolic activity	71
Figure 32: Structure of hemin	72
Figure 33: Influence of hemin on metabolic activity on differentiated Caco-2 cells.....	73
Figure 34: Influence of hemin on P19 neuronal cell metabolic activity	74
Figure 35: Influence of CHL compounds on FXN expression in differentiated Caco-2 cells	77
Figure 36: Influence of CHL-compounds on FXN expression in differentiated P19 neuronal cells	78
Figure 37: Influence of hemin on FXN expression in differentiated Caco-2 cells.....	80
Figure 38: Influence of hemin on FXN expression in differentiated P19 neuronal cells	81
Figure 39: Influence of other substances on FXN content in differentiated Caco-2 cells.....	83
Figure 40: Influence of other substances on FXN content in differentiated P19 neuronal cells	84
Figure 41: Testing the Caco-2 monolayer integrity by using phenol red exclusion	85
Figure 42: Testing the Caco-2 cell monolayer integrity by using TEER measurement ...	86
Figure 43: Caco-2/recipient co-culture model with P19 neuronal cells	87
Figure 44: Effect of CHL compounds on FXN level in Caco-2 cells cultivated in hanging cell culture inserts	88
Figure 45: Effect of CHL compounds on FXN level in P19 neuronal cells after passaging a Caco-2 cell monolayer.	89

III. List of tables

Table 1: Cultivation of P19 neuronal cells.....	41
Table 2: Serial dilution of Mg- and Cu-CHL	45
Table 3: Preparation of further exogenous substances	54
Table 4: Preparation scheme of BioRad protein quantification standard curve	57
Table 5: Preparation scheme of frataxin-ECLIA standard curve	63

IV. List of abbreviations

AAV	Adeno-associated virus
ACE	Angiotensin-converting-enzyme
ADI	Acceptable daily intake
BSA	Bovine serum albumin
CEPO	Carbamylated EPO
CHL	Chlorophyllin
CM-1	Cryoprotective medium
CS	Calf serum
DFO	Deferoxamine
DMEM	Dulbecco's Modified Eagle's Medium
DMSO	Dimethyl sulfoxide
ECLIA	Electrochemiluminescence immunoassay
EDTA	Ethylenediaminetetraacetic acid
ELISA	Enzyme-linked immunosorbent assay
EPO	Erythropoietin
FARR	FRDA with retained reflexes
FCS	Fetal calf serum
FXN	Frataxin
HDACi	Histone deacetylase inhibitor
HEPES	4-(2-hydroxyethyl)-1-piperazineethanesulfonic acid
IFNγ	Interferone gamma
iNOS	Inducible nitric oxide synthase
IRE	Iron responsive element
ISC	Iron-sulfur cluster
ISCU	Iron-sulfur cluster assembly enzyme
ISD11	Cysteine desulfurase enzyme
Isu1	ISCU homologue in yeast
LOFA	Late onset Friedreich's ataxia

MEM	Minimum Essential Medium Eagle
MPP	Mitochondrial processing peptidase
MSD®	Meso Scale Discovery®
MSD-SULFO-TAG™	Ruthenium (III) tris-bipyridine-(4-methylsulfonate) NHS ester
MTT	3-(4,5-Dimethylthiazol-2-yl)-2,5-diphenyltetrazolium bromide
NFS1	Cysteine desulfurase enzyme
NQO1	NADPH quinone oxidoreductase 1
PBMC	Peripheral blood mononuclear cell
PBS	Phosphate buffered saline
PMSF	Phenylmethanesulfonyl fluoride
PPAR-γ	Peroxisome proliferator-activating receptor-gamma
rhuEPO	Recombinant human EPO
ROS	Reactive oxygen species
SCC	Sodium copper chlorophyllin
TAT	Trans-Activator of transcription
TEER	Transepithelial Electrical Resistance
TPA	Tripropylamine

1. Aim of the study

Friedreich ataxia (FRDA) was discovered in 1863 by the German neurologist and pathologist Nikolaus Friedreich, describing at first the elementary clinical and pathological features of this hereditary illness. [FRIEDREICH, 1863 and 1867]

With an incidence of 1:50,000 Caucasians, FRDA is the most common autosomal recessive form of ataxia in the white population. The mean age of onset is in the first half of puberty, demonstrating the first typical symptoms of gait instability and generalized clumsiness. [KOEPPEN, 2011] [PANDOLFO, 2009]

According to the unique pathophysiology, during FRDA progression a typical combination of signs and symptoms can be observed. [PANDOLFO, 2009] The first neurodegeneration occurs in the dorsal root ganglia (DRG), followed by affecting the spinals and the dentate nucleus in the cerebellum. [MARMOLINO, 2011]

An overexpression of GAA triplet repeats in the first intron of the *FXN gene*, located on the proximal long arm of chromosome 9, results in a reduced frataxin expression of 5–30% compared to healthy people. [MARTELLI et al., 2012]

Frataxin is a mitochondrial protein, which is ubiquitously expressed and necessary to survive, which was shown in knockout experiments of multicellular organisms. [PANDOLFO, 2012]

There is still a controversial debate about the exact function of this protein, but evidence based knowledge provides that frataxin is an important factor in iron homeostasis, the synthesis of Iron-Sulfur-Clusters (ISCs) and in the cellular defence of reactive oxygen species (ROS). [SCHMUCKER and PUCCIO, 2010]

FRDA is still an incurable illness without any sustainable therapeutic treatment. Beside palliative and symptomatic treatments, intense research work developed therapeutic strategies according to the pathological mechanisms. [RICHARDSON et al., 2013] [SCHMUCKER and PUCCIO, 2010]

As it was demonstrated by Sarsero et al., hemin is a potent inducer of frataxin gene expression. [SARSERO et al., 2003] Due to its reported neurotoxicity [DANG et al., 2011] our group was searching for other non-toxic porphyrin compounds.

One of these non-toxic porphyrin compounds is chlorophyllin (CHL), which belongs to a mixture of water-soluble salts and is technically derived from the naturally green pigment chlorophyll. During the synthesis process the central atom magnesium is mainly replaced by copper and the phytol tail is removed.

Chlorophyllin compounds are currently used as colour additive in food, drugs and cosmetics and they are therapeutically used as internal deodorant or for accelerating wound healing. Additionally, several studies demonstrate that CHL is a potent antimutagenic, anticarcinogenic and antioxidative agent. [TUMOLO and LANFER-MARQUEZ, 2012]

Different metal ions may action as the central atom of chlorophyllins, like magnesium, iron, zinc or copper. Iron- and copper-ions released from the porphyrin ring may participate in redox reactions. As a safe alternative we decided therefore to investigate the effect of Mg-CHL where the central atom if released does not participate in redox reactions.

Due to its wide range of uses as a health and food additive and its similar structure to hemin, we assumed that chlorophyllin may be a non-toxic alternative to increase frataxin expression.

In previous studies our group found that chlorophyllin compounds significantly increased FXN expression in various cell types as well as in primary lymphocytes from FRDA patients (unpublished data).

The amount of residual frataxin in FRDA patients varies between reports from 4 to 35% of controls and asymptomatic carriers also show reduced frataxin levels (between 64–68% of controls). [CAMPUZANO et al., 1997] [DEUTSCH et al., 2010] [SACCA et al., 2011] [STEINKELLNER et al., 2010]

Interestingly, a study with 50 healthy individuals found that, despite a narrow range of GAA-repeats in FRDA gene in healthy individuals, frataxin protein levels varied up to threefold. [BOEHM et al., 2011] This suggests that in addition to the number of GAA-repeats possibly other mechanisms might influence frataxin expression. This leads us to the hypothesis that stimulation of frataxin expression with non-toxic exogenous substances to the level of asymptomatic FRDA carriers could represent a therapeutic option for the treatment of FRDA patients.

Therefore the aim of this *in vitro* study was to identify a safe dose for chlorophyllin compounds effective to up-regulate frataxin expression. The expected results should prepare a scientific basis for CHL-studies *in vivo*.

2. Introduction

2.1. The history of Friedreich's Ataxia

Friedreich's ataxia (FRDA) was discovered in the year 1863 by the German pathologist and neurologist Nikolaus Friedreich (**Figure 1**). During the years 1863-1877 he described elementary clinical and pathological features in his publications, whereby he also recognized that this form of ataxia is hereditary. [FRIEDREICH, 1863 and 1876]

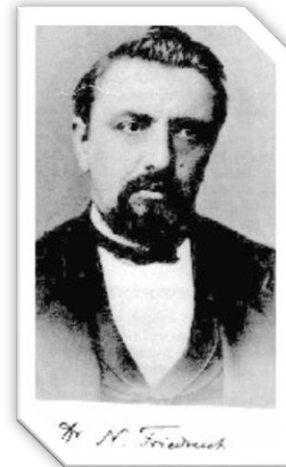


Figure 1: Nikolaus Friedreich ^[1]

His detailed microscopic descriptions let him to assume, that the abnormal thinness of the spinal cord is the primary disease of FRDA, without mentioning the lesion of the dentate nucleus, which was described and established by Mott in 1907. [MOTT, 1907]

During the following decades a lot of misdiagnoses were performed. Especially the Charcot-Marie-Tooth disease, which also affects the peripheral nervous system and therefore shows similar symptoms, was often wrong assumed. Referring to this fact, in 1981 Harding classified the symptoms of FRDA, according to the results of a study with 150 cases, for providing a differential diagnosis. [HARDING, 1981]

After mapping the mutated gene responsible for FRDA on the chromosome 9 [CHAMBERLAIN et al., 1988] eight years later, in 1996, Campuzano et al. published the identification of the FXN gene (former named as X25 gene) and its responsible mutations causing FRDA. The encoded protein was called frataxin and also the involvement in the iron metabolism was recognized. [CAMPUZANO et al., 1996]

The following years after this revelation were characterized by searching the precise function of frataxin, which is still unknown, but necessary for developing an effective treatment. [KOEPPEN, 2011]

2.2. Clinical features of FRDA

Friedreich's ataxia (FRDA) affects 1:50,000 Caucasians and is responsible for about the half of all hereditary ataxia cases. [PANDOLFO, 2009] According to this incidence, FRDA is the most common autosomal recessive ataxia in the white population. The carrier frequency is assumed in a range of 1:50 to 1:100 and is only found in peoples of European, North African, Middle Eastern and Indian origin. [KOEPPEN, 2011]

This multisystemic disease affects primarily young people, with a mean age of onset in the first half of puberty, without any preference to their gender. The first typical presenting symptoms are gait instability and generalized clumsiness, where the illness is mainly recognized. [KOEPPEN, 2011]

As it was described by Friedreich, the main feature of ataxia is determined to be progressive and unremitted, [SANTOS et al., 2010] whereas at the beginning of the illness the phases of stability are frequent. [PANDOLFO, 2009]

The cardinal clinical features are followed by dysarthria and the incidence of extensor plantar responses (Babinski-signs) (**Figure 2a**). Other neurological signs are lower limb muscle weakness and the diminishing of vibration sense. [DELATYCKI et al., 2000]

Besides the development of skeletal deformities, like pes cavus and scoliosis (**Figure 2b**) two thirds of patients exhibit cardiomyopathy, which is the most frequent cause of death within FRDA patients. Additionally, ocular abnormalities (nystagmus, optic atrophy, or fixation instability) and hearing loss may be developed. After a mean duration of 15 years after onset, patients develop diabetes mellitus and glucose intolerance. [SANTOS et al., 2010]

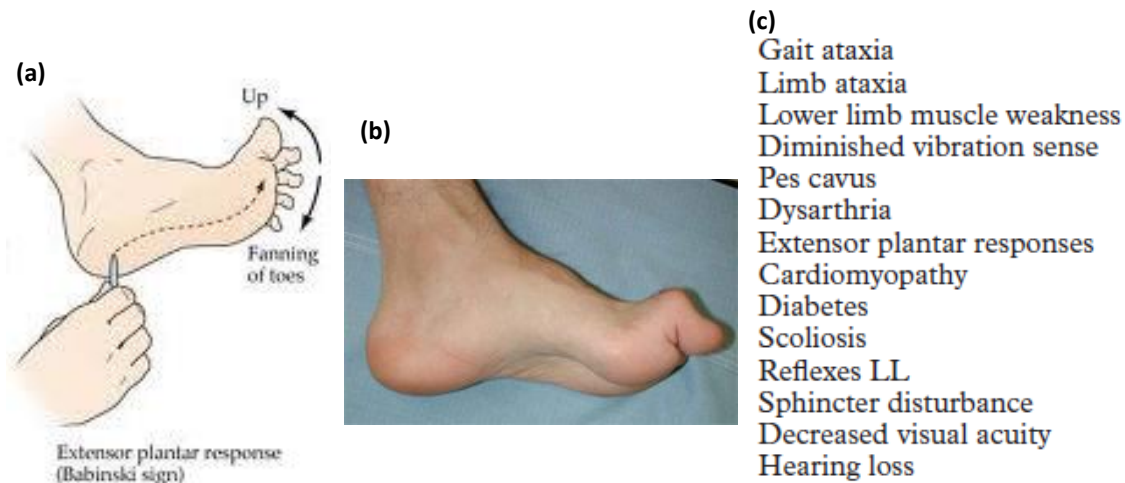


Figure 2: Clinical features of FRDA. (a) Babinski-sign [2]; (b) Pes Cavus [3]; (c) Specific signs and complications of FRDA [mod. from DELATYCKI et al., 2000]

Like the variability of the symptoms, also the disease progression is inconstant. Patients with a mild disease progression are often still able to walk decades after onset, while those affected with severe progression need a wheelchair within a few years. The mean duration of losing the abilities to walk, stand and sit without support is between 10 to 15 years after onset. [PANDOLFO, 2009]

The mix of cerebellar and sensory ataxia results in a progressive impairment in the daily routine of a patient, by decreasing the ability to do precision things, like writing, dressing and other daily activities. Additionally an intermittent and later constant support is necessary and dysarthria will progress until spoken words are incomprehensible. Cognitive functions are usually not affected; however these impairments may inhibit academic, professional and personal development. [PANDOLFO, 2009] [SANTOS et al., 2010]

To distinguish between FRDA and other common recessive ataxias, Harding's study provides according to his observations in a cohort of 150 patients, the incidence of clinical signs, which are confirmed by several different studies (**Figure 2c**). [DÜRR et al., 1996] [DELATYCKI et al., 2000] Nevertheless for an exact diagnosis laboratory and genetic analysis is necessary, due to the fact that other ataxic disorders tend to mimic FRDA signs. [FOGEL and PERLMAN, 2007]

Fulfilling all the clinical features of Harding describes the typical form of FRDA. Moreover there are further atypical forms of FRDA, complying an FRDA-like phenotype except at least one essential clinical criterion. [SANTOS et al., 2010] An onset after 25 years of age describes one of such an atypical form of FRDA, the late-onset FRDA (LOFA). The clinical signs are the same, but differences are found concerning severity, duration and progression of this disease. [SANTOS et al., 2010] [KOEPPEN, 2011]

Further atypical types includes the Acadian type and FRDA with retained reflexes (FARR), describing less severe forms of the classical FRDA type. [SANTOS et al., 2010]

2.3. Pathophysiology

Compared with other hereditary ataxias, the neuropathology of FRDA shows significant differences. It is specific to this disorder and reflects a typical combination of signs and symptoms, by involving degeneration of the spinal cord, the peripheral nerves and the cerebellum. [PANDOLFO, 2009]

Characteristically observed neurodegeneration begins in the dorsal root ganglia (DRG), with a loss of large sensory neurons and posterior columns. Degeneration is going on in the corticospinal and spinocerebellar tracts of the spinal cord and the dentate nucleus in the cerebellum (**Figure 3**). [MARMOLINO, 2011]

Observations of Koeppen et al. demonstrate that the cytoplasm of DRG neurons in FRDA is replaced through satellite cells by surrounding them until they are completely invaded. Assuming this proliferation as a result of neuronal atrophy may not be established due to the fact that neuronal loss can also be caused by a primary disease process in satellite cells. Staining with the S-100 α protein, a marker for neural crest derived cells indicates an interesting difference between satellite and Schwann cells in FRDA. Satellite cells are able to remain S-100 α -reactive, while Schwann cells lose their immunoreactivity. This finding led to the assumption, that FRDA primarily affects

satellite and Schwann cells, whereas the loss of neuronal and axonal cells is a secondary result. [KOEPPEN et al., 2009]

The posterior and lateral columns of the cervical spinal cord in FRDA patients are degenerated, which can be detected by magnetic resonance imaging (MRI). Both losses of position and vibration sense, as well as removing reflexes are the results of these degenerations. [PANDOLFO, 2009]

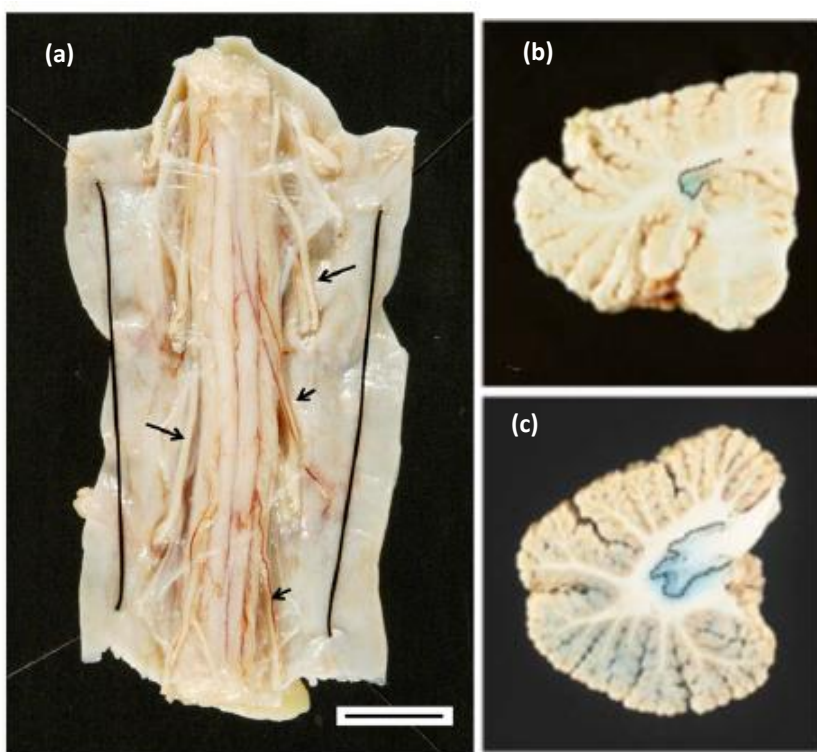


Figure 3: Degeneration of the thoracic spinal cord and the dentate nucleus. (a) The thoracic spinal cord in FRDA. The transverse diameter of the spinal cord is less than 1 cm (bar). Size comparison of the dentate nucleus in (b) FRDA and (c) in normal control. [mod. from KOEPPEN, 2011].

Characteristic for these regions is the demyelination of fibers and gliosis. Sural nerve biopsies demonstrate a significant reduction of the density of large myelinated fibers, whereas small or unmyelinated fibers are normal or moderately reduced. These neurophysiological abnormalities in the peripheral nervous system display a severe reduction or complete loss of sensory nerve action potentials and a mild nerve-conduction velocity decrease, which explains the loss of deep tendon reflexes. [MARMOLINO, 2011], [SANTOS et al., 2010]

Further severe neuronal loss is observed in the Clarke columns, which is responsible for the proprioceptive component of FRDA. Atrophy is observed in the spinocerebellar tracts as well as mainly in the distal portions of the corticospinal motor tracts, describing a “dying back” degenerative process. [MARMOLINO, 2011]

Decreased touch, pain and temperature perception occurs according to these degenerations. In progressive disease the pyramidal tracts of patients are also affected resulting in developing Babinski-sign and muscular weakness. In case of severe sensory neuronopathy, reflexes are retained and pyramidal involvement leads to hyperreflexia and spasticity in patients. [PANDOLFO, 2009]

In the cerebellum, the dentate nucleus is severely affected at the beginning stage. The cortex remains unaffected until Purkinje cell loss is observed. All clinical features of FRDA like ataxia, dysarthria, gait instability and profound sensory loss are caused by progressive atrophy of sensory and cerebellar pathways. [SANTOS et al., 2010]

The majority of patients additionally shows hypertrophic cardiomyopathy, resulting from an increase of the thickness of the ventricular and inter-ventricular septum walls (**Figure 4**). [MARMOLINO, 2011] It is the most common symptom beside the neurological features and responsible for premature death, especially in patients with earlier age of onset. Initial symptoms of hypertrophic cardiomyopathy are shortness of breath and palpitations, sometimes existing before FRDA is recognized. [PANDOLFO, 2009]

As it was observed in different cohort studies, the incidence of diabetes mellitus in FRDA patients varies between 8–32%. [SANTOS et al, 2010] It is classified as a combination of peripheral insulin resistance and insulin deficiency, but not according to the autoimmune attack typical for type I diabetes. [MARMOLINO, 2011]

By using synaptophysin immunostaining a lack and progressive destruction of the islets of Langerhans in diabetic FRDA patients can be displayed. In non-diabetic patients there are more pancreatic β -cells and the islets cells are larger. In contrast the β -cells

of diabetic FRDA patients lose their precise outline and become alike to the enclosing pancreas. [KOEPPEN, 2011]

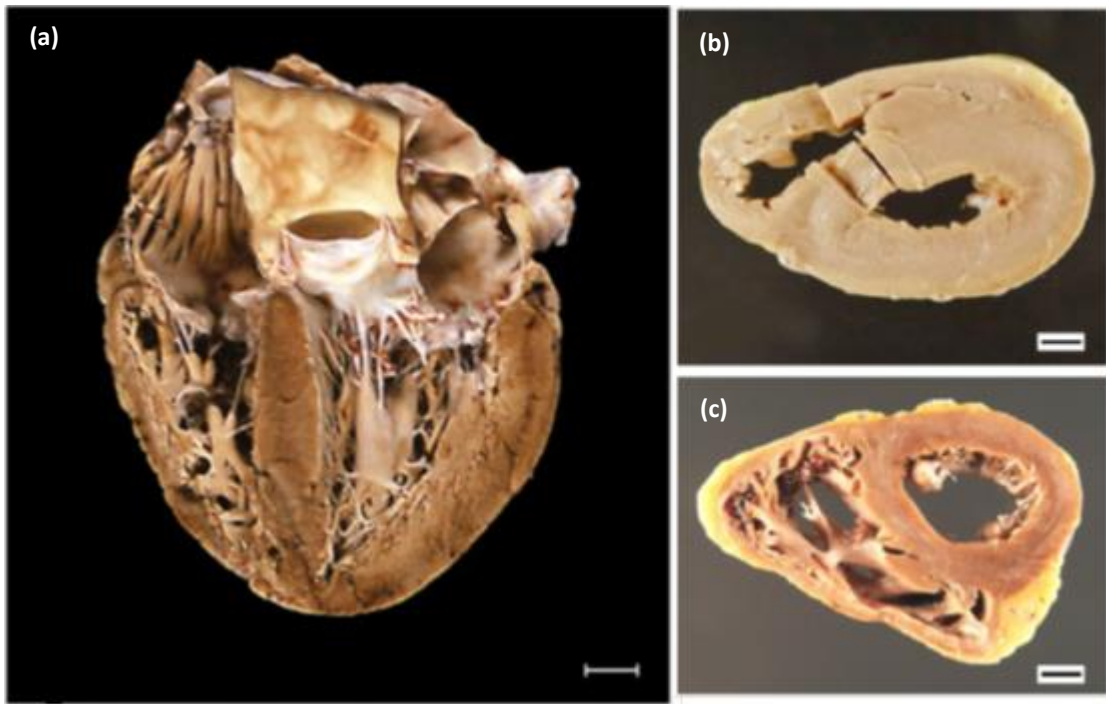


Figure 4: Hypertrophic cardiomyopathy in FRDA. (a) Left and right ventricular walls are greatly thickened. The myocardium is discoloured, lacking the normal dark and homogeneous appearance of normal heart [mod. from MARMOLINO; 2011] **(b)** Concentric cardiac hypertrophy and discoloration of the myocardium. The left ventricles are narrowed. **(c)** Cardiac hypertrophy affecting only the left ventricular wall and interventricular septum. The right ventricle is dilated. [mod. from KOEPPEN, 2011] Bars: 1 cm.

2.4. Genetic pathogenesis

2.4.1. FXN gene

The concerned gene in FRDA, the *FXN gene*, is mapped on the proximal long arm of chromosome 9, enclosing the region 9q13-9q21.1. [SANTOS et al., 2010] This gene is composed of seven exons (exons 1-4, 5a, 5b, and 6) comprising 85 kb of genomic DNA. [PUCCIO and KOENIG, 2000] The major mRNA transcript (1.3 kb) encloses the exons 1 to 5a, encoding the 210 amino acids containing protein frataxin (isoform A). Due to its N-terminal signal it gets directly located to mitochondria. [PANDOLFO, 2009]

Expression of the FXN gene and protein production is ubiquitous, while these levels show tissue specificity correlating with the main features of the disease. In adults the highest level of expression is observed in the heart and spinal cord. Lower levels are expressed in the cerebellum, liver, skeletal muscle and pancreas, followed by the cerebral cortex with the lowest expression. Responsible for this various distribution of frataxin expression, could be the different dependence on mitochondrial metabolism of these non-dividing cells and may explain the reason that only certain tissues are affected in FRDA disease. [SANTOS et al., 2010]

2.4.2. FXN gene mutations

Within the first intron of the frataxin gene a GAA triplet-repeat expansion is present, ranging from 70 up to 1700 triplet-repeats. Most of the patients show a number between 600 and 900 triplet-repeats. In comparison, healthy people possess from 6 to 36 triplet-repeats. [SCHMUCKER and PUCCIO, 2010]

This GAA-hyperexpression is accompanied by a transcriptional silencing of the FXN-gene, which is elicited due to a mechanism involving the heterochromatinization of the locus. This gene mutation results in an about 5-30% reduced level of normal structured and functional frataxin, compared to healthy people. [MARTELLI et al., 2012]

96% of FRDA patients carry this GAA-triplet expansion on both alleles, correlating with a strongly reduced frataxin expression and resulting in a severe type of FRDA. There is an inverse correlation between the size of GAA repeat expansion and the age of onset, the severity of the disease and the occurrence of non-neurological signs like cardiomyopathy, scoliosis and diabetes (**Figure 5**). [PUCCIO and KOENIG, 2000]

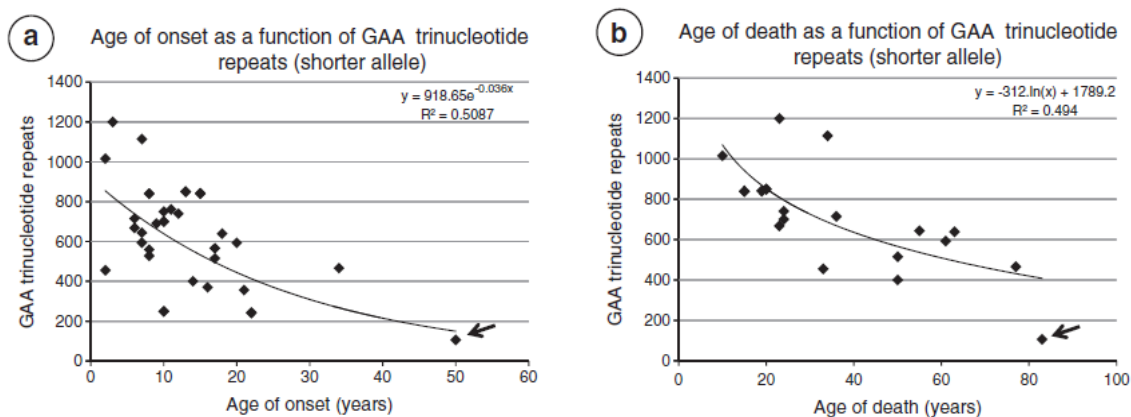


Figure 5: Influence of GAA trinucleotide repeats in FRDA. (a) Correlation between GAA triplet repeats and age of onset. **(b)** Correlation between GAA expansion and age of death. [mod. from KOEPPEN, 2011]

The remaining 4% are heterozygous, showing the GAA-triplet-repeat expansion only on one allele, the other allele carrying a point mutation, which leads to the production of non-functional or only partially functional frataxin. [MARTELLI et al., 2012]

In difference to the nonsense mutation, the missense mutations are only present in the second half of the protein, assuming that this is an important functional domain. Patients with point mutations show nearly the same clinical features as homozygous FRDA patients, with few exceptions. One of the most frequent point mutation is the G130V mutation which is always presented with an atypical feature, like moderate ataxia, slow progression or absence of dysarthria. Like the other point mutations, it is associated with a milder presentation of the illness. [PUCCIO and KOENIG, 2000]

2.4.3. Gene silencing due to the expanded GAA repeats

The expanded GAA triplet repeats are responsible for the loss of transcriptional activity of the FXN gene and the associated reduction of the mature protein frataxin. This inhibition of FXN transcription is described as the principal and critical step in developing FRDA. There exist three possible explanations for transcriptional silencing by GAA repeats in intron 1 (**Figure 8**):

- formation of non-B DNA structures (triplex and “sticky DNA”)
- persistent RNA·DNA hybrid formation
- heterochromatin formation. [WELLS, 2008]

“Sticky DNA” formation was observed as a novel behaviour of long GAA·TTC (150 and 270 repeats) tracts by Sakomoto et al. in 1999. This non-B DNA structure is adopted by the self-association of two R·R·Y (purine·purine·pyrimidine) triplexes (**Figure 6**) under the influence of negative supercoiling. [SAKOMOTO et al., 1999]

According to this unique formation, the DNA molecule is transformed into a dumbbell-shaped structure (**Figure 6**), resulting in blocking nearly all biological processes *in vitro* including transcription, replication, repair and recombination. “Sticky DNA” is a strong transcription inhibitor by impounding the RNA polymerases due to directly binding to the DNA structure. [WELLS, 2008]

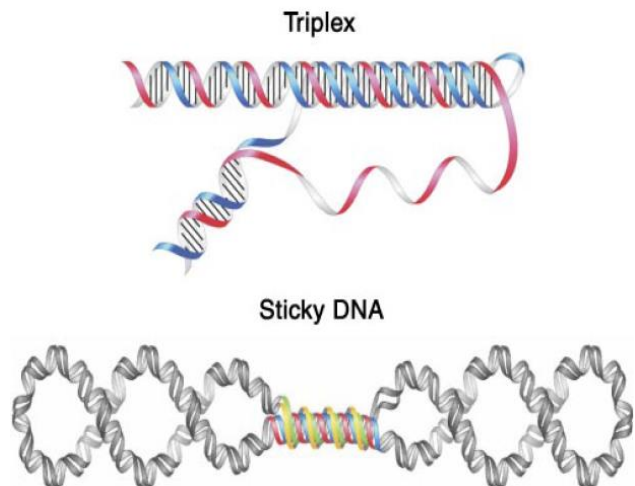


Figure 6: Models of an intramolecular DNA triplex and sticky DNA structures. [WELLS, 2008]

The threshold of GAA·TTC repeats to form a “sticky DNA” is observed at about 59 repeats, showing a clear correlation to the pathogenicity of FRDA, where the shortest pathologic allele was reported with 66 repeats. [PANDOLFO, 2008]

The formation of stable RNA·DNA hybrids during transcription of GAA·TTC repeats in *E. coli* as well as *in vitro* by defined transcription reactions using T7 RNA polymerase was reported by Grabczyk et al. Their data show that an extensive RNA·DNA hybrid formation *in vitro* is associated with arresting the T7 polymerase in the distal end of the GAA·TTC tracts. RNA·DNA hybrids are observed at the presence of about 40 triplets, which is near the pathological threshold of the GAA·TTC repeats causing genomic instability in FRDA disease. According to this linkage, it can be assumed that RNA·DNA hybrid formation is responsible for the GAA·TTC repeat instability in the cell. [GRABCZYK et al. 2007]

Further mechanism of transcriptional silencing is based on the packaging of DNA within chromatin. The repetitive GAA·TTC tracts have the ability to package genomic regions and transform them into inaccessible heterochromatin structures, which leads to gene silencing (**Figure 7**).

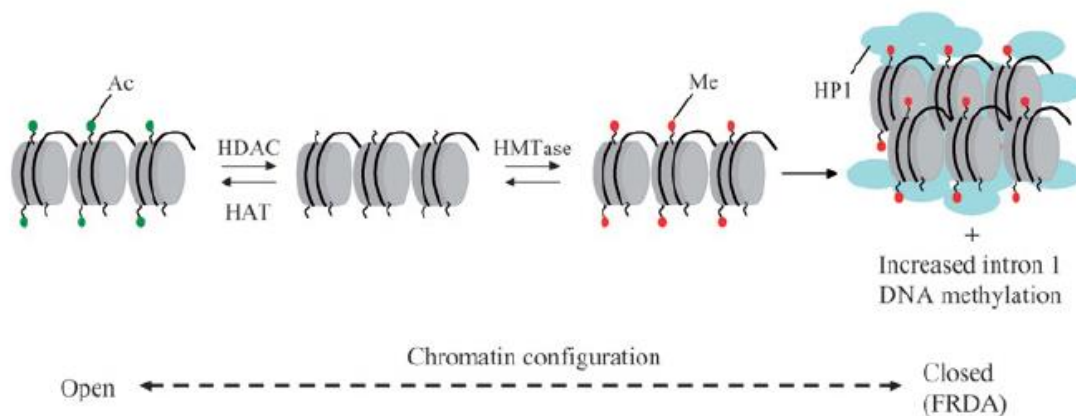


Figure 7: A model for heterochromatin formation in FRDA. An overexpression of GAA triplet repeats induces a non B-DNA formation which generates acetylated histones (Ac, green) of normal alleles through an increased activity of histone deacetylase (HDAC) and histone methyltransferases (HMTase) to methylated histones (Me, red). Additionally, heterochromatin protein 1 (HP1) enforces chromatin compaction and increases DNA methylation. Histone acetyltransferase (HAT) and histone deacetylase (HDAC) inhibitors are able to reverse methylation and increase frataxin expression. [HERBERT and WHITTON, 2007]

First evidence about expanded GAA repeats and heterochromatin formation was reported from studies in transgenic mice. Based on these results, silencing correlates with a reduction of promoter accessibility, which was additionally stimulated by the position effect variegation (PEV) modified heterochromatin protein 1. Notably, the GAA·TTC repeats associated variegation was not restricted to classical heterochromatic regions. Restrictions occurred on irrespective chromosomal locations, which lead to assume that heterochromatin-mediated silencing has an epigenetic mechanism *in vivo*. [WELLS, 2008] [SAVELIEV et al., 2003] [MARMOLINO, 2011]

Chromatin condensation is associated with post-translational modification of histones, like changes in acetylation, methylation, phosphorylation and ubiquitination. In lymphocyte DNA from FRDA patients, an increase in histone H3 lysine 9 (H3K9) trimethylation and a decrease in acetylation at H3K14, H4K5, H4K8 and H4K12 - all markers of a heterochromatic state in vicinity of expanded GAA·TTC triplet repeats, were observed. The responsible mechanism for inducing these changes is still unknown, but it is important to know, that these modifications can be reverted by specific histone deacetylase inhibitors (HDACi), resulting in a substantial increase of frataxin expression in cells from patients with FRDA. [PANDOLFO, 2009]

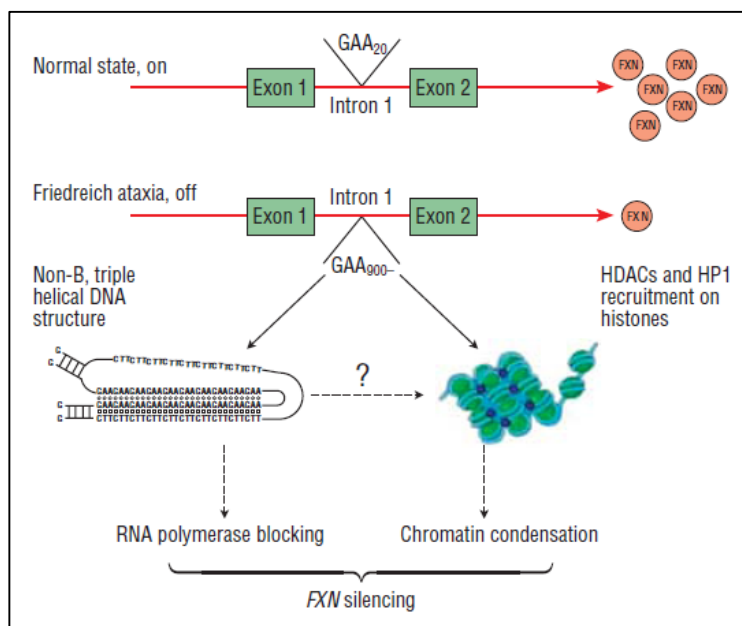


Figure 8: Mechanisms of FXN silencing by the expanded GAA repeat. FXN. HP1=heterochromatin protein 1, HDAC=histone deacetylases. [PANDOLFO, 2008]

2.5. Frataxin

2.5.1. Structure and mitochondrial maturation

Frataxins are small, highly conserved mitochondrial proteins, comprising 100 up to 220 amino acids, and they are ubiquitously expressed. The structure of frataxin displays, beside the hydrophobic core, a 5- to 7-stranded β -antiparallel sheet (**Figure 9**). [PANDOLFO and PASTORE, 2009]

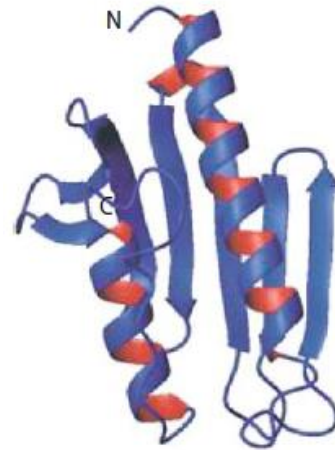


Figure 9: Structure of human frataxin.
[mod. from PANDOLFO and PASTORE, 2009]

Its surface is mostly uncharged and is assumed to be responsible for protein-protein interactions. The β sheet is flanked by two α helices ($\alpha 1$ and $\alpha 2$) on the non-conserved N- and the strongly conserved C-terminal regions. [MUSCO et al., 2000]

The most important feature on the surface is an acidic ridge of semi-conserved residues. It is distributed along the first helix, providing a highly negatively charged surface. [PANDOLFO and PASTORE, 2009] [SCHMUCKER and PUCCIO, 2010]

Eukaryotic frataxin is encoded in the nucleus, translated by ribosomes in the cytoplasm and finally imported into mitochondria for proteolytic maturation. Maturation is processed by the mitochondrial processing peptidase (MPP) by a two-step cleavage of the precursor polypeptide (23 kDa) (**Figure 10**). [PANDOLFO and PASTORE, 2009]

During first cleavage, the precursor form is converted into a ~19 kDa intermediate form, by removing the mitochondrial target sequence. The second cleavage forms three matured proteins, whereas the main matured form is found between Lys80 and Ser81. This 130 amino acids (~ 17 kDa) containing protein shows complete function, as it is able to rescue aconitase defects in frataxin-deficient cells. [CONDO et al., 2007]

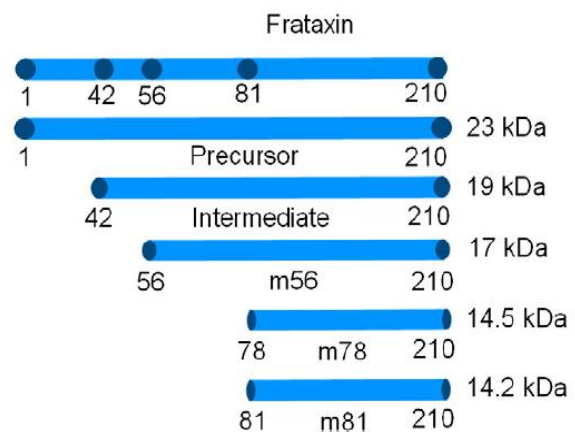


Figure 10: Representation of different frataxin forms.
[MARMOLINO, 2011]

In vivo the longer forms are observed assembled, creating larger structures, whereas this oligomerization could not be demonstrated *in vitro* with the two shorter forms. While it has been shown that this assembly to oligomers is essential for detoxification of redox-active iron, the occurrence of forming oligomers by human frataxin is not known. It could be assumed, based on the different isoforms with various N-terminal lengths and frataxin from different origins, that the proteins follow different oligomerization pathways and assemble into different types of oligomers. However it is important to note that the research community still disagree about the ability of oligomerization and the functional importance *in vivo*. [SÖDERBERG et al., 2013]

2.5.2. Functions of frataxin

As it was shown in knockout experiments, multicellular organisms (mice, worms, flies, plants) with a complete lack of frataxin are not able to survive, assuming that this protein is substantial for long-term survival. [PANDOLFO, 2012]

Although the exact function is still a controversially debate, evidence based knowledge provides that frataxin is involved and plays an important role in iron metabolism. [SCHMUCKER and PUCCIO, 2010]

2.5.2.1. Iron-sulfur cluster biogenesis

The synthesis of iron-sulfur clusters (ISCs) is one of the most important iron-related metabolic pathways, playing a crucial role in various cellular activities. In prokaryotes and eukaryotes, iron-sulfur clusters are essential for the function of several metalloproteins (iron-sulfur proteins), as well as for their structure and stability. The most common biological ISC-types are [2Fe-2S] and [4Fe-4S] clusters. [PANDOLFO, 2012]

Iron-sulfur clusters are acting as acceptors or donators of single electrons, catalysing enzymatic reactions or function as regulatory proteins. Thereby they are essential components of i.e. the respiratory electron transfer complexes or the enzymes of the Krebs cycle - aconitase and succinate dehydrogenase. [ROUAULT and TONG, 2008]

In higher eukaryotes iron-sulfur cluster biogenesis takes place in mitochondria and in the cytosol, noting that cytosolic iron-sulfur cluster synthesis seems to be dependent on mitochondrial integrity and a still unknown export component from the mitochondria through the carrier ABCB7 in mammals. For mitochondrial iron-sulfur cluster biogenesis in higher eukaryotes a lot of different factors are responsible, but with partially still unknown functions. [PANDOLFO, 2012]

The involvement of frataxin in the iron-sulfur cluster biogenesis

De novo iron-sulfur cluster biogenesis starts by assembling of inorganic iron and sulfur into an ISC on the scaffold protein ISCU or Isu1 in yeast. Sulfur is provided by the cysteine desulfurase proteins NFS1 and ISD11 by producing a persulfide intermediate. According to the work with mammalian recombinant proteins, the results demonstrate that frataxin interacts with a preformed complex consisting of NFS1, ISCU and ISD11. Due to this interaction, the cysteine desulfurase activity is increased, resulting in the assumption that frataxin modulates the capacity of NFS1 to provide sulfur for ISC formation. In contrast to the iron-dependent activation of NFS1 cysteine desulfurase activity by frataxin, the interaction of frataxin with the ISCU-NFS1-ISD11 complex can be performed when iron is absent. [MARTELLI et al., 2012]

These findings demonstrate that frataxin is essential for a significant iron-sulfur cluster synthesis, due to the fact that the complex is in an off state when frataxin is absent. In case of a too low frataxin level, as it occurs in FRDA patients, reduced activities of various iron-sulfur proteins, like aconitase from the Krebs cycle, or the respiratory chain complexes I, II and III are observed. By impairing the activity of these iron-sulfur proteins, the intracellular energy production is decreased. [PANDOLFO, 2012]

2.5.2.2. Alterations in iron metabolism and oxidative stress

Based on the impaired iron-sulfur cluster synthesis, the iron metabolism is altered in two major ways. The first way concerns the generation of free radicals in mitochondria. Mitoferrin 1 and 2 are membrane carriers, which are necessary to import ferrous iron into mitochondria. This reduced form of iron tends to become oxidized and forms insoluble precipitates when not rapidly used in a biosynthetic process. These complexes have been detected in mitochondria from frataxin-depleted yeast, from conditional frataxin KO mice, and in the myocardium of FRDA patients.

Because ferrous iron is oxidized by reactive oxygen species (especially H_2O_2) in mitochondria according to the Fenton reaction ($\text{Fe}^{2+} + \text{H}_2\text{O}_2 \rightarrow \text{Fe}^{3+} + \text{OH}^\cdot$), the highly toxic hydroxyl radical is generated. In addition to this radical production, further ROS (reactive oxygen species) also become more abundant in mitochondria of frataxin-deficient cells due to respiratory chain dysfunction. Normally, electrons of the respiratory chain are transported to complex IV (cytochrome c oxidase), where they reduce molecular oxygen to water. In case of an insufficient iron-sulfur cluster synthesis the respiratory chain complexes are impaired. This leads to an increasing leakage of electrons from the respiratory chain, directly forming superoxide with molecular oxygen, which is transformed into hydrogen peroxide by mitochondrial superoxide dismutase, supporting the Fenton reaction with the second reactant.

On one side, ROS are able to directly damage many cellular components, i.e. proteins, nucleic acids and lipids and on the other side, the increased ROS productions activates signalling pathways, which usually should be protective or cell death-promoting,

comprising the phenomenon of “oxidative stress”. In frataxin-deficient cells, an activation of the “stress kinase” pathway has been detected, which could play a role in the pathogenesis of FRDA. This enforced stress signalling pathway increases vulnerability which could end in stress-induced apoptotic cell death. Additionally, in frataxin-deficient cells protective antioxidant response is diminished due to impairment of the nuclear factor-erythroid 2-related factor 2 and the peroxisome-proliferator activated receptor gamma coactivator 1-alpha pathways, both involved in antioxidant responses. [PANDOLFO, 2012]

The second major implication of an impaired iron-sulfur-cluster concerns the activity of the cytosolic iron response proteins IRP1 and IRP2. Iron homeostasis in higher eukaryotes mainly occurs at the post-transcriptional level by binding of these regulatory proteins in the 5' or 3' untranslated regions of specific mRNAs of the Iron Responsive Element (IRE). [MARMOLINO, 2011]

In case of a low cytosolic iron status, IRP1 loses a labile iron atom of its cubane ISC and its function as cytosolic aconitase is diminished, which turns IRP1 into a RNA-binding protein. Inducing a cytosolic iron increase by IRP activation finally leads to IRP2 degradation and regeneration of the IRP1 iron-sulfur cluster, which forms it back into a cytosolic aconitase. Under normal conditions, this negative feedback mechanism assures the cellular iron homeostasis. The impaired ISC biogenesis due to frataxin deficiency changes IRP function by resulting in a higher amount of IRP1 molecules where ISC are absent. The fact that frataxin-deficient cells show iron accumulation in mitochondria results in activation of IRP1-mediated cellular response. This intensifies translation of transferrin receptor mRNA whereby cellular iron uptake becomes increased. Normally, iron is then transferred to mitochondria, where it is used for heme and ISC synthesis, as well as for the restoration of IRP1 iron sulfur cluster. This leads to an increase of cytosolic iron levels and the IRP response is stopped. This response is prevented in case of frataxin deficiency because of the impaired ISC synthesis. Thereby iron is oxidized and accumulates in mitochondria, which turns a homeostatic response into a pathogenic vicious cycle (**Figure 11**). [PANDOLFO, 2012]

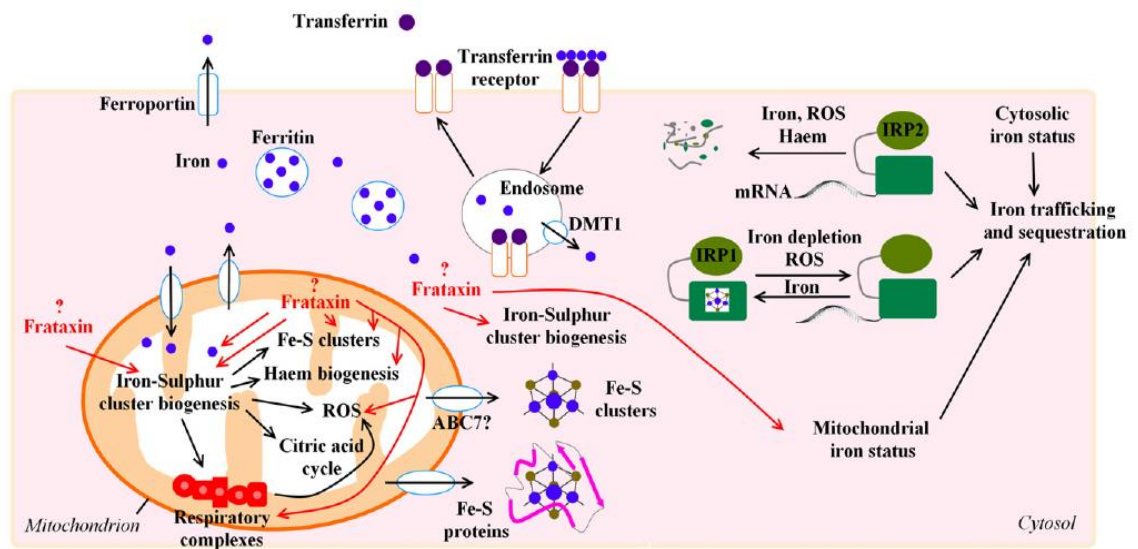


Figure 11: Iron homeostasis and possible function of frataxin. Frataxin has been suggested to be involved in iron-sulfur cluster biogenesis, iron homeostasis, ROS production, respiratory chain function, and haem biogenesis. ABC7: ATP binding cassette transporter 7, DMT1: divalent metal transporter 1, IRP1: iron regulating protein 1, ROS: reactive oxygen species. [MARMOLINO, 2011]

2.6. Treatment of Friedreich's ataxia patients

2.6.1. Therapeutic approaches

Despite intense research, there is still no sustainable treatment option for FRDA patients. The current treatment and therapeutic strategies in FRDA are divided into several categories. Beside palliative and symptomatic treatments (e.g. use of wheelchairs, β -blockers, ACE-inhibitors, physical therapy), [RICHARDSON et al., 2013], several therapeutic strategies according to the pathological mechanisms have been developed (**Figure 12**). [SCHMUCKER and PUCCIO, 2010]

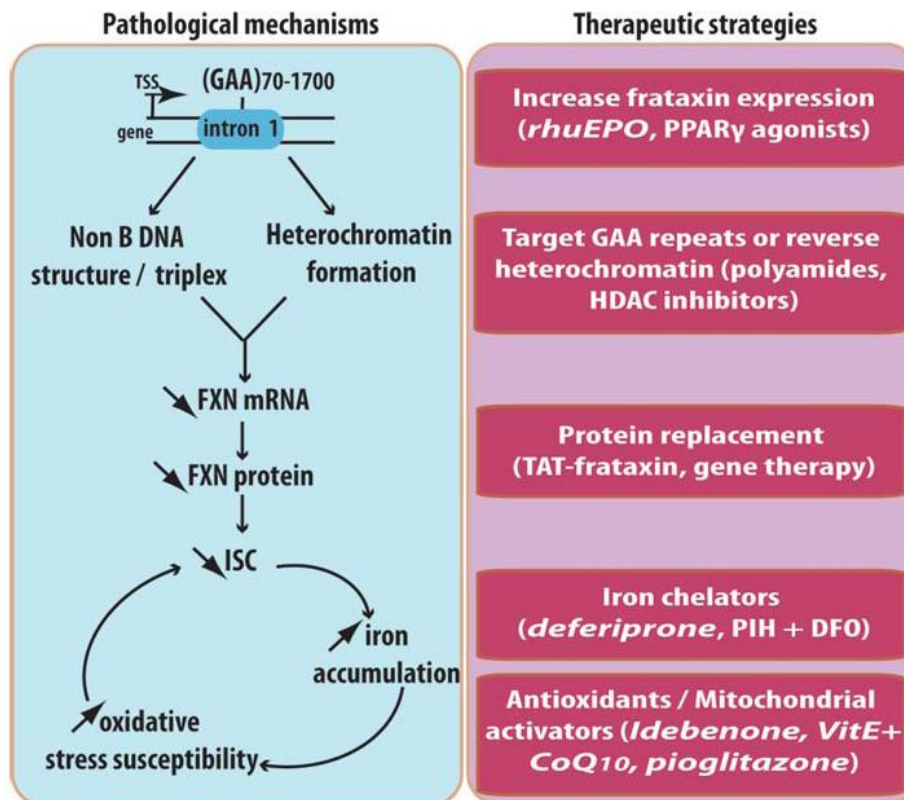


Figure 12: Therapeutic strategies development according to pathological mechanisms of FRDA. *rhuEPO*: recombinant human erythropoietin, PPAR: peroxisome proliferator-activated receptor, HDAC: histone deacetylase, PIH: pyridoxal isonicotinoyl hydrazine, DFO: deferrioxamine, VitE: vitamin E, CoQ10: coenzyme Q10. [SCHMUCKER and PUCCIO, 2010]

Due to the identification of the mutation causing FRDA, the expanding knowledge of frataxin function and pathogenesis, different therapeutic approaches for FRDA are

currently in development. The focus of these strategies is to increase the frataxin expression or to interrupt the pathogenetic cascade downstream of frataxin deficiency, which already succeeded in well-established research studies. Gene therapy and protein-replacement are future approaches with auspicious research work in pre-clinical development. [MARMOLINO, 2011]

2.6.1.1. Antioxidants and increasing mitochondrial function

Concerning the knowledge of generating free radicals and thereby increased oxidative sensitivity in frataxin deficient cells, a lot of work has been done in investigating the potential of antioxidants as therapeutic approach in FRDA. [RICHARDSON et al., 2013] [MARMOLINO, 2011]

Idebenone

Idebenone, a synthetic analogue of coenzyme Q₁₀ has been the first drug in FRDA treatment reaching Phase III clinical trials. It penetrates the membrane more efficiently than CoQ₁₀, acts as an electron carrier between complex I/II to III of the electron transport chain and diminishes intracellular ROS, improving oxidative phosphorylation and aerobic respiration in FRDA. [RICHARDSON et al., 2013] Results of conducted clinical trials [DI PROSPERO et al. 2007], [LAGEDROST et al., 2011], [LYNCH et al., 2010] provide improvements of neurological symptoms after long-term application. In combination with the well-established safety and tolerability of high-dose idebenone, it seems that idebenone remains to be a treatment option for pediatric FRDA patients. [MEIER et al., 2012]

Further selected antioxidants

Combinations with coenzyme Q₁₀ and vitamin E provide an increased ATP production, resulting in an improved cardiac function and diminished clinical progression. [PANDOLFO, 2013]

The lipid-soluble antioxidant and respiratory chain stimulator molecule EPI-A0001, an α -tocopherol-ubiquinone hybrid, provided evidence of safety in a Phase I study [PANDOLFO, 2013] and improved neurological functions in a Phase II RCT. [LYNCH et al. 2012]

A further antioxidant and metabolic stimulator is the drug EPI-743. Beside, the antioxidant capacity, it targets the enzyme NAD(P)H quinone oxidoreductase 1 (NQO1), improving mitochondrial function. Currently a phase II RCT study is in progress to assess the visual changes of EPI-743 in FRDA patients. [Internet: Friedreich's Ataxia Research Alliance (FARA), 26.05.2013] [Internet: U.S. National Institutes of Health: ClinicalTrials.gov_NCT01728064, 26.05.2013]

The well-known PPAR- γ ligand Pioglitazone is currently used in a Phase III RCT, exploring its effect on neurological function in FRDA patients. Pioglitazone is commonly used in diabetes type II treatment and is able to induce the expression of many enzymes involved in mitochondrial metabolism, including the superoxide dismutase. Currently there are no results of this still ongoing study. [Internet: Friedreich's Ataxia Research Alliance (FARA), 26.05.2013] [Internet: U.S. National Institutes of Health: ClinicalTrials.gov_NCT00811681, 26.05.2013]

2.6.1.2. Iron chelation strategy to decrease iron toxicity & increase ISCs

The commitment of iron chelators in FRDA treatment is discussed controversially, because of the non-systemic distribution of iron overload, accumulating mostly in the heart tissue. Further, the impaired ISC biogenesis and iron involvement in frataxin regulation are able to arise doubts about the application of iron decreasing drugs in FRDA. Therefore beneficial drugs must have the potential only to redistribute iron from overloaded mitochondria to depleted cytosol, crossing also the blood-brain-barrier. [MARMOLINO, 2011]

Because deferoxamine (DFO), the most commonly used iron chelator, penetrates the membrane very poorly and additionally facilitates iron depletion by chelating iron from the extracellular compartment and the cytosol, it is not very useful in FRDA treatment.

In contrast to DFO, orally administered deferiprone demonstrates a higher affinity to transferrin, thereby preventing iron depletion and, additionally, can easily cross the blood brain barrier. Due to these properties, deferiprone is assumed to be a potential therapeutic drug in FRDA treatment. [PANDOLFO, 2013]

2.6.1.3. Erythropoietin for stabilizing or enhancing frataxin expression

Erythropoietin (EPO) is an endogenous glycoprotein hormone, controlling erythropoiesis by acting as stimulator of erythrocyte precursor development in the bone marrow. Currently it is therapeutically used for the treatment of anaemia, especially in dialysis and cancer patients or prior surgeries associated with a high loss of blood. [Internet: Friedreich's Ataxia Research Alliance (FARA), 27.05.2013]

Primary results of an *in vitro* study delivered a significant dose-dependent increase of frataxin expression in rhuEPO treated cells. In addition to the safe profile of rhuEPO as therapeutic agent, these observations provided the scientific basis for studying the effects of rhuEPO in FRDA patients. [STURM et al. 2005] Results of an open-label, phase IIa proof-of-concept study demonstrate a persistent and significant increase of frataxin levels after rhuEPO treatment, accompanied with a decrease of oxidative stress in all patients. [BOESCH et al., 2007]

These outcomes were supported by the results of a further 6-month open-label clinical pilot study, additionally showing an improvement of ataxia symptoms measured on FARS and SARA rating scores. Only the hematopoietic effects are the main safety concern of using rhuEPO in nonanemic patients. In addition a decrease of serum ferritin levels and otherwise an increasing serum transferrin level were observed, suggesting an iron mobilisation or redistribution into haemoglobin. To overcome the possible increased erythropoietin response in some patients and hence resulting safety concerns, EPO derivatives without hematopoietic activity might be a powerful treatment in FRDA. [BOESCH et al., 2008]

Prompted by these requirements, in an *in vitro* study the effect on frataxin expression using the non-hematopoietic derivative carbamylated erythropoietin (CEPO) was tested, observing a similar increase of frataxin expression in cultured cell lines, but without EPO-receptor binding, suggesting a diminished risk of polycythaemia. [STURM et al., 2010]

Epoetin alfa was tested in an open-label, Phase IIa clinical trial, suggesting a higher and sustained frataxin expression after administration of a single high dose, compared to low doses or repeated administration schemes, without haemoglobin increase. [SACCA et al., 2011]

In January 2013, a still ongoing Phase II RCT study started to evaluate the effect of epoetin alfa on physical performance of FRDA patients as primary endpoint. Drug safety and tolerability, its effect on frataxin expression, cardiac symptoms and disease progression are determined as secondary endpoints of this study. [Internet: U.S. National Institutes of Health: ClinicalTrials.gov_NCT01493973, 27.05.2013]

2.6.1.4. Increase of Frataxin or frataxin gene expression

Histone deacetylase inhibitors (HDACi)

As already mentioned in chapter 2.4.2., an overexpression of GAA triplet repeats is responsible for a reduced frataxin expression. One possible causal mechanism is the chromatin-condensing effect of GAA repeat expansion, which can be detected in their vicinity as silent chromatin, a characteristic epigenetic marker. By interfering with the histone deacetylase, HDACi are able to reconstitute an active chromatin conformation from its silent form and restore the normal function of the gene. [MARMOLINO, 2011]

Experiments performed by Hermann et al. demonstrate a 1.5–2.5-fold increase of frataxin levels in PBMC after treatment with a specific group of benzamide HDACi. It is assumed that for frataxin upregulation their target specificity for HDAC1 and HDAC3 as well as their slow-on slow-off kinetics is important. A further positive property is the long-lasting increase, suggesting an intermittent exposure as effective treatment. Data

from knock-in animals indicate a frataxin level increase in various tissues, including also the most affected heart tissue and CNS. [PANDOLFO, 2013]

The company RepliGen determined the HDACi RG2833 as a potential candidate in FRDA treatment, due to its oral availability and target specificity. Currently RG2833 is in Phase I clinical trial, evaluating the safety and dosage of the drug. A followed HDACi, RepliGen started pre-clinical studies with the compound RG3250. Results may indicate some advantages over RG2833 such as better pharmacology, metabolic stability and brain penetration. [Internet: BabelFamily - The international project to defeat Friedreich's Ataxia, 27.05.2013] [Internet: Friedreich's Ataxia Research Alliance (FARA), 27.05.2013]

Nicotinamide

Nicotinamide, the amide of vitamin B3, niacin or nicotinic acid, is under investigation to enhance the frataxin level in FRDA. Vitamin B3 is naturally available with the uptake of a broad variety of foods. Further the liver synthesizes niacin from the essential amino acid tryptophan, which is significantly found in milk and milk products. Niacin and its derivatives are essential compounds of the coenzymes NAD⁺ and NADP⁺, which are necessary as hydrogen carrier, in metabolisms.

Currently, a Phase II open-label trial is still ongoing, assessing if nicotinamide is an effective upregulator of frataxin gene expression in FRDA patients, and if so to determine an optimum dosage. [Internet: U.S. National Institutes of Health: ClinicalTrials.gov_NCT01589809, 27.05.2013]

Resveratrol

Resveratrol is a polyphenolic phytochemical, naturally occurring in e.g. red grapes, plums, raspberries and Japanese knotweed. High concentrations are found in fresh pressed red grape juice and red wine. Its well established antioxidant and neuroprotective properties, as well as the ability of increasing frataxin level *in vivo* and *in vitro*, are suggesting resveratrol as a potential agent for the treatment of FRDA patients. Assessing the effect of resveratrol on oxidative stress markers, clinical

features and cardiac parameters in FRDA patients is currently performed in a phase II open-label trial. [Internet: U.S. National Institutes of Health: ClinicalTrials.gov_ NCT01339884, 27.05.2013]

Interferon gamma

Treatment with interferon gamma (IFN γ) demonstrates an increase of frataxin level in cellular and animal models. This effect is presumably generated by the intense involvement of IFN γ in controlling iron distribution and availability. IFN γ modulates the expression of important compounds of iron metabolism.

Beside the involvement in iron metabolism, IFN γ additionally acts as an immune regulator by inducing components of the NAD(P)H oxidase complex and iNOS as well as by controlling the ROS and NO production. Further, results from IFN γ treated FRDA mice show an improvement of neuronal symptoms. [TOMASSINI, 2012] Based on these positive observations, a pilot study of IFN γ in FA patients is planned for evaluating safety and tolerability of IFN γ , and to assess a possible effect on frataxin levels in patients. [Internet: Friedreich's Ataxia Research Alliance (FARA), 29.05.2013]

2.6.1.5. Gene therapy and protein replacement

Preclinical investigations of herpes virus, lentivirus and adeno-associated virus (AAV)-based vectors provide a further potent possibility for FRDA treatment (**Figure 13**).

Gene-based Friedreich ataxia treatment:

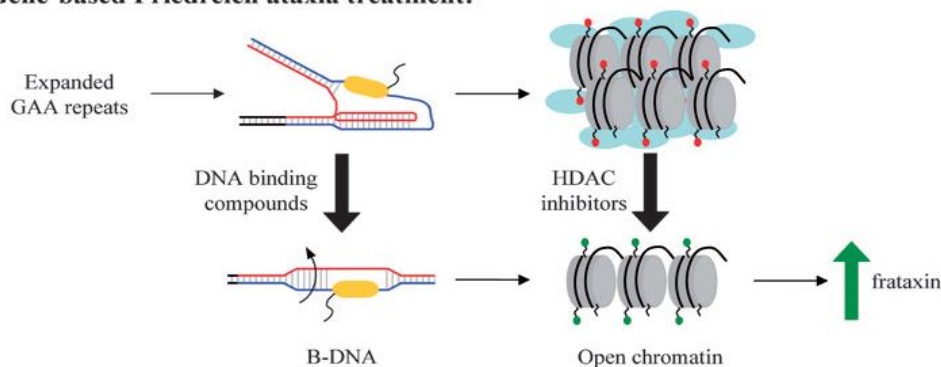


Figure 13: Gene-based strategy as possible treatment in FRDA. Ideally, gene based treatment could reverse non B-form DNA structures and heterochromatin formation to increase frataxin expression. HDAC: histone deacetylase. [mod. from HERBERT and WHITTOM, 2007]

Especially AAV is a quite promising vector due to its various serotypes, which are effectively delivered to the mainly affected tissues in FRDA disease (CNS, DRGs, heart). Before effects of gene therapy can be assessed in clinical studies, terms of delivery and safety have to be determined. [PANDOLFO, 2013]

The requirements for an effective protein replacement therapy are the penetration into the CNS and into the mitochondria. [PANDOLFO, 2013] To fulfil these demands, Piyush et al. used the cell penetrating peptide TAT. Therefore they evaluated if a TAT-Frataxin (TAT-FXN) fusion protein is able to diminish the clinical picture of FRDA in patient fibroblasts and in a severe phenotype of a FXN knock out mouse. Their data show beneficial improvements in the mouse model, like expanding life span by 53% or advances in the relief from cardiac symptoms. Based on these results, protein replacement therapy is assumed to be a further attractive treatment, requiring more preclinical work. [VYAS et al., 2012]

2.7. Chlorophyllin

Chlorophyllin compounds are technically derived from the natural green pigment chlorophyll, found in cyanobacteria and the chloroplasts of plants and algae. It enables them to perform photosynthesis by absorbing sun light for energy production in the organisms, which makes chlorophyll a critical component in photosynthesis and the oxygen production in the world (**Figure 14**).

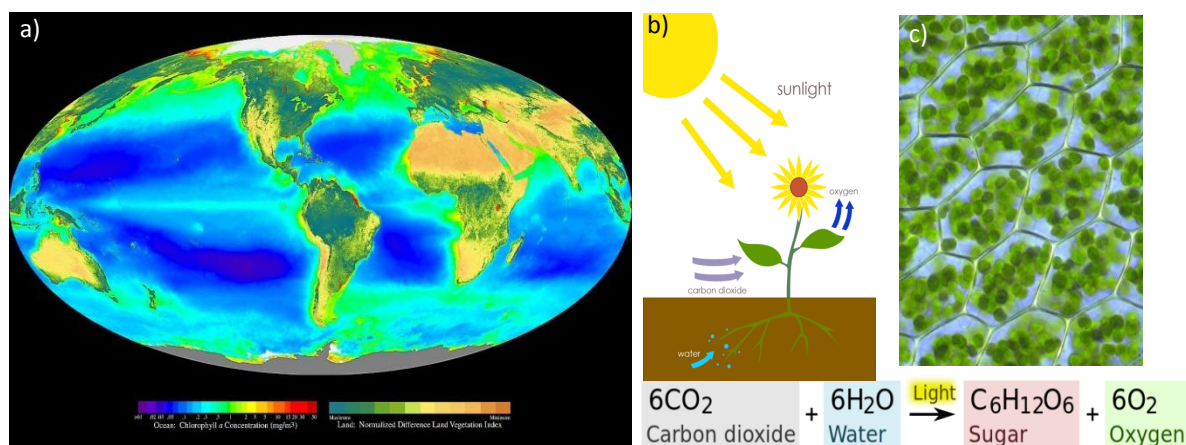


Figure 14: Photosynthesis and the critical role of chlorophyll. (a) Global distribution of photosynthesis. Dark blue and green regions indicate high photosynthetic activity. (b) Schematic representation of photosynthesis in plants and the resulting stoichiometric equation. (c) Plant cells with visible chloroplasts, the centre of photosynthesis. [4]

Like heme, the chromophor of haemoglobin, chlorophyll also possesses a porphyrin ring as basic structure, containing magnesium instead of iron as central atom. Due to the attached long phytol tail, chlorophyll is a water-insoluble compound.

Chlorophyllin (CHL) compounds belong to the group of semi-synthetic chlorophyll derivatives. During the manufacturing process the phytol tail is removed, resulting in a water-soluble mixture of salts of chlorophyll. Further the centrally coordinated Mg²⁺ is replaced with other metals, mainly Cu²⁺. Trisodium copper chlorin e₆ and disodium copper chlorin e₄ are the most commonly found compounds in commercially available chlorophyllin mixtures (**Figure 15**). [FERRUZZI and BLAKESLEE, 2007]

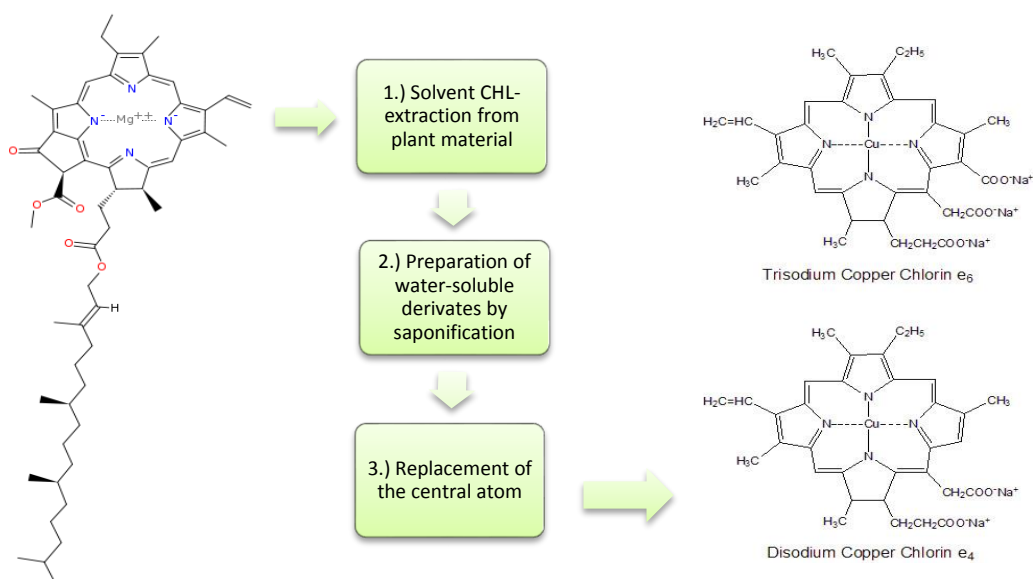


Figure 15: Manufacturing process of chlorophyllin derivatives from chlorophyll a. [5], [6]

Chlorophyll and chlorophyllin, as well as their copper containing derivatives are commonly used as food colouring agents in several food categories, marked in the EU with E 140 and E 141. Because of their non-toxicological profiles, these compounds belong to the group of food colorants without any upper level (quantum satis). [Verordnung (EU) Nr. 1129/2011]

While the intake of chlorophylls (E 140) is without any concerns, for chlorophyllin compounds containing copper (E 141) an ADI (=acceptable daily intake) of 15 mg/kg/day is established. [Internet: Die Verbraucher Initiative e.V. (Bundesverband): E141 – Kupferkomplexe der Chlorophylle, 12.06.2013] However, chlorophyll and chlorophyllin supplements should be avoided by pregnant or lactating women, because the safety for this group has not been tested. [Internet: Linus Pauling Institute, 12.06.2013]

Chlorophyllin supplements are therapeutically used as internal deodorant, e.g. it is orally administered to incontinent patients for reducing urinary and fecal odour, patients with colostomies and ileomies or patients with the hereditary disorder trimethylaminuria to prevent their typically “fishy” or foul odour. Further topical administration of chlorophyllin solutions is used for accelerating wound healing. [TUMOLO and LANFER-MARQUEZ, 2012]

2.7.1. Bioavailability and metabolism

Based on an *in vitro* digestion study, investigating the stability of sodium copper chlorophyllin, Ferruzzi et al. observed a higher presence of the catabolite copper chlorin e₄, compared to copper chlorin e₆. This indicates a higher stability of copper chlorin e₄ as well as an oxidative related degradation of copper chlorin e₆. Further, as it is described by Egner et al. and Gomes et al., the individual components are differently available in human body tissue. [TUMOLO and LANFER-MARQUEZ, 2012] Egner et al. observed a high amount of copper chlorin e₄ ethyl ester in human blood serum after 4 months consumption of 300 mg SCC/per day. The component copper chlorin e₄ was only detectable in a minor amount and copper chlorin e₆ was absent, indicating that SCC components are selectively bioavailable. [FERRUZZI and BLAKESLEE, 2007] Additionally, Gomes et al. also observed the absence of copper chlorin e₆ in blood serum and tissues (liver and kidney) and the presence of copper chlorin e₄ in both in rats. A significant reduction of lipid peroxidation in rat brain after copper CHL administration provides further evidence of absorption and bioavailability, although the exact mechanisms are still unknown (**Figure 16**). [TUMOLO and LANFER-MARQUEZ, 2012]

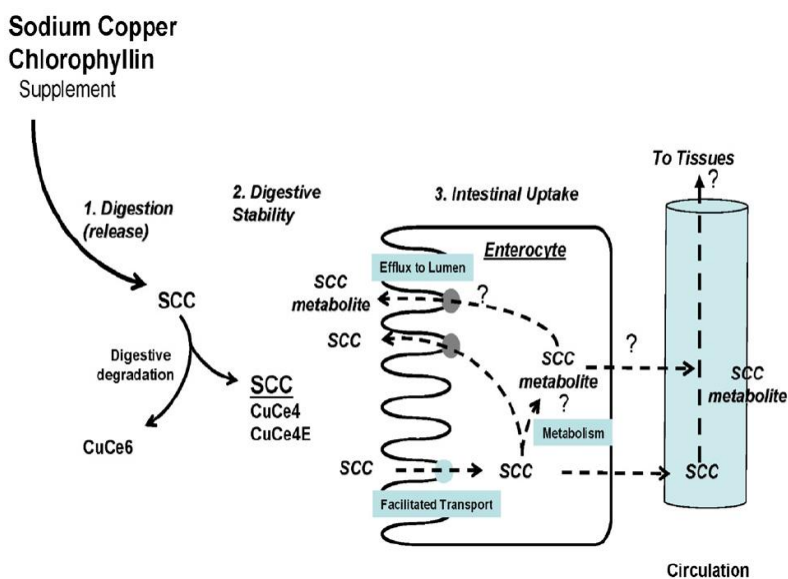


Figure 16: Possible schema of digestion and absorption of sodium copper chlorophyllin (SCC). SCC is primarily divided into the derivatives Cu-Chlorin e₄ and Cu-chlorin ethyl ester by digestive degradation. The uptake of these derivatives proceeds by a facilitated process, whereas SCC metabolites are effluxed back to the luminal compartment (potentially by the BCRP/ABCG2 transporter system) and a portion of SCC metabolites passes the enterocytes and enters the blood circulation. CuCe6: Cu-chlorin e₆. [FERRUZZI and BLAKESLEE, 2007]

2.7.2. Biological effects and disease prevention

The antimutagenic potential of chlorophyll and chlorophyllin compounds was assessed in several *in vitro* assays with strains of *Salmonella typhimurium*. Mutagenic compounds in natural as well as in processed food include polycyclic aromatic hydrocarbons, heterocyclic amines and aflatoxin-B₁. Conducted studies observed a dose-dependent inhibition of the effect of these mutagenic compounds after chlorophyll and Cu-CHL treatment. [TUMOLO and LANFER-MARQUEZ, 2012]

It is assumed that the antimutagenic and chemopreventive activity of Cu-CHL is due to a chlorophyllin-mutagen complex formation. Thereby the porphyrin ring of the Cu-CHL molecule interacts with aromatic rings in the mutagenic compounds, resulting in a diminished bioavailability of the mutagens and subsequently a reduced DNA-adduct formation. [TUMOLO and LANFER-MARQUEZ, 2012]

An additional antimutagenic effect of Cu-CHL is achieved by modulating the activity of cytochrome P450 enzymes, a necessary enzyme group to metabolize endogenous and exogenous substances that unfortunately has also the potential to transform procarcinogens to harmful carcinogens. *In vitro* studies with Cu-CHL demonstrate that it is able to inhibit cytochrome P450 activity on one side, and on the other side enforcing phase II biotransformation enzymes, which are responsible for elimination of harmful substances. [Internet: Linus Pauling Institute, 12.06.2013]

Cu-CHL also demonstrates antioxidative potential against oxidative stress or radiation-generated ROS, thus possible reducing the risk of several oxidant-related diseases. Compared with chlorophyll derivatives, the highest antioxidant activity is present in Cu-CHL, maybe due to the presence of copper in the porphyrin ring.

Additionally, chlorophyll and chlorophyllin are shown to be significant inducers of mammalian phase II enzymes, like NAD(P)H:quinone oxidoreductase 1 (NQO1), protecting the cells against reactive electrophiles and oxidizing compounds. [TUMOLO and LANFER-MARQUEZ, 2012]

3. Materials and Methods

3.1. Cell Culture

The most important aspect to prevent contaminations (e.g. bacteria, yeasts or mould) in cell culture is to work under sterile conditions. To reduce the contamination risk, all steps are performed in a laminar flow workbench (SafeFAST Elite; FASTER), which has to be cleaned with 70% ethanol and run 15 min before starting to work.

All items and solutions, which are necessary for work under the laminar flow workbench, have to be free of contaminations. Therefore the working materials are bought sterile or become decontaminated with following methods:

- **Heat sterilization** – for materials made of glass (e.g. bottles, glass-pipettes): using a sterilization oven (WTB Binder), sterilized for 12 hours at 180 °C.
- **Autoclaving** – for materials made of plastic (e.g. pipette tips, dest. water): using an autoclave (Certoclav), at a temperature of 120-140 °C for 20 min and 2 bar pressure.
- **Sterile filtration** – for solutions (e.g. incubation solutions, cell medium): using a membrane filter with a pore diameter < 0.22 µm (Rotilab).
- **Disinfection of surfaces** – with 70% ethanol and UV-light.
- **Disinfection of the hands** – during work under the laminar flow workbench gloves must be worn all the time, which are disinfected with 70% ethanol.

For cell cultivation an incubator (Binder) with constant temperature of 37 °C and 5% CO₂-atmosphere is used.

3.2. Cell lines

In this master thesis two different cell lines were used. One cell line, the human colon carcinoma cell line (Caco-2 cells) is used as an *in vitro* model to investigate intestinal uptake.

Mouse embryonic carcinoma P19 cells, differentiated to neural cells by retinoic acid [McBURNEY, 1993], were used as a model for neural cells which is the most affected cell type in Friedreich's ataxia patients.

3.2.1. Caco-2 cells

3.2.1.1. Culture medium (DMEM)

For preparing the cell culture medium, powdered Dulbecco's Modified Eagle's Medium (DMEM), high Glucose (4.5 g/l), with L-Glutamine (PAA Laboratories GmbH) is dissolved in 8.0 litres (80% of the end volume) distilled water under constant stirring. The distilled water must have a temperature between 15 and 30 °C to protect the vitamins and amino acids from degradation. When the cell culture powder is completely dissolved, 3.7 g sodium bicarbonate per litre is added. Further the pH value is adjusted to 7.2 by adding 1 M NaOH or 1 M HCl. Finally the solution is filled up with distilled water to the end volume of 10.0 litres.

After this preparation, DMEM is pumped into sterilized 500 ml bottles under sterile working conditions. For this, a peristaltic pump (Masterflex; Cole Parmer Instrument Co.) equipped with a membrane filter with a pore size of 0.20 µm (Sartolab P plus, Sartorius) is used.

The bottles filled with DMEM are stored in the dark at 4 °C until use.

3.2.1.2. Culture medium modification (modified DMEM)

To provide optimal growth conditions for Caco-2 cells, 450 ml of the DMEM culture medium is supplemented under sterile conditions with the following substances:

- 50.0 ml FCS (fetal calf serum), (BIOCHROM SUPERIOR)
- 5.0 ml L-Glutamin (200 mM) (100x), (PAA Laboratories GmbH)
- 0.5 ml Gentamycin (50 mg/ml), (GEBRU Biotechnik GmbH)

The modified DMEM is stored at 4 °C and must be used within 4 weeks after date of modification.

3.2.1.3. Cell culturing and sub-culturing

The Caco-2 cells are cultivated in 75 cm² sterile culture flasks (FALCON®) at a density of 1.8 million cells per 10.0 ml medium. To reach a logarithmic growth of the cells, the modified DMEM has to be renewed every 2-3 days, since the essential substances of the medium are catabolized by the cells during cultivation in the incubator.

When the cells have overgrown 80% of the culture flask surface, the cell density has to be reduced. The adherent Caco-2 cells must be therefore detached from the surface. This is initiated by removing the used medium and washing the cells with 2-3 ml of sterile PBS (1x) for complete removal of the trypsin-inhibiting-activity of FCS containing medium. Afterwards the cells are treated with 2 ml Trypsin-EDTA (1x) (PAA Laboratories GmbH). After 2 min of incubation at room temperature, most of the incubation mixture is removed and the flask is placed into the incubator (37 °C) for 5-10 min. When the cells are completely detached from the bottom of the flask Trypsin activity is stopped by addition of fresh modified DMEM to the cells. After cell counting a suitable amount of cell suspension is transferred to a new flask and filled with fresh modified DMEM to a final volume of 10 ml.

Caco-2 cells must be splitted approximately twice per week to a density of 1.8 million cells in 10 ml medium in a 75 cm² sterile culture flask.

3.2.1.4. Cell counting

Cell number was determined with an electronic cell counter (Microcellcounter CC-108; Sysmex). Preparing cell suspensions with a defined cell density is important for sub-culturing when used in the experiments.

Therefore the adherent cells must be detached from surface by digestion with Trypsin-EDTA. From the resulting cell suspension 0.5 ml are transferred to a microcentrifuge tube (EPPENDORF), 200 µl of the cell suspension are transferred to a special vessel and diluted with 9.8 ml cell counter solution (Cellpack PK-30L, Sysmex). After mixing this solution thoroughly the cells are ready to be analysed in the Microcellcounter. The result displays the total cell number, but notably that it does not differ between dead and live cells.

3.2.1.5. Cryopreservation of Caco-2 cells

Caco-2 cells can be stored over a long time at a temperature of -160 °C by using liquid nitrogen. This cryopreservation provides a resource for viable cells for later cultivation.

After cell counting the required amount of cell suspension (appr. 2 million cells/ml) must be transferred into a 15 ml centrifuge tube and centrifuged at 250*g for 5 min at 4 °C. Further the supernatant must be removed carefully from the cell pellet which is resuspended with the appropriate volume of cryoprotective medium (CM-1) (Cell line service). The resulting suspension must be filled immediately into cryotubes (Cryovial) and be cooled with ice until the whole work is done. After all tubes are filled, they are getting placed into a special freezing container (Nalgene Cryo 1 °C Freezing Container). This container is normally filled with propanol and stored at 4 °C. After placing the cryotubes into the freezing container, it is further stored at -80 °C, where the temperature of the cell suspension is decreasing 1 °C per hour. After 80 hours the cryotubes can be transferred to a liquid nitrogen tank.

This slow progress of freezing should prevent a destruction of the cell membranes resulting in a degradation of proteins.

3.2.1.6. Thawing of Caco-2 cells

In contrast to the freezing process, thawing of cells must be done fast to protect them from any damage. Therefore the frozen cryotubes are incubated with continuous agitation in a water bath at 37 °C until the cell suspension is completely thawed. The cell suspension is transferred into a 15 ml centrifuge tube filled with 8 ml modified DMEM. Afterwards the tube is centrifuged at 250*g for 10 min at 21 °C. The supernatant, including the cryoprotective medium, is removed and the cell pellet is resuspended with an appropriate amount of modified DMEM. This solution is transferred into a 75 cm² cultivation flask and cultivated at 37 °C with 5% CO₂-atmosphere.

3.2.2. P19 cells

3.2.2.1. Culture medium (α -MEM)

As culture medium for the P19 cell line MEM Alpha Modification with L-Glutamine and ribonucleosides (PAA Laboratories GmbH) is used. This culture-medium is bought in sterile 500 ml bottles as a ready to use solution and can be stored at 4 °C.

3.2.2.2. Culture medium modifications

Culture medium has to be modified with various supplements in reference to its further use.

- **Modified culture medium (modified α -MEM)** – this medium is used for cultivation of undifferentiated P19 cells. The following sterile supplements (all from PAA Laboratories GmbH) are added to 450 ml culture medium:
 - 37.5 ml CS (Calf Serum)
 - 12.5 ml FCS (fetal calf serum)
 - 5.0 ml L-Glutamine (200 mM) (100x)
 - 5.0 ml Non-essential amino acids solution (100x)
 - 0.5 ml Gentamycin (50 mg/ml)

- **Modified neuron medium** – this medium is used during differentiation of P19 cells to neuronal cells. The following sterile supplements (all from PAA Laboratories GmbH) are added to 464 ml culture medium:
 - 19.0 ml CS h.i. (Calf Serum, heat inactivated)
 - 6.5 ml FCS h.i. (Fetal Calf Serum, heat inactivated)
 - 5.0 ml L-Glutamine (200 mM) (100x)
 - 5.0 ml Non-essential amino acids solution (100x)
 - 0.5 ml Gentamycin (50 mg/ml)

Heat inactivation of CS and FCS is performed by incubation at 55 °C in a tempered water bath for 30 min.

3.2.2.3. *Cell culturing and sub culturing*

Undifferentiated P19 cells (**Figure 17a**) are cultivated in 75 cm² sterile culture flasks (FALCON®) at a density of 1 million cells per 20 ml modified α -MEM. The used medium has to be renewed every 2-3 days for ensuring a logarithmic growth of the cells.

When the cells reach their highest density, they stop proliferation due to contact induced inhibition. In this case these adherent cells must be detached from the surface of the culture flask. This is performed by incubating the cells with 1-2 ml Trypsin-EDTA (1x) (PAA Laboratories GmbH) at room temperature for 2 min. Then the Trypsin-EDTA (1x) is almost completely removed and the cells are further incubated for 4-5 min at 37 °C in the incubator, until the cells are completely detached from the surface of the flask. With addition of fresh modified α -MEM to the cells, Trypsin activity is inhibited. After resuspending the cells they are now ready for counting and the required amount of cell suspension can be transferred to a new sterile flask.

Passaging of undifferentiated P19 cells is performed 2-3 times per week.

3.2.2.4. *Cell counting, cryopreservation and thawing of P19 cells*

Cell counting, cryopreservation and thawing of P19 cells is performed as described for the Caco-2 cell line under the points from 3.2.1.4. to 3.2.1.6.

Instead of modified DMEM medium, P19 cells require modified α -MEM for seeding the cells into the flask.

3.2.2.5. *Differentiation of P19 cells to neuronal cells*

Undifferentiated P19 cells are pluripotent stem cells and can be differentiated to neuronal cells by adding retinoic acid. [McBURNEY, 1993] The complete differentiation process into neurons is concluded at day 10 (**Table 1**).

Day 0	Seeding the undifferentiated P19 cells into petri dishes <ul style="list-style-type: none"> - 0.30 million cells/ml modified neuron medium - 0.25 µl retinoic acid (5mM solved in DMSO)/ml modified neuron medium - incubating at 37 °C, 5% CO₂-atmosphere for 48 hours
Day 2	Renewal of the modified neuron medium <ul style="list-style-type: none"> - transferring 3 petri dishes to one 50 ml centrifuge tube - waiting for 10 min - centrifugation at 200*g for 10 min at 4 °C - resuspend the cell pellet in fresh modified neuron medium - transfer to the petri dishes - incubating at 37° C, 5% CO₂-atmosphere for 120 hours
Day 7	Plating the cells into microtiter plates <ul style="list-style-type: none"> - coating the plates with 0.1% gelatine-solution, 30 min - remove the modified neuron medium by centrifugation - resuspend the cell pellet in sterile PBS/EDTA (1xPBS, 1mM EDTA, pH 7.4) - diluting the suspension with modified α-MEM to a density of 0.4 million cells/ml - transferring to the wells - incubating at 37 °C, 5% CO₂-atmosphere for 72 hours
Day 10	Cells are completely differentiated to neurons and ready for further use

Table 1: Cultivation from undifferentiated embryonic P19 cells to differentiated P19 neuronal cells.

Day 0 – Seeding the undifferentiated P19 cells into petri dishes

Differentiation to neuronal cells starts with seeding the undifferentiated P19 cells into bacterial petri dishes (Sterilin) for building cell aggregates. Therefore 10 ml of modified neuron medium and 2.5 µl of retinoic acid (5 mM in DMSO) are filled into each petri

dish. After preparing these components, the required amount of cell suspension, containing 3 million cells is transferred into each petri dish.

The petri dishes are incubated at 37 °C and 5% CO₂-atmosphere for 48 hours.

Day 2 – Renewal of the modified neuron medium

After 48 hours of incubation, the cell aggregates need fresh modified neuron medium. For this, the contents of 3 petri dishes are transferred into one 50 ml centrifuge tube (BioGreiner). The tubes are now allowed to stand for 10 minutes until the cells are sunken to the ground followed by centrifugation at 200*g for 10 min at 4 °C. During this time the empty petri dishes can be refilled with 5 ml fresh modified neuron medium and 2.5 µl of retinoic acid per dish to prevent them from drying.

After centrifugation of the cell aggregates the old medium is removed without destroying the cell pellet. Each cell pellet is resuspended and separated with 15 ml fresh modified neuron medium. From this cell suspension 5 ml are transferred to a previously prepared petri dish.

Finally the dishes are cultivated at 37 °C and 5% CO₂-atmosphere again for further 120 hours.

Day 7 – Plating the cells into microtiter plates

Before plating the cells into microtiter plates, they are coated with a sterile 0.1% gelatine-solution (Sigma G2500). 96-well-plates are coated with 150µl/well 0.1% gelatine-solution and 6-well-plates are coated with 1.5 ml/well coating solution. After 30 minutes of incubation at room temperature the gelatine-solution is removed from the wells.

In the meantime the used modified neuron medium from the petri dishes can be removed by centrifugation as described above at day 2. Each cell pellet is resuspended with 1-2 ml sterile PBS/EDTA (1xPBS, 1mM EDTA, pH 7.4) and by adding 5 ml of modified α-MEM. For determination the total cell number the content of all centrifuge

tubes are collected in one tube and cell number of this cell suspension is determined counted (see point 3.2.1.4.).

According to the results from the cell counter, the cell suspension for the plates must be diluted with modified α -MEM to a density of 0.4 million cells/ml. For 96-well-plates, 200 μ l cell suspension/well must be used. For plating the cells into a 6-well-plate, each well is filled with 2 ml cell suspension.

The plates are incubated at 37 °C, 5% CO₂-atmosphere for 72 hours.

Day 10 – Cells are completely differentiated to neurons and ready for further experiments

At day 10, the P19 cells are completely differentiated to neuronal cells (**Figure 17c**) and ready for further experiments.

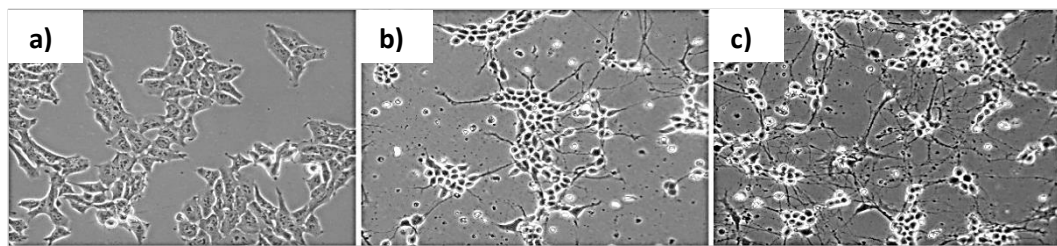


Figure 17: Differentiation of embryonic P19 cells to neuronal cells. ^[7] **a)** Embryonic P19 cells before beginning of differentiation, **b)** P19 cells at day 9 of differentiation, **c)** P19 cells are completely differentiated to neuronal cells, visible by the developed axonal connections.

3.3. Cytotoxicity Assays

To define a non-toxic concentration of the different chlorophyllin compounds for the cells, three different cytotoxicity assays are performed. Concentrations up to 50 μ M of Mg- or Cu-chlorophyllin are tested by MTT-assay, Neutral red uptake and Resazurin uptake.

3.3.1. Preparation of the cells

Caco-2 cells and differentiated neuronal cells are seeded into 96-well-plates to perform the above mentioned cytotoxicity assays.

Caco-2 cells are plated at a density of 45,000 cells/ml in modified DMEM medium, using 150 μ l per well. The plates are cultivated for up to 21 days at 37 °C and 5% CO₂-atmosphere. The medium must be renewed every 2-3 days.

The undifferentiated P19 cells must be differentiated, plated and cultivated as described in point 3.2.2.5.

3.3.2. Preparation of the incubation solutions

The cells are incubated with Mg- and Cu-chlorophyllin at concentrations ranging from 0.39 μ M up to 50.0 μ M. In addition to these compounds the cytotoxicity of hemin is assessed at the same concentrations.

From all compounds stock solutions (1mM) were prepared by dissolving Mg- CHL (Paninkret) and Cu-CHL (Sigma) in PBS (1x). Hemin (Fluka) is dissolved in NaOH (1 M). These resulting stock solutions are sterilised by filtration through a 0.22 μ m membrane filter and protected from light.

For preparing the different concentrations of the compounds, their stock-solutions are diluted with modified DMEM in case of Caco-2 cells and modified α -MEM for the neuronal cells, both containing heat inactivated FCS.

Stock solutions of Mg- and Cu-CHL can be stored in aliquots in the dark at -20 °C (stock aliquots were always discarded after thawing) whereas the stock solution for hemin must always be prepared fresh.

The serial dilution is performed according to the following scheme:

Solution	Concentration [μM]	Preparation	Dilution
1	50.0	Stock solution (1 mM) diluted with medium	1:20
2	25.0	Sol. 1 diluted with medium	1:1
3	12.5	Sol. 2 diluted with medium	1:1
4	6.25	Sol. 3 diluted with medium	1:1
5	3.12	Sol. 4 diluted with medium	1:1
6	1.56	Sol. 5 diluted with medium	1:1
7	0.78	Sol. 6 diluted with medium	1:1
8	0.39	Sol. 7 diluted with medium	1:1
Control	-	only medium	-

Table 2: Serial dilution of Mg- and Cu-CHL.

3.3.3. Incubation of the cells

When the cells were ready for the experiments the medium was removed from the wells and the cells were incubated with different concentrations of the compounds. To each well 200 μl of the incubation mixture were added and the cells were incubated at 37 °C and 5% CO₂-atmosphere for 24 hours.

At the end of the incubation time different cytotoxicity assays were performed.

3.3.3.1. MTT-Assay

The background for proving the metabolic activity of cells with this colorimetric assay is this ability to reduce the yellow and water-soluble tetrazolium dye MTT [3-(4,5-Dimethylthiazol-2-yl)-2,5-diphenyltetrazolium bromide] to the purple and insoluble formazan in living cells (**Figure 18**).

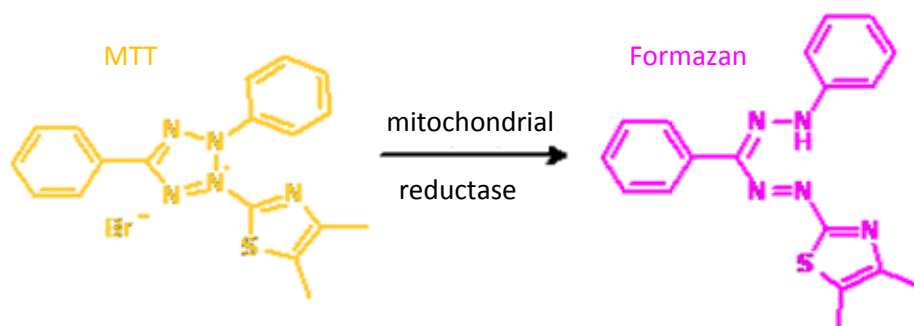


Figure 18: Reduction of MTT to formazan by the mitochondrial reductase in living cells.^[8]

Test performance

For the MTT-assay the following solutions must be prepared:

- *MTT-solution*
powdered MTT must be solved in PBS (1x) reaching a concentration of 5 mg MTT/ml. After solving completely the solution must be filtered by a 45 µm membrane filter and stored protected from the light. Unused MTT-solution can be frozen at -20 °C and stored in the dark.
- *MTT-solvent-solution*
this solution consists of isopropanol with 0.1% nonident P40 (Fluka) and 4 mM HCl.

After incubation of the cells with the compounds of interest, the incubation medium is removed and the cells are washed once with culture medium to ensure complete

removal of the incubation medium. Further each well is filled with 100 µl fresh modified medium and 20 µl MTT-solution, incubated at 37 °C and 5% CO₂-atmosphere for 30 min. After proving the colouring of the cells by visual inspection (Nikon TMS-F microscope) the plates are emptied manually and each well is filled with 150 µl MTT-solvent-solution. The coloured crystals are solved by continuous agitation (The Belly Dancer, Stovall, Life Science, Inc.) protected from light. After 20 minutes the absorbance at 595 nm and 620 nm is recorded in an absorbance plate reader (ANTHOS Zenyth 3100, Microplate multimode reader). Results are calculated and analysed by MS Excel 2010 and Graph Pad Prism 5.0.

3.3.3.2. Neutral red uptake

Neutral red (**Figure 19**) uptake is a further colorimetric assay to assess metabolic activity of cells. Neutral red is a dye which changes its

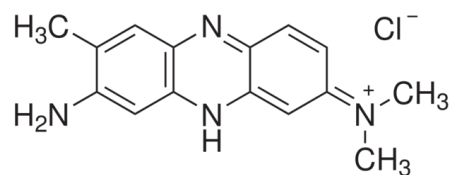


Figure 19: Structure of neutral red.^[9]

colour from yellow to red according to a modification of the pH from an alkaline to an acidic milieu. Based on this property neutral red is able to stain lysosomes because of their pH value of 5. Therefore red staining of the cells indicates that the cells are still viable and able to transport neutral red to the lysosomes.

Test performance

For this assay the following solutions are prepared:

- *Neutral Red solution 0.4%*
a solution with 0.4% neutral red (Fluka) dissolved in distilled water. After solving the dye completely, the solution must be sterilized by filtration through a 0.45 µm membrane. Freshly prepared MTT solution can be stored in the dark at 4 °C until further usage.

- *Diluted Neutral Red solution (1:80)* – for cell treatment, the *Neutral Red solution 0.4%* is diluted with the cell type specific modified culture medium at a ratio of 1:80.
- *Extraction Mixture* – this solution is composed of 50% ethanol and 1% acetic acid, filled up with distilled water.

At the end of the incubation time, the solutions are removed from the cells and the wells are washed with culture medium once to completely eliminate the incubation medium. In the next step the cells are incubated with 200 μ l of diluted Neutral Red solution (1:80) per well at 37 °C and 5% CO₂-atmosphere for 3 hours. Then the incubation medium is removed and the cells are washed with PBS (1x) once. To solve the dye, 200 μ l of extraction mixture are added per well and the plates are constantly shaken on the Belly Dancer for 20 min. Afterwards absorbance at 540nm is recorded in a absorbance plate reader (Victor², Wallac 1420 Multilabel counter). Analysis is performed by using GraphPad Prism 5.0.

3.3.3.3. Resazurin Assay

The Resazurin-Assay is another test to examine the cell metabolic activity. Resazurin is a blue, non-fluorescent dye, which is reductively transformed by living cells to the red, fluorescent resorufin. **(Figure 20)** In case of damaged or dead cells, the oxidation-reduction potential of the cells is reduced or absent, resulting in a non-transformation of resazurin.

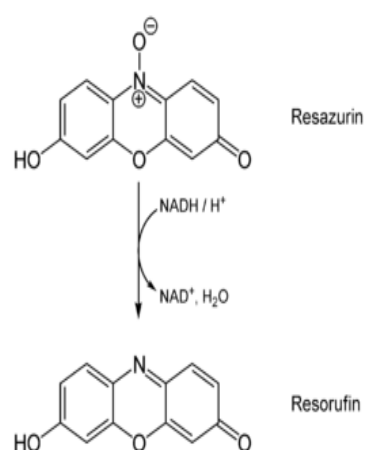


Figure 20: Reduction of resazurin to resorufin.^[10]

Test performance

For the resazurin assay the following solutions are needed:

- *DMEM without phenol red* is prepared by solving 10 g of the powdered medium (SIGMA) in 1 litre of distilled water, stirring until the powder is completely dissolved. Further 1.2 g/l NaHCO₃ and 1 ml Gentamycin (50mg/ml) must be added. Now the medium must be filtered through a 0.45 µm membrane and can be stored at -20 °C protected from the light.
- *Phenol red-free DMEM with HEPES (20mM)*
- *Resazurin-solution (4mM)*
Resazurin Sodium Salt (Sigma) is dissolved in distilled water and can be stored light-protected at -20 °C.
- *Resazurin-solution (3µM)*
The *resazurin-solution (4mM)* is diluted in *phenol red-free DMEM with HEPES (20mM)* to reach a concentration of 3 µM resazurin.

To assess the viability of the cells with this assay, the incubation solutions from the cells are removed. Then the cells are further washed with phenol red-free DMEM. Each well is filled with 200 µl of the resazurin-solution (3µM). Then fluorescence (Ex535nm/Em595nm) is recorded in a fluorescence plate reader (ANTHOS Zenyth 3100, Microplate multimode reader). The first fluorescence measurement starts immediately after addition of the resazurin-solution and is then repeated in intervals of 15 minutes for 165 min. Results are analysed with the program GraphPad Prism 5.0.

3.4. Permeability measurement of Caco-2 cells

To perform bioavailability tests it is necessary that Caco-2-cells are complete differentiated (**Figure 21**). For testing this time point of confluence the Phenol Red Exclusion and the Transepithelial Electrical Measurement (TEER) are recommended to test for confluency and monolayer integrity.

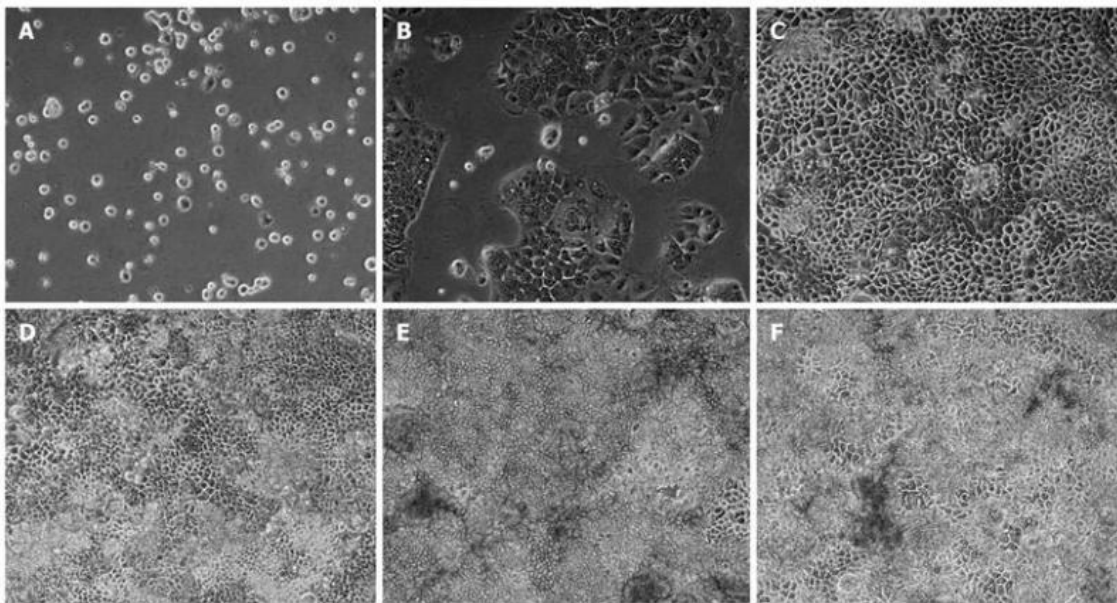


Figure 21: Microscopic images of Caco-2 cells on several days of cultivation. Isolated Caco-2 cells (A) are developing to a confluent monolayer (F) during time of cultivation. A: 0 d; B: 3 d; C: 5 d; D: 7 d; E: 11 d; F: 17 d. ^[11]

3.4.1. Preparation of the cells

For permeability measurements the cells are seeded into hanging cell culture inserts (Millipore, 0.4 μm PET) which are placed in advance into a 6-well-plate (Cellstar, Greiner) filled with 3 ml modified DMEM. After moistening the inserts, 2 ml containing the appropriate amount of cells must be placed on the apical side of each insert. According to the instruction of the supplier (Millipore) an optimal growth of the cells can be reached with a density of 20,000 cells/cm² (90,000 cells per insert).

The cells are cultivated at 37 °C and 5% CO₂-atmosphere.

3.4.1.1. Phenol Red Exclusion

The Phenol Red Exclusion provides a photometric measurement for proofing the monolayer integrity of the cells [MAZNAH, 1999]. This method is based on measuring the intensity of phenol red in the lower chamber which correlates with the cell growth.

Test performance

For this test modified DMEM and DMEM without phenol red are used. The required amount of DMEM without phenol red must be completed with 10% heat inactivated FCS. After removing the used medium from the wells, the lower chamber must be washed three times with DMEM without phenol red to remove all colour residues in this chamber. First the basolateral wells must be filled with 2.5 ml DMEM without phenol red containing FCS. Afterwards the apical side is filled with 2.5 ml modified DMEM (containing phenol red).

For assessing the values of time point zero (T_{0h}), immediately after filling the wells according to the description before, 0.5 ml must be transferred from each chamber to a microcentrifuge tube. After this the plates are incubated at 37 °C and 5% CO₂-atmosphere. After 2.5 hours of incubation 0.5 ml from each chamber must be transferred to a microcentrifuge tube again, assessing the values after this incubation time ($T_{2.5h}$). The remaining medium must be removed and after washing the wells with DMEM culture medium, the wells can be filled as described under point 3.4.1. Further 5 µl NaOH (1M) are added to each tube to get a basic pH and then 200 µl from each tube transferred into a 96-well-plate and phenol red absorbance is measured photometrically at 540 nm (ANTHOS Zenyth 3100, Microplate multimode reader).

Phenol Red Diffusion [%] was calculated in MS Excel and GraphPad Prism 5.0:

$$\text{Phenol Red Diffusion [\%]} = (T_{2.5h \text{ lower chamber}} - T_{0h \text{ lower chamber}}) * 100 / T_{0h \text{ upper chamber}}$$

$T_{2.5h \text{ lower chamber}}$ → using the mean value of $T_{2.5h \text{ lower chamber}}$

$T_{0h \text{ lower chamber}}$ → using the mean value of $T_{0h \text{ lower chamber}}$

$T_{0h \text{ upper chamber}}$ → using the mean value of $T_{0h \text{ upper chamber}}$

3.4.1.2. *Transepithelial Electrical Resistance (TEER) Measurement*

The TEER measurement is performed with the Millicell®-ERS (Electrical Resistance System) (Millipore). This method provides a fast and easy way to measure the cell monolayer health and cell confluency. Millicell®-ERS has specialized small size electrodes, each equipped with a silver/silver chloride pellet on the tip.

Before beginning the measurement some steps must be fulfilled to ensure proper operation:

- *Testing the meter (without electrode connection to the meter)*
 - switch the meter to the mode “R” (resistance)
 - turn the power on
 - push the button “TEST”

The meter is ok if it displays the following values:

1,000 Ω \pm 1 % (if the range is switched to 2,000 Ω) or
1 K Ω (if the range is switched to 20 K Ω)

- *Testing the electrodes*
 - plug in the electrodes into the electrode port on the meter
 - immerse the electrode tips into a sterile culture medium or electrolyte solution
 - for resistance measurement switch the meter to the “R” mode
 - turn the power on
 - the meter should now read “0”
 - push the button “MEASURE” and the shown value must be under 200 Ω
- *Sterilizing the electrodes*
 - immerse the electrode tips for 15 min, but not longer than 30 minutes in 70% ethanol during the connection of the electrodes to the meter

Now the Millicell®-ERS is ready for resistance measurements. For this the meter must be switched to the mode “R” and the range must be adjusted at 2,000 Ω. After setting these conditions the meter can be turned on and the electrode tips are placed into the wells, thereby ensuring that the tips are completely covered by the medium.

Then the “MEASURE” button must be pushed until the shown value is constant. Before measuring the next well the electrode tips should be rinsed with 70% ethanol and then with sterile culture medium.

When the measurement is finished, the electrodes must be cleaned thoroughly with distilled water before they are getting dry. For short term storage (less than 14 days) the electrodes can be placed into an electrolyte solution, otherwise the electrodes can be protected by a cover and must be stored in the dark.

Calculation of TEER values are calculated in MS Excel and GraphPad Prism 5.0:

$$\text{TEER } [\Omega \times \text{cm}^2] = (\text{TEER}_{\text{sample}} [\Omega] - \text{TEER}_{\text{blank}} [\Omega]) \times \text{membrane surface area } [\text{cm}^2]$$

$\text{TEER}_{\text{sample}} [\Omega] \rightarrow$ using the mean TEER value of the samples

$\text{TEER}_{\text{blank}} [\Omega] \rightarrow$ using the mean TEER value of the blanks

3.5. Cultivation of Caco-2 cells and differentiated neuronal cells for the experiments

To assess influence of various compounds on frataxin expression, Caco-2 and differentiated neuronal cells are seeded into 6-well plates. Caco-2 cells are plated out at a density of 96,000 cells/ml in modified DMEM, with 2 ml cell suspension/well. The cells are cultivated at 37 °C and 5% CO₂-atmosphere until complete differentiation (at least 21 days). Cell culture medium renewal is performed every 2-3 days.

P19 cells are differentiated and seeded in 6-well plates as described under point 3.2.2.5. The cells are completely differentiated to neuronal cells at day 10 and ready for further use.

3.5.1. Incubation of the cells with different compounds

For assessing a time-dose dependent effect of various compounds on the frataxin level in differentiated cells, the cells are incubated with different concentrations of the compounds for 1, 24 or 48 hours. The incubation media containing Mg- and Cu-chlorophyllin or hemin are prepared according to the description under point 3.3.2. Further the effect of Mg-CHL, idebenone and erythropoietin (EPO) (NeoRecormon®, Roche) alone or of different combinations of these compounds (**Table 3**) to the frataxin level is investigated in both cell types.

Solutions	Preparation (amount is added to 6 ml medium, containing FCS h.i. and CS h.i.)
5 µM Mg-CHL	30 µl Mg-CHL (1 mM) 6 µl 70% EtOH
3 U/ml EPO	3 µl EPO (2,000 I.U./300 µl) 6 µl 70% EtOH
10 µM idebenone	6 µl idebenone (10 mM/l) solved in 70% EtOH
5 µM Mg-CHL + 3 U/ml EPO	30 µl Mg-CHL (1 mM) 3 µl EPO (2,000 I.U./300 µl) 6 µl 70% EtOH
5 µM Mg-CHL + 10 µM idebenone	30 µl Mg-CHL (1 mM) 6 µl idebenone (10 mM/l)
3 U/ml EPO + 10 µM idebenone	3 µl EPO (2,000 I.U./300 µl) 6 µl idebenone (10 mM/l)
Control	6µl 70% EtOH

Table 3: Preparation of further exogenous substances.

3.5.2. *In vitro* model to study intestinal drug uptake and bioactivity of the compounds

Caco-2 cells are a widely used *in vitro* model to investigate the uptake and transport of different substances. In this case the time dependent effect of 50 μ M Mg- and Cu-CHL on FXN-levels in differentiated neuronal cells is assessed, following application of the compounds from the apical side of a monolayer of differentiated Caco-2 cells. Therefore Caco-2 cells are cultivated in hanging cell culture inserts (Millipore, 0.4 μ m PET) which are placed into 6-well plates containing differentiated neuronal cells as recipient cells (to test bioactivity in target cells) (**Figure 22**).

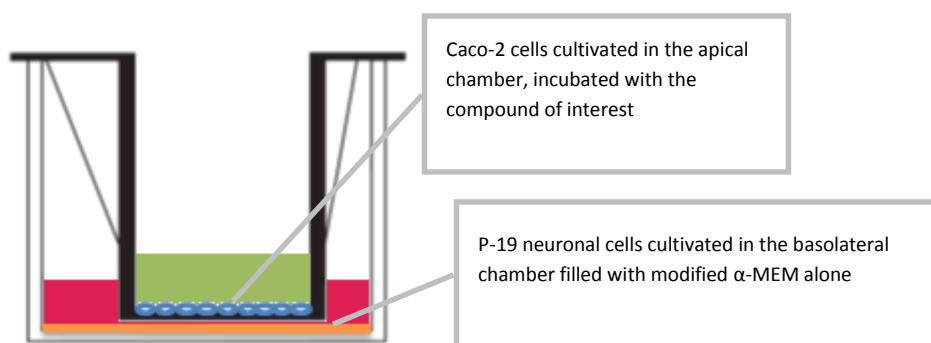


Figure 22: Caco-2/recipient co-culture model with P19 neuronal cells.

The simultaneous cultivation begins by seeding the Caco-2 cells as described under point 3.4.2. at a density of 90,000 cells/insert, and further cultivation at 37 °C and 5% CO₂-atmosphere for 21 days. Since completion of differentiation of Caco-2 cells and P-19 neuronal cells differs, differentiation of P19 cells has to start on day 12 after starting Caco-2 cell cultivation in the hanging inserts. At day 21 of Caco-2 cell cultivation in the hanging inserts, both cell types are differentiated and ready for the experiments.

For each experiment the incubation medium containing 50 μ M of the compounds of interest (Mg- or Cu-CHL) is freshly prepared in modified DMEM containing heat inactivated FCS.

At first the medium from all apical inserts (containing differentiated Caco-2 cells) as well as from all basolateral wells (containing the differentiated P-19 neuronal cells) is removed. Then 2 ml of fresh modified α -MEM (containing heat inactivated FCS and CS) per well is added to cells in the basolateral chamber whereas 2 ml of the previously prepared Mg- or Cu-CHL containing incubation medium are placed on the apical side of each insert. Then the cells are incubated for 1, 24 or 48 hours at 37 °C and 5% CO₂-atmosphere.

3.5.2.1. *Cell harvesting and production of cell lysates*

After termination of incubation time the cells can be harvested. The plates are placed on ice for 5 min to stop further metabolic activity. The incubation solution is removed and the cells are washed with PBS (1x) once. To harvest the cells each well is filled with 1 ml PBS (1x) and the cells are scrapped carefully from the surface, collected and centrifuged with 500*g, at 4 °C for 10 min in an Eppendorf centrifuge. After centrifugation the supernatant must be sucked of without destroying the cell pellet and the pellet is immediately frozen at -80 °C. The cells can be snap-frozen by dipping the tubes shortly into 90% ethanol (precooled to -80 °C) and then stored at -80 °C until further analysis.

Cell lysates are prepared from the frozen cell pellets. Therefore 1x cell lysis buffer was prepared by dilution of the commercially available 5x cell lysis buffer (Promega) with distilled water (1:5). To 1 ml 1x lysis buffer the following amounts of protease inhibitors are added:

- 10 μ l PMSF (Sigma) in DMSO (1mM)
- 10 μ l NaF (Merck) in distilled water (10mM)
- 10 μ l Protease Inhibitor Cocktail (P8340), (Sigma)

Only freshly prepared lysis buffer is used and stored on ice until use.

The frozen cell pellets from the deep freezer are directly placed on ice. To prevent protein degradation the further steps must be managed quickly and on ice.

The cell pellets are resuspended in lysis buffer and incubated on ice for 20 min. The required amount of lysis buffer depends on the size of the cell pellet:

- Caco-2 cells – 100-200µl lysis buffer
- P-19 Neuronal cells – 20µl lysis buffer

Then the cell lysates are centrifuged with 10,000*g, at 4 °C for 12 min. The supernatant (= cell lysate) is transferred to another tube and is used for protein and frataxin quantification. To store the lysate for later analysis it must be snap-frozen by immersion of the tube in -80 °C ethanol and can be stored at -80 °C until use.

BioRad protein quantification assay

Protein quantification of the cell lysates is performed according to the protein quantification assay of Bradford. [BRADFORD, 1976] This method is based on the binding of Coomassie brilliant blue G-250 to proteins in an acidic milieu. In presence of proteins the absorption maximum changes from 465 nm (without proteins) to 595 nm, by changing the colour from green/brown to blue. The intensity of absorption at 595 nm correlates with the protein concentration in the solution.

To assess the unknown protein quantity in the lysates, a standard curve ranging from 2-10 µg protein/ml is generated. Bovine serum albumin (BSA) with a concentration of 1 mg/ml is therefore used as standard stock solution. To generate the standard curve the stock solution is diluted 1:10 with distilled water. Subsequently different dilutions of the protein standard are prepared as shown in the following scheme:

Protein concentration [µg/ml]	BSA (0.1mg/ml) [µl]	Distilled water [µl]
0	-	800
2	20	780
4	40	760
6	60	740
8	80	720
10	100	700

Table 4: Preparation schema of BioRad protein quantification standard curve.

According to the protein content of the samples, the required amount of lysate must be filled up with distilled water to an exact volume of 800 μl . For Caco-2 cells and P-19 neuronal cells 2-10 μl cell lysate is sufficient to reach values within the standard curve.

By adding 200 μl of BioRad-reagent (Bio-Rad Laboratories GmbH) and vortexing each standard and sample thoroughly, the colour reaction is started. Next, 200 μl of each solution are transferred in duplicates into a 96-well plate. At least 20 but maximally 40 minutes after adding the BioRad-reagents absorbance at 595 nm is recorded on a absorbance platereader (Victor², Wallac 1420 Multilabel Counter).

Standard curve calculation and calculating the unknown values is performed by the programme Graph Pad Prism 5.0. (**Figure 23**).

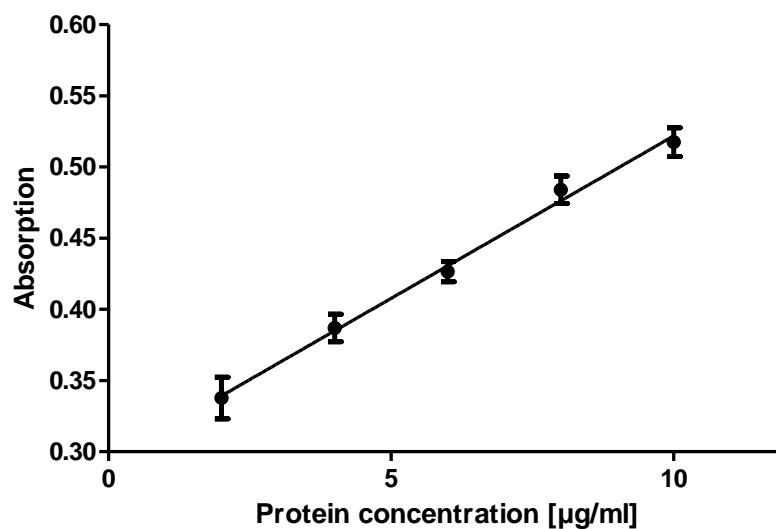


Figure 23: Standard curve for BioRad protein quantification assay.

Quantification of frataxin by ECLIA

Frataxin levels are quantified by using the Meso Scale Discovery platform. The frataxin-ECLIA (Electrochemiluminescence Immunoassay) is based on the principle of inducing

Ruthenium (II) tris-bipyridine-(4-methylsulfonate) NHS ester (MSD SULFO-TAG label)

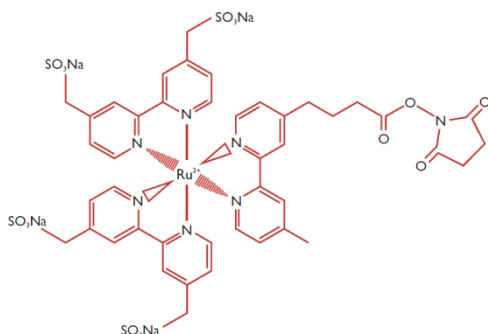


Figure 24: MSD SULFO-TAG label (Ruthenium (III) tris-bipyridine-(4-methylsulfonate) NHS ester). ^[12]

an “antibody-antigen-antibody” formation, which is the common technique of preparing a Sandwich-ELISA (Enzyme-linked Immunosorbent Assay). The main difference lies in the fact that the detection antibody used in the MSD-ECLIA has an electrochemiluminescent label with the non-radioactive and stable reagent MSD SULFO-TAG™ (**Figure 24**).

Preparing the “antibody-antigen-antibody” formation in a MULTI-ARRAY™ plate

The primary monoclonal antibody (“capture antibody”) is unspecifically bound to the carbon surface (**Figure 25**) of a MULTI-ARRAY™ plate (MA2400 96 High Binding Plate), whereas the detected antigen in the sample can be bound to it with high specificity. After washing to remove all unbound substances, only the requested antigen remains.

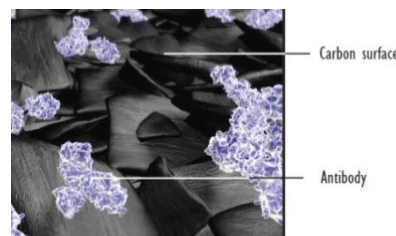


Figure 25: Carbon surface of a MULTI-ARRAY™ plate. ^[12]

Additionally to the first antibody, a second polyclonal “capture antibody” can be used to amplify the signal emitted later. It is important that this second antibody binds to another epitope on the antigen, in order to not disturb the binding of the first antibody.

Finally, the binding of a third antibody (“detection antibody”) labelled with MSD SULFO-TAG™ to the second antibody completes the “antibody-antigen-antibody” formation.

The diagram illustrates the structure and operation of a multi-array plate. At the top left, a 3D view of a 'MULTI-ARRAY Plate' is shown with a grid of wells. A red circle highlights a single well, which is magnified in the top right to show a cross-section of the well structure, labeled with '1' and '2' for the top and bottom electrodes, and 'A' and 'B' for the side walls.

The bottom part of the diagram shows the electrochemical luminescence mechanism. It depicts a 'Working Electrode' (labeled 'Working Electrode' at the bottom) and a 'Counter Electrode' (labeled 'Counter Electrode' at the bottom). The 'Working Electrode' is coated with a 'first antibody' (red square) and a 'second antibody' (yellow star). The 'first antibody' is bound to 'frataxin' (red square) and the 'second antibody' is bound to 'detection antibody' (yellow star). The 'detection antibody' is bound to 'frataxin' (red square) and the 'second antibody' is bound to 'frataxin' (red square). The 'detection antibody' is bound to 'frataxin' (red square) and the 'second antibody' is bound to 'frataxin' (red square).

The mechanism involves the electrochemical oxidation of TPA (Tetrakis(4-pyridyl)methane) at the working electrode, generating TPA^{•+} and releasing H⁺. The TPA^{•+} then reacts with Ru(bpy)₃²⁺ to form the excited state Ru(bpy)₃^{2+*}, which emits light (measured signal). The process is initiated by electrochemical energy (E_{chem}) and results in luminescence (E_{lum}).

60

Measurement of FXN in cell lysates

For measuring the FXN content in the cell lysates the following antibodies are used:

- *First antibody ("capture antibody") is directed against human frataxin:*
mouse anti-human frataxin monoclonal antibody (MAB1594), (Chemicon)
- *Second antibody binds to human frataxin and enforces the detection signal :*
frataxin (H-155) rabbit polyclonal antibody (Santa Cruz Biotechnology)
- *Third antibody ("detecting antibody") binds to the heavy and light chains of rabbit IgG:*
goat polyclonal anti-rabbit MSD-SULFO-TAG™ labelled (Meso Scale Discovery)

The following solutions must be prepared for the assay in advance:

- *1% BSA-solution:* 1 g MSD-BSA solved in 100 ml MSD-PBS (1x)
- *3% BSA-solution ("Blocking solution"):* 3 g MSD-BSA solved in 100 ml MSD-PBS (1x)
- *Washing solution:* PBS (1x) including 0,05% TWEEN 20 (Merck-Schuchardt)

These solutions can be stored at 4 °C until use.

The following solutions have to be freshly-prepared:

- *Lysis buffer (1 ml):*
200 µl 5x cell lysis buffer (PROMEGA) + 800 µl distilled water mixed with:
 - 10 µl PMSF (Sigma) in DMSO (1 mM)
 - 10 µl NaF (Merck) in distilled water (10 mM)
 - 10 µl Protease Inhibitor Cocktail (P8340) (Sigma)
- *Lysis buffer/SDS (200 µl for two approaches):*
195 µl lysis buffer + 5 µl SDS 10% (8% lysis buffer/0.02% SDS 10% per approach)

- *BSA/SDS buffer (for 20 samples):*
1,377 µl 1% BSA-solution + 3 µl SDS 10% (1% BSA/0.02% SDS 10% per sample)
- *Reading Buffer (1x):*
5 ml MSD Reading Buffer (4x) + 15 ml distilled water

1) Coating the MULTI ARRAY™ plate with the first antibody (Ms α Fx, Chemicon)

The stock solution of the first antibody is frozen and stored at -20 °C and is a dilution of 1:10 of the original commercially available antibody. For measurement it must be further diluted according to the following steps:

- 2.5 µl of the antibody stock solution (1:10) is diluted with MSD-PBS (1x) to a range of 1:800.
- 50.0 µl of the 1:800 diluted antibody is diluted at a range of 1.5:10 with MSD-PBS (1x).

5 µl of this diluted antibody are transferred by reverse pipetting to the centre of each well and is incubated for 1h at room temperature, covered by an aluminium foil.

In case of overnight incubation, the plate is sealed carefully by a plastic wrap and stored at 4 °C.

2) Blocking

At the end of the incubation time, the coating solution is removed and each well is filled with 125 µl blocking solution. This step ensures that all free binding sites are blocked to prevent unspecific binding. The plate is sealed and incubated at room temperature for 1h 30min under constant agitation (The Belly dancer, Stovall Life Science, Inc.).

3) Washing

After removal of the blocking solution the wells are washed with 150 µl washing solution for 3 times.

4) Preparation of standards and samples

To prepare the standard curve 30 µl of a frataxin-solution (0.4 ng/µl, stored at -80 °C) is mixed with 270 µl of 1% BSA-solution, resulting a standard-stock-solution with a concentration of 40 pg FXN/µl. Now 75 µl of this standard-stock-solution are mixed with 63 µl 1% BSA-solution to get standard 0 (Std. 0 = 500 pg/well). Further standards are prepared according to the following scheme (each prepared for 3 wells) (**Table 5**):

Standard	FXN concentration [pg/well]	Preparation
Std. 1	250	69 µl Std. 0 + 69 µl 1% BSA
Std. 2	125	69 µl Std. 1 + 69 µl 1% BSA
Std. 3	62.5	69 µl Std. 2 + 69 µl 1% BSA
Std. 4	31.3	69 µl Std. 3 + 69 µl 1% BSA
Std. 5	15.6	69 µl Std. 4 + 69 µl 1% BSA
Std. 6	7.80	69 µl Std. 5 + 69 µl 1% BSA
Std. 7	3.90	69 µl Std. 6 + 69 µl 1% BSA
Blank value	0.00	69 µl 1% BSA

Table 5: Preparation schema of frataxin-ECLIA standard curve.

To obtain equal final volumes of each standard (69µl), from standard 7 a volume of 69µl is removed and discarded. Then 7µl of lysis buffer/SDS are added to all standards and the blank.

The samples are also prepared in 3-fold to have enough volume to run the assay in duplicates. To obtain a final volume of 75µl (25µl/well are used in the assay) 7 µl of the cell lysates are mixed with 69 µl BSA/SDS buffer.

For the assay 25 µl/well of each standard and sample are transferred in duplicates to the wells by reverse pipetting, and incubated in the covered plate at room temperature for 1h 30 min under constant agitation on the belly dancer.

The protein content of the cell lysates should range between 6-10 µg protein per well, depending on the cell type. This amount of protein/well ensures that the frataxin levels lie within the frataxin standard curve. When volumes smaller than 7µl of the cell lysate have to be used, lysis buffer is added to a final volume of 7µl.

5) Washing and incubation with the second antibody (RabAntiFx, polyclonal Santa Cruz):

The second antibody is diluted 1:1,000 with BSA 1% in PBS. At the end of the incubation time, the incubation mixture is removed and the wells are washed with 150 µl/well washing solution for three times. Then 30 µl of the diluted second antibody is added to each well by reverse pipetting, and the plate covered by a plastic wrap is incubated for 1h at room temperature on the belly dancer.

6) Washing and incubation with the third antibody (MSD Goat α Rabbit):

The third antibody is diluted with BSA 1% to reach a concentration of 0.75 mg/ml (4 ml BSA 1% + 6 µl MSD Goat α Rabbit).

After emptying and washing the plate as described before , 30 µl per well of the third antibody are added by reverse pipetting, and the sealed plate is incubated for 1 hour at room temperature on the belly dancer.

7) Washing and incubation with the Reading Buffer (1x):

Before incubation with the Reading Buffer (1x), the plate must be emptied and washed with 150 µl/well washing solution for three times. Afterwards each well is filled with 150 µl Reading Buffer (1x) by reverse pipetting and electrochemiluminescence is measured immediately in the MSD Sector® Imager 2400. Calculations are performed using Graph Pad Prism 5.0 software (**Figures 27 and 28**).

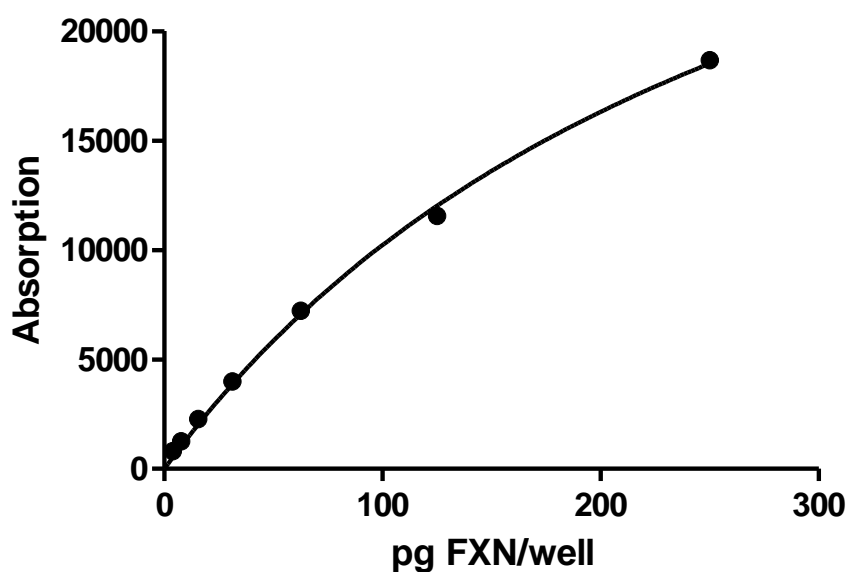


Figure 27: Standard curve for frataxin-ECLIA measurement.

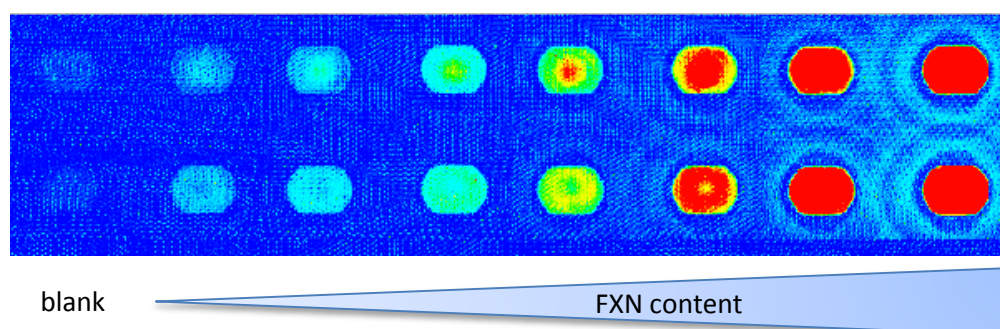


Figure 28: ECL signal of the frataxin standards detected with a CCD camera in the MSD Sector Imager 2400.

3.6. Statistics

Results were calculated and analysed by MS Excel 2010 and GraphPad Prism 5.0. Controls were averaged and normalised to 100% and compared to the average values of the samples.

Paired two-tailed t-test was used to determine the level of significance compared to controls. Significant differences are specified as $^*(p < 0.05)$, $^{**}(p < 0.01)$ and $^{***}(p < 0.001)$.

4. Results and Discussion

Main issue of this *in vitro* study was to identify a non-toxic dose to assess bioactivity of chlorophyllin on Caco-2 cells and P19 neuronal cells, to prepare a safe scientific basis for chlorophyllin studies *in vivo*.

Since the reduced frataxin level is critical in FRDA patients, increasing expression of this protein could represent an effective target for therapeutically treatment.

Sarsero et al. demonstrated a significant increase of FRDA gene expression when cells were exposed to various hemin concentrations (up to 100 μ M) [SARSERO et al., 2003]. Based on these findings, it could be hypothesized that such effects could also be expected by using other compounds with similar structure.

Chlorophyllins are such a group of compounds with common chemical base structure similar to hemin and our group identified chlorophyllin compounds as potent inducers of frataxin expression in FRDA lymphocytes (unpublished data).

Neuronal cells belong to the most affected tissues in FRDA and the use of orally available compounds is the preferred route for drug application. In this regard toxicity and bioactivity of the compounds of interest were tested in this study in P19 neuronal cells as a model for neuronal cells and differentiated Caco-2 cells as a model for intestinal cells, representing the first target after oral drug uptake.

Since there are no published data available about the impact of chlorophyllin on the frataxin expression in Caco-2 cells and P19 neuronal cells, dose-time-dependent cytotoxicity assays were performed to examine a useful non-toxic dosage for further experiments.

Frataxin expression in Caco-2 and P19 neuronal cells was assessed by frataxin-ECLIA measurement after treatment with the compounds of interest, as described in chapter Material and Methods.

4.1. Cytotoxicity of porphyrin compounds

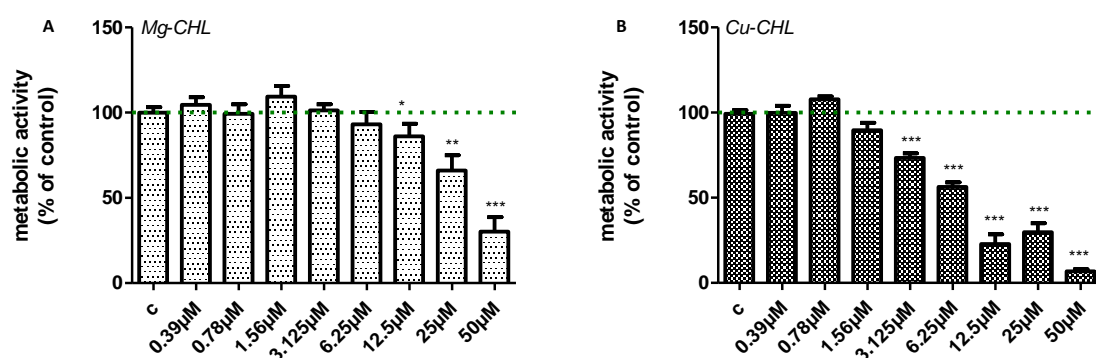
To define a secure concentration of the different porphyrin compounds for the cells, three different cytotoxicity assays were performed. Concentrations up to 50 μM of Mg-CHL, Cu-CHL or hemin were tested by MTT-assay, Neutral red uptake and resazurin reduction. Implementation of different measurement methods is necessary to determine comparable results, since each method measures different effects on metabolic activity.

4.1.1. Metabolic activity of cells following incubation with CHL compounds

Metabolic activity of non-differentiated Caco-2 cells following CHL incubation

Intestinal cells are the first target potentially harmed by oral drugs. Therefore we investigated toxicity of chlorophyllin in an intestinal cell-model, using Caco-2 cells cultivated for 17 days. According to chapter 4.3. Caco-2 cells need 21 days to form an intact monolayer of differentiated cells. Therefore at cultivation day 17 differentiation of the cells is not completed. Based on the background of the metabolic activity assays, the results demonstrate a dose-dependent decrease of metabolic activity in non-differentiated Caco-2 cells (**Figure 29**) with both chlorophyllin compounds tested. From these results it can be assumed that higher concentrations of Mg-CHL and Cu-CHL are able to inhibit ongoing proliferation of the cells. Another explanation for the dose-dependent decrease in non-differentiated Caco-2 cells could be a reduced metabolic activity and viability.

MTT-Assay



Neutral-Red uptake

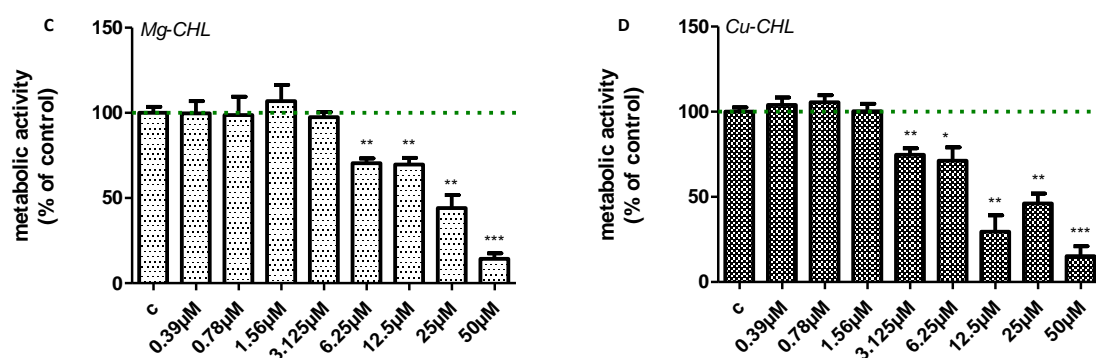


Figure 29: Influence of CHL compounds on metabolic activity of non-differentiated Caco-2 cells.

Caco-2 cells were seeded into 96-well tissue culture plates at a density of 9×10^3 cells per well and cultivated for 17 days in modified DMEM culture medium containing 1% L-glutamine and 0.1% gentamycin. Afterwards the cells were treated with Mg-CHL (A), (C) and Cu-CHL (B), (D) solutions at concentrations ranging from $[0.39 \mu\text{M}]$ up to $[50.00 \mu\text{M}]$ for 24 hours at 37°C and 5% CO_2 atmosphere. Controls (c) were incubated with modified DMEM alone.

Metabolic activity was assessed by MTT-assay (A), (B) and neutral red uptake (C), (D) as described in Materials and Methods. Significant differences vs. control are marked with * ($p < 0.5$), ** ($p < 0.01$) and *** ($p < 0.001$). Shown are the means \pm SEM in % of control (control = 100%); ($n=12$).

Metabolic activity of differentiated Caco-2 cells following CHL incubation

In differentiated Caco-2 cells (**Figure 30**) the metabolic activity up to the maximal tested dose of Mg-CHL and Cu-CHL is comparable to untreated cells, assuming that the cells are fully proliferated and the compounds have no negative impact on metabolic activity.

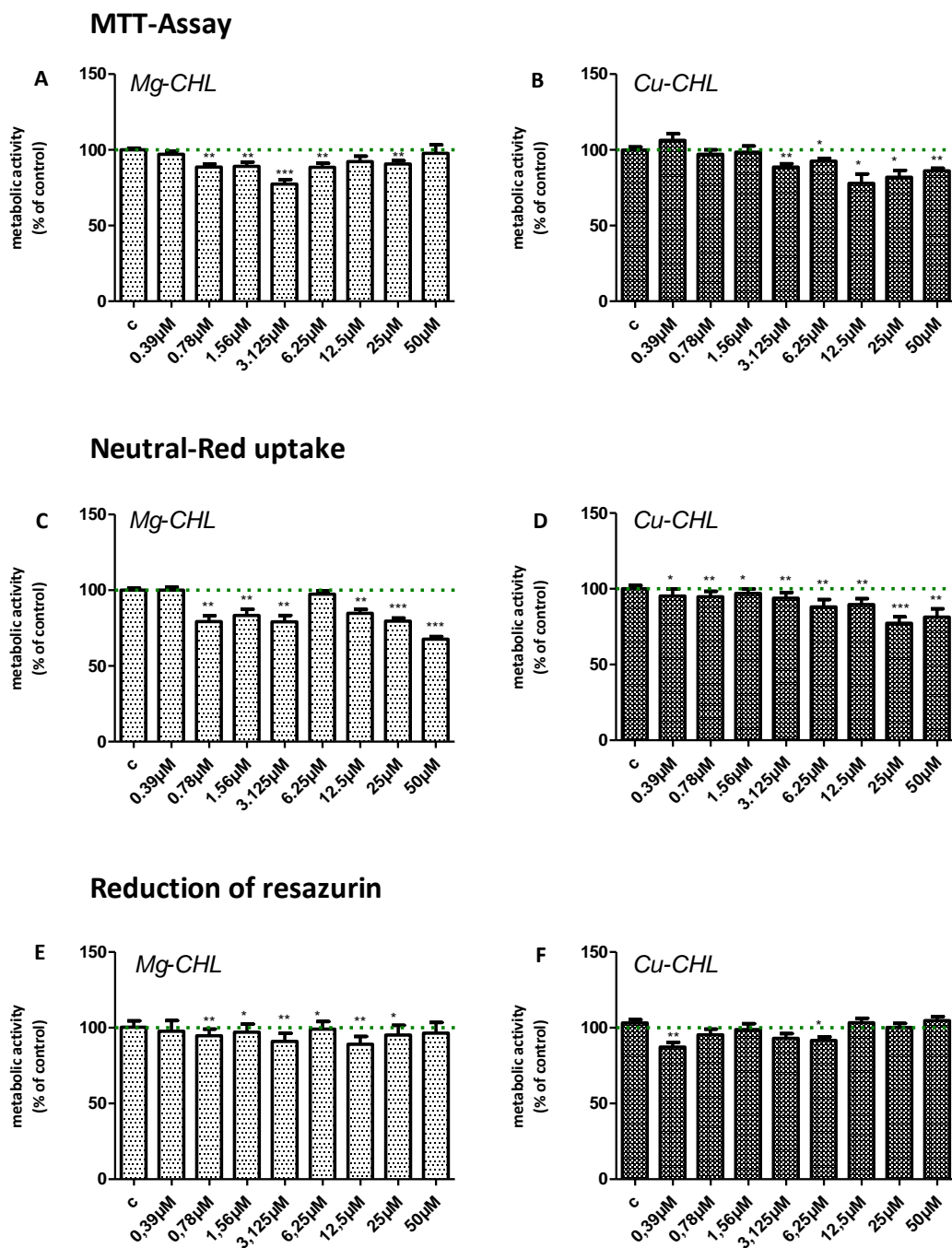


Figure 30: Influence of CHL compounds on metabolic activity of differentiated Caco-2 cells.

Caco-2 cells were seeded into 96- tissue culture plates at a density of 9×10^3 cells per well and cultivated for 21 days in modified DMEM culture medium containing 1% L-glutamine and 0.1% gentamycin. Afterwards the cells were treated with Mg-CHL (A), (C), (E) and Cu-CHL (B), (D), (F) solutions at concentrations ranging from $[0.39 \mu\text{M}]$ up to $[50 \mu\text{M}]$ for 24 hours at 37 °C and 5% CO₂ atmosphere in modified DMEM culture medium containing heat inactivated FCS. Controls (c) were incubated for the same period with modified DMEM containing heat inactivated FCS alone.

*Metabolic activity was assessed by MTT-assay (A), (B), neutral red uptake (C), (D) and reduction of resazurin (E), (F) as described in Materials and Methods. Shown are the means \pm SEM in % of control (control = 100%); (n=12). Significant differences vs. control are marked with * ($p < 0.5$), ** ($p < 0.01$) and *** ($p < 0.001$).*

In conclusion the results from the different cytotoxicity assays in Caco-2 cells indicate that there is no difference between Mg-CHL and Cu-CHL in regard to metabolic activity in differentiated as well as in non-differentiated Caco-2 cells. Both compounds show no toxicity in completely differentiated Caco-2 monolayers (day 21 of cultivation), whereas before complete differentiation (day 17 of cultivation) a dose-dependent toxicity was observed. For further experiments Caco-2 cells were cultivated for at least 21 days.

Metabolic activity of P19 neuronal cells after CHL incubation

Because neuronal cells are the most affected cell type in FRDA, we investigated the effects of CHL compounds on metabolic activity in differentiated P19 neuronal cells. Unexpectedly Mg-CHL and Cu-CHL treatment of neuronal P19 cells results in a significant increase of their metabolic activity (**Figure 31**), indicating that CHL compounds are able to trigger metabolic activity.

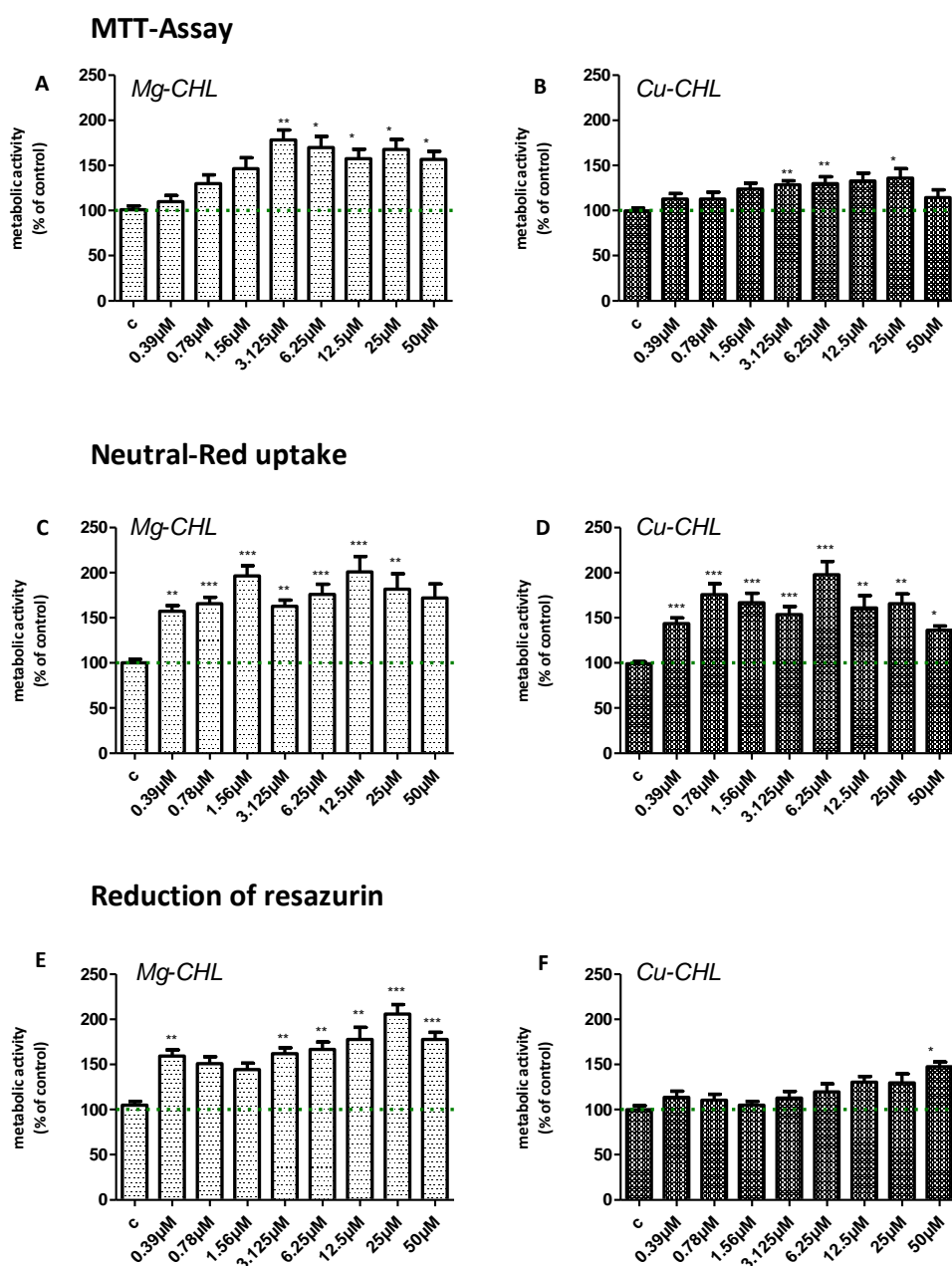


Figure 31: Influence of CHL compounds on P19 neuronal cell metabolic activity.

P19 cells were differentiated to P19 neuronal cells by retinoic acid as described in Materials and Methods. The completely differentiated neuronal cells were seeded into 96-well microtiter plates at a density of 8×10^4 cells per well and incubated with Mg-CHL (**A**), (**C**), (**E**) and Cu-CHL (**B**), (**D**), (**F**) solutions at concentrations ranging from $[0.39 \mu\text{M}]$ up to $[50 \mu\text{M}]$ for 24 hours at 37 °C and 5% CO₂ atmosphere in modified α -MEM containing heat inactivated FCS and CS. Controls (c) were incubated with modified α -MEM containing heat inactivated FCS and CS.

Metabolic activity was assessed by MTT-assay (**A**), (**B**), neutral red uptake (**C**), (**D**) and reduction of resazurin (**E**), (**F**) as described in Materials and Methods. Shown are the means \pm SEM in % of control (control = 100%); (n=12). Significant differences vs. control are marked with * ($p < 0.5$), ** ($p < 0.01$) and *** ($p < 0.001$).

In conclusion the results from the different cytotoxicity assays in neuronal P19 cells indicate that there is no difference between Mg-CHL and Cu-CHL on metabolic activity. Since no toxicity was observed in CHL treated P19 neuronal cells, doses up to 50 μM were used in further experiments.

4.1.2. Metabolic activity of cells following incubation with hemin

Additionally to CHL compounds, the cells were treated with the iron containing substance hemin (**Figure 32**). Its biosynthesis in the mitochondria competes with ISC-synthesis, assuming that hemin supplementation could change mitochondrial iron content or iron utilisation, affecting FRDA gene expression.

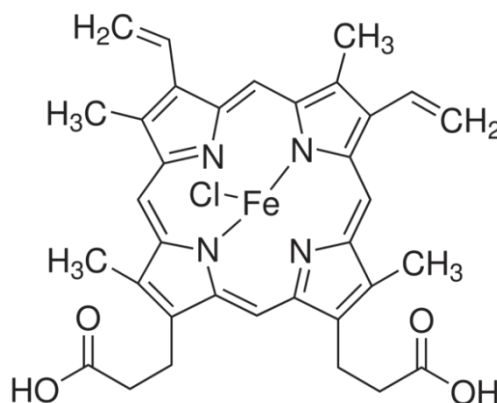


Figure 32: Structure of hemin.^[13]

Although Sarsero et al. demonstrated an increase of FXN expression [SARSERO et al., 2003] studies indicate that hemin is neurotoxic. [DANG et al., 2011] Therefore we assessed its impact on metabolic activity in our cell models.

Metabolic activity of differentiated Caco-2 cells following hemin incubation

Hemin significantly reduced metabolic activity in differentiated Caco-2 cells at higher concentrations only in the neutral-red uptake (**Figure 33**).

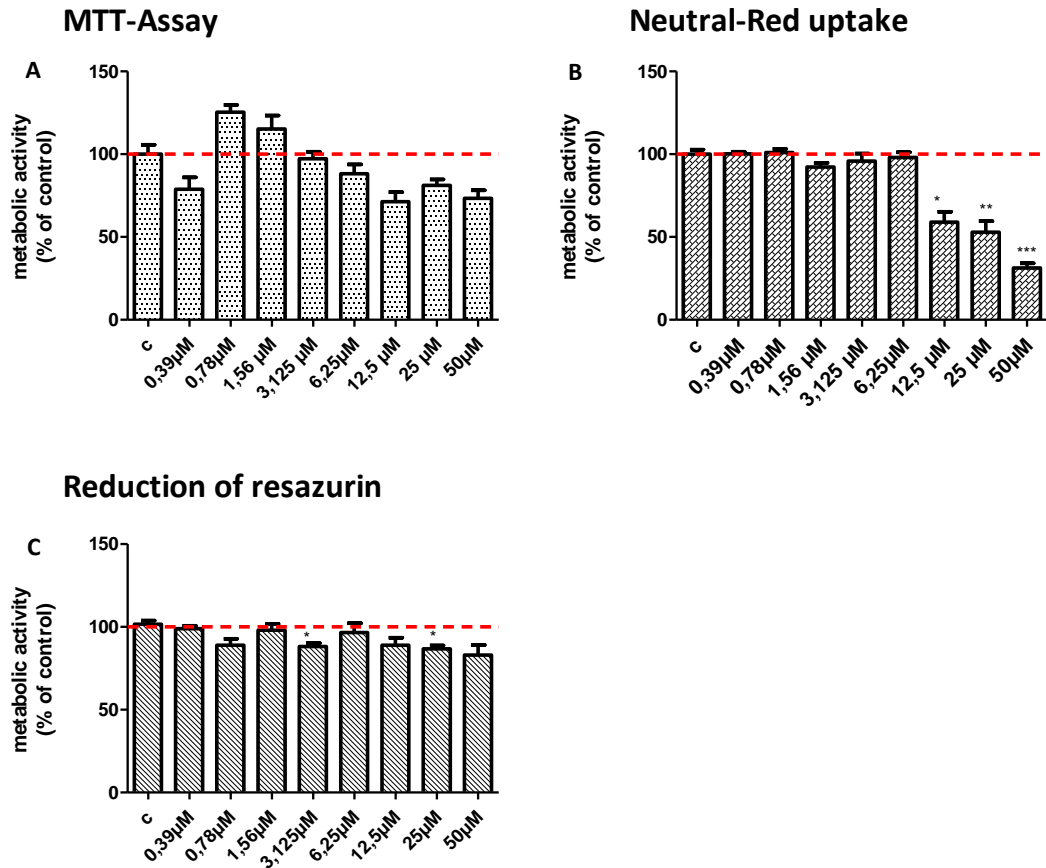


Figure 33: Influence of hemin on metabolic activity on differentiated Caco-2 cells.

Caco-2 cells were seeded into 96-well tissue culture plates at a density of 9×10^3 cells per well and cultivated for 21 days in modified DMEM culture medium; containing 1% L-glutamine, 0.1% gentamycin. Afterwards the cells were treated with hemin solutions at concentrations ranging from $[0.39 \mu\text{M}]$ up to $[50 \mu\text{M}]$ in modified DMEM containing heat inactivated FCS for 24 hours at 37°C and 5% CO_2 atmosphere. Controls (c) were incubated with modified DMEM containing heat inactivated FCS alone.

Metabolic activity was assessed by MTT-assay (**A**), neutral red uptake (**B**) and reduction of resazurin (**C**) as described in Materials and Methods. Shown are the means \pm SEM in % of control (control = 100%); ($n=6$). Significant differences vs. control are marked with * ($p < 0.5$), ** ($p < 0.01$) and *** ($p < 0.001$).

Metabolic activity of P19 neuronal cells following hemin incubation

Sarsero et al. demonstrated an increase of FXN expression with hemin [SARSERO et al., 2003], but another study revealed that hemin is neurotoxic. [DANG et al., 2011] Therefore we assessed metabolic activity of P19 neuronal cells following hemin incubation by three different cytotoxicity assays.

In contrast to chlorophyllin compounds, incubation with hemin induces only a modest increase in metabolic activity in P19 neuronal cells, and there was no cytotoxicity observed up to the highest concentration tested in all three assays (**Figure 34**).

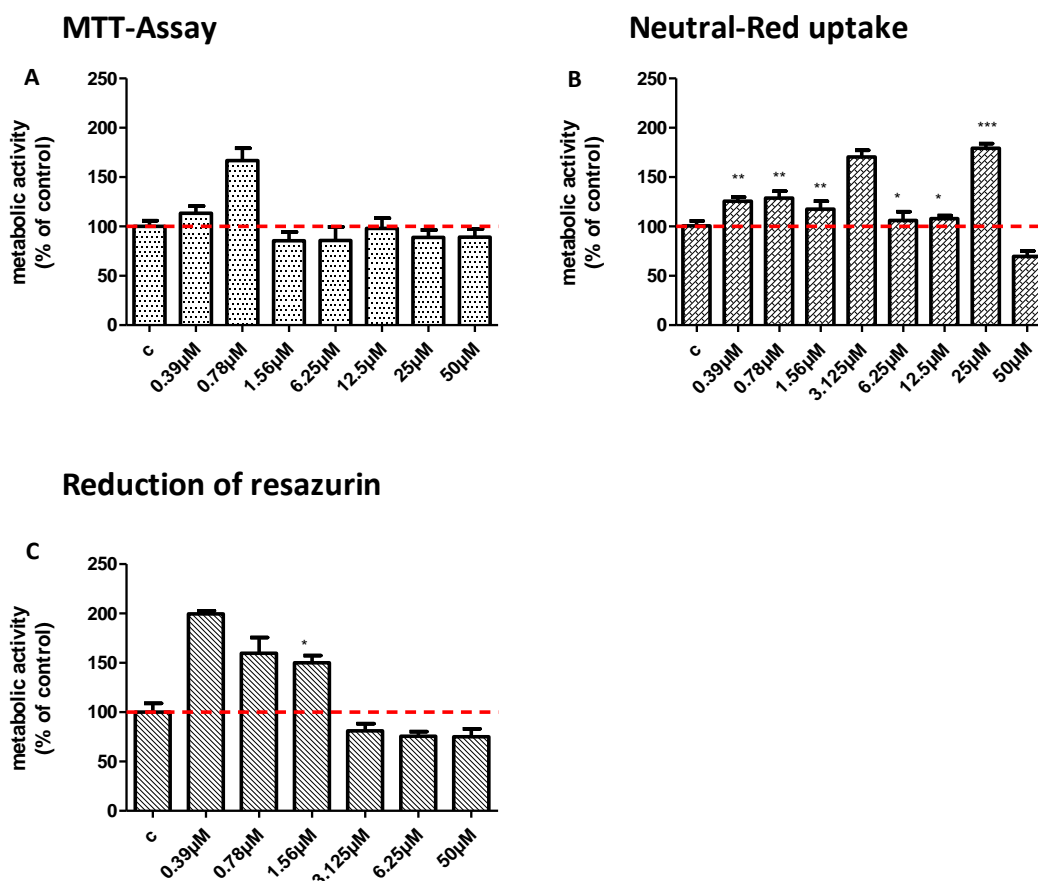


Figure 34: Influence of hemin on P19 neuronal cell metabolic activity.

P19 cells were differentiated to neuronal cells by treatment with retinoic acid as described in Materials and Methods. The completely differentiated neuronal cells were seeded into 96-well microtiter plates at a density of 8×10^4 cells per well and incubated with hemin at concentrations ranging from $[0.39 \mu\text{M}]$ up to $[50 \mu\text{M}]$ in modified α -MEM containing heat inactivated FCS and CS for 24 hours at 37 °C and 5% CO₂ atmosphere. Controls (c) were incubated with modified α -MEM containing heat inactivated FCS and CS.

*Metabolic activity was assessed by MTT-assay **(A)**, neutral red uptake **(B)** and reduction of resazurin **(C)** as described in Materials and Methods. Shown are the means \pm SEM in % of control (control = 100%); (n=6). Significant differences vs. control are marked with * ($p < 0.05$), ** ($p < 0.01$) and *** ($p < 0.001$).*

4.2. Effect of exogenous substances on frataxin expression

In a study with 50 healthy individuals our group found that, despite an only narrow range of GAA-repeats in the FRDA-gene in healthy individuals, frataxin protein levels varied up to threefold [BOEHM et al., 2011]. This suggests that in addition to the number of GAA-repeats possibly other mechanisms than GAA-repeat length might influence frataxin expression. It is therefore important to recognize compounds which are able to increase frataxin levels. Stimulation of frataxin expression with non-toxic exogenous substances to the level of asymptomatic FRDA carriers could therefore represent a therapeutic option for the treatment of FRDA patients.

To determine the influence of exogenous substances on FXN expression, the cellular FXN content was assessed by frataxin-ECLIA measurement as described in “Materials and Methods”. The FXN content was normalized to the total protein content of the lysates, which was quantified by the BioRad protein assay (chapter 3.5.2.1.).

4.2.1. Effect of chlorophyllin compounds on frataxin expression

Effect of Mg-CHL and Cu-CHL on frataxin expression in differentiated Caco-2 cells

Differentiated Caco-2 cells at day 21 of cultivation were incubated with different concentrations of Mg-CHL and Cu-CHL for different time periods. Frataxin levels in the lysates were assessed by frataxin-ECLIA and normalized to the total protein content.

Compared to the untreated control both chlorophyllin compounds increased frataxin expression within one hour, while this effect could not be observed following longer incubation times. Interestingly, in the untreated control cells frataxin expression was not stable and increased from 0.2 pg FXN/μg protein to 0.4 pg FXN/μg protein at 24 hours and dropped to 0.3 pg FXN/μg protein at 48 hours. This may explain the fact that no further increase in frataxin expression with chlorophyllin could be observed at these time points (**Figure 35**).

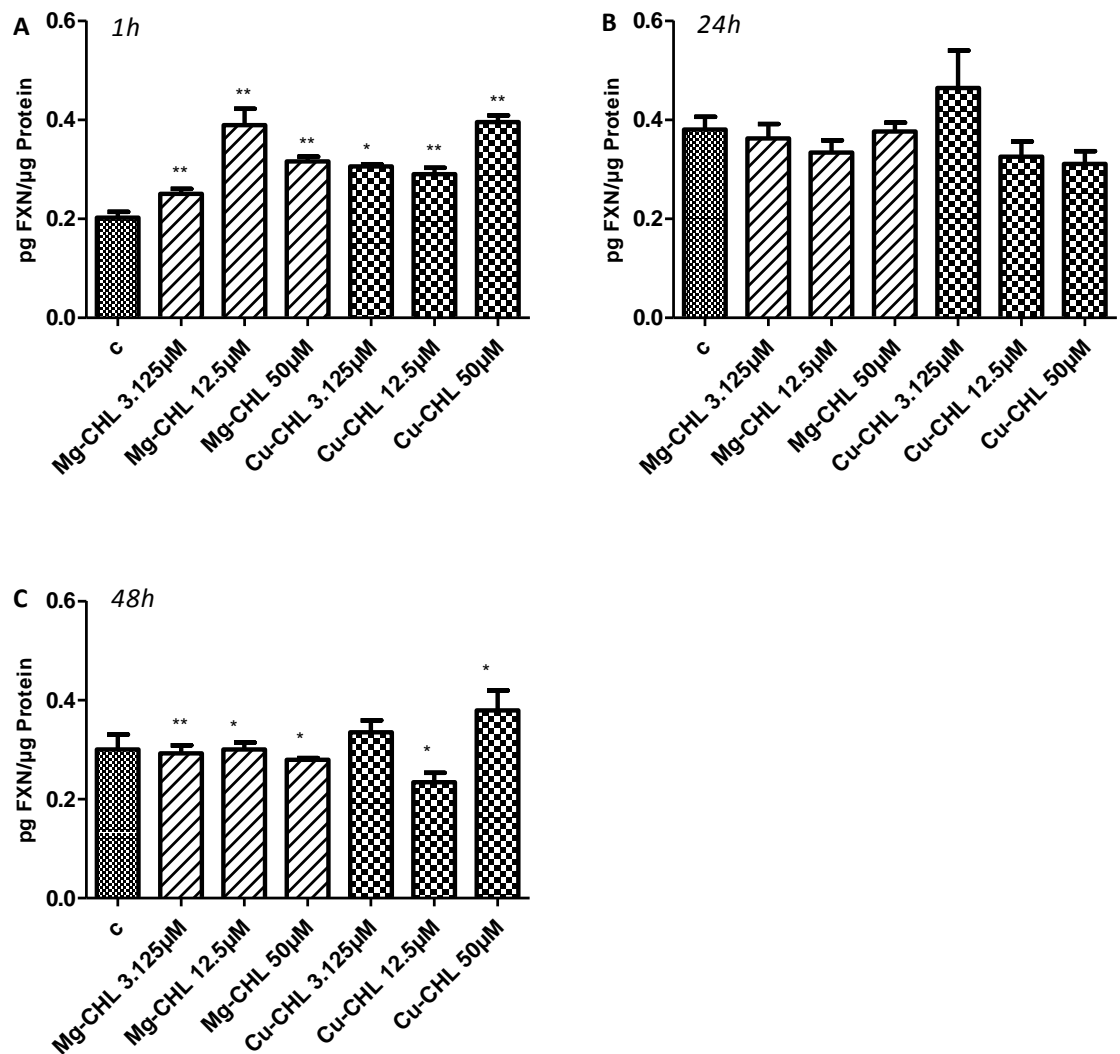


Figure 35: Influence of CHL compounds on FXN expression in differentiated Caco-2 cells.

Caco-2 cells were seeded into 6-well tissue culture plates at a density of 19.2×10^4 cells per well and cultivated for 21 days in modified DMEM culture medium; containing 1% L-glutamine, 0.1% gentamycin. Afterwards the cells were treated with Mg-CHL and Cu-CHL solutions at concentrations of [3.125μM], [12.5μM] and [50.0μM] for (A) 1hour, (B) 24 hours and (C) 48 hours at 37 °C and 5% CO₂ atmosphere. Controls (c) were incubated with modified DMEM containing heat inactivated FCS alone.

*Frataxin content [pg FXN/μg Protein] was assessed by frataxin-ECLIA measurement as described in Materials and Methods. Shown are the means ± SEM; (n=4). Significant differences vs. control are marked with * ($p < 0.5$), ** ($p < 0.01$) and *** ($p < 0.001$).*

Effect of Mg-CHL and Cu-CHL on frataxin expression in P19 neuronal cells

Based on the findings of the cytotoxicity assays the influence of chlorophyllin compounds on frataxin expression in P19 neuronal cells was assessed. Since neuronal cells are among the most affected tissues in FRDA it was of interest to investigate the impact of chlorophyllin compounds on these cells at non-toxic concentrations.

Frataxin levels remained stable during 48 hours of incubation and frataxin levels of treated cells were comparable to the untreated control (**Figure 36**).

In contrast to these data, previous results indicating an increase in frataxin expression, which were assessed by Western blot analysis and by the Frataxin Protein Quantity Dipstick Assay Kit from Mitoscience. To verify these results a comparative study with all three methods will be necessary.

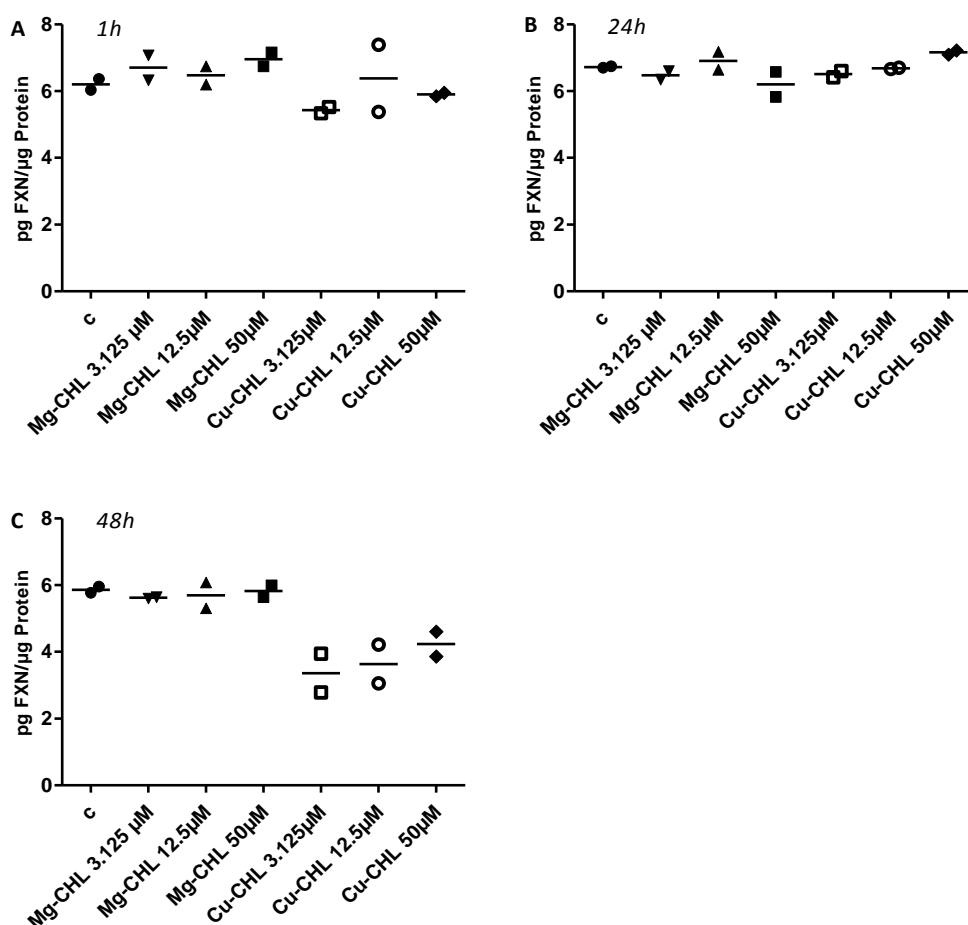


Figure 36: Influence of CHL-compounds on FXN expression in differentiated P19 neuronal cells.

P19 cells were differentiated to P19 neuronal cells by retinoic acid as described in Materials and Methods. The completely differentiated neuronal cells were seeded into 6-well microtiter plates according at a density of 8×10^4 cells per well and incubated with Mg-CHL and Cu-CHL at concentrations of [3.125 μ M], [12.5 μ M] and [50.0 μ M] in modified α -MEM containing heat inactivated FCS and CS for (A) 1 hour, (B) 24 hours and (C) 48 hours at 37 °C and 5% CO₂ atmosphere. Controls (c) were incubated with modified α -MEM containing heat inactivated FCS and CS only.

Frataxin content [pg FXN/ μ g Protein] was assessed by frataxin-ECLIA measurement as described in Materials and Methods. Shown are the means of two experiments.

4.2.2. Effect of hemin on frataxin expression

Sarsero et al. demonstrated a significant increase of FRDA gene expression when cells were exposed to various hemin concentrations (up to 100 μ M) [SARSERO et al., 2003]. Therefore it was of interest to assess the impact of hemin on frataxin expression in differentiated Caco-2 cells as well as in neuronal P19 cells.

Effect of hemin on frataxin expression in differentiated Caco-2 cells

Again in the untreated control cells, frataxin levels were not stable and showed an increase of frataxin expression at 24 hours of incubation and were still slightly elevated at 48 hours compared to frataxin expression at 1 hour. Although cytotoxicity assays in 96-well tissue culture plates up to 50 μ M hemin could be performed, cells cultivated in 6-well tissue culture plates immediately detached at 50 μ M hemin from the surface. Therefore only the effect of 3.125 μ M and 12.5 μ M hemin on frataxin expression could be assessed. There was a slight but significant increase of frataxin expression within one hour, but at longer incubation times we observed significantly reduced frataxin levels (**Figure 37**).

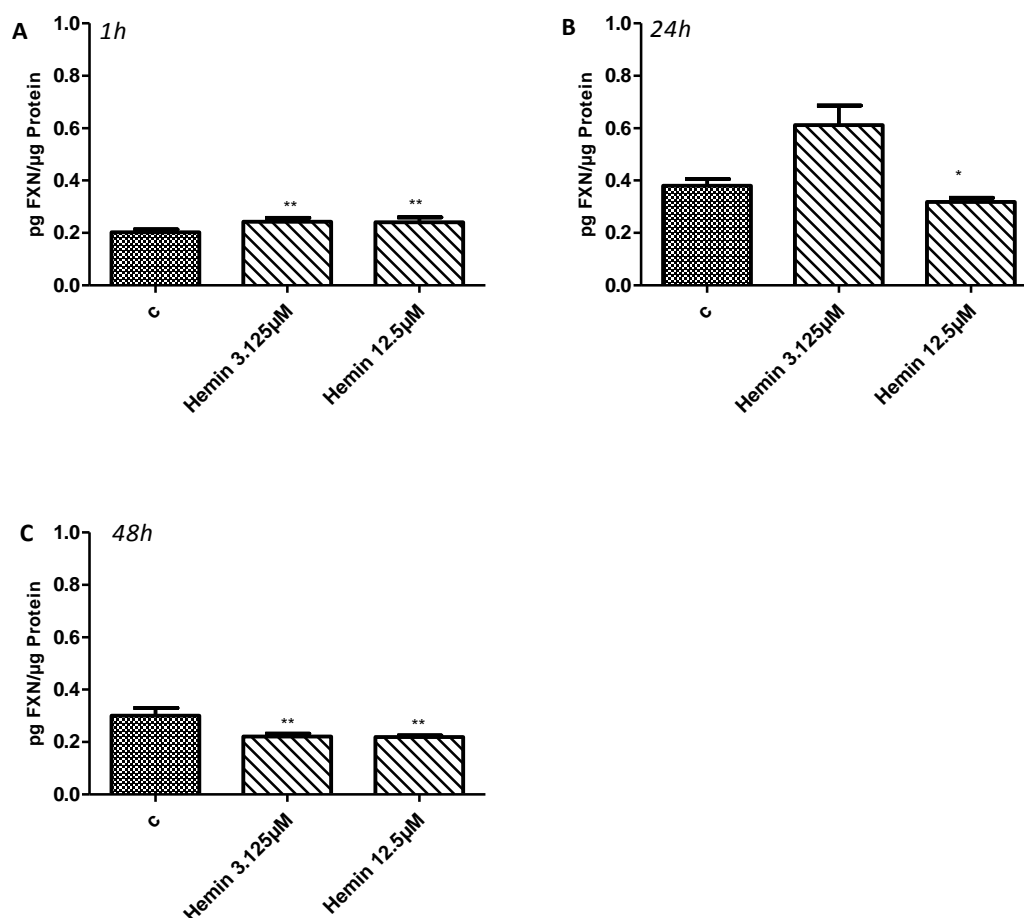


Figure 37: Influence of hemin on FXN expression in differentiated Caco-2 cells.

Caco-2 cells were seeded into 6-well tissue culture plates at a density of 19.2×10^4 cells per well and cultivated for 21 days in modified DMEM culture medium; containing 1% L-glutamine, 0.1% gentamycin. Afterwards the cells were treated with hemin at concentrations of [3.125μM], [12.5μM] and [50.0μM] in modified DMEM containing heat inactivated FCS for (A) 1hour, (B) 24 hours and (C) 48 hours at 37 °C and 5% CO₂ atmosphere. Controls (c) were incubated with modified DMEM containing heat inactivated FCS alone.

*Frataxin content [pg FXN/μg Protein] was assessed by frataxin ECLIA measurement as described in Materials and Methods. Shown are the means \pm SEM; (n=4). Significant differences vs. control are marked with * ($p < 0.5$), ** ($p < 0.01$) and *** ($p < 0.001$).*

Effect of hemin on frataxin expression in P19 neuronal cells

Although cytotoxicity assays in 96-well tissue culture plates up to 50 μ M hemin could be performed with P19 neuronal cells, cells cultivated in 6-well tissue culture plates immediately detached at 50 μ M hemin from the surface. Therefore only the effect of 3.125 μ M and 12.5 μ M hemin on frataxin expression is shown in figure 38.

When P19 neuronal cells were treated with different concentrations of hemin for various incubation times, frataxin levels remained comparable to untreated cells.

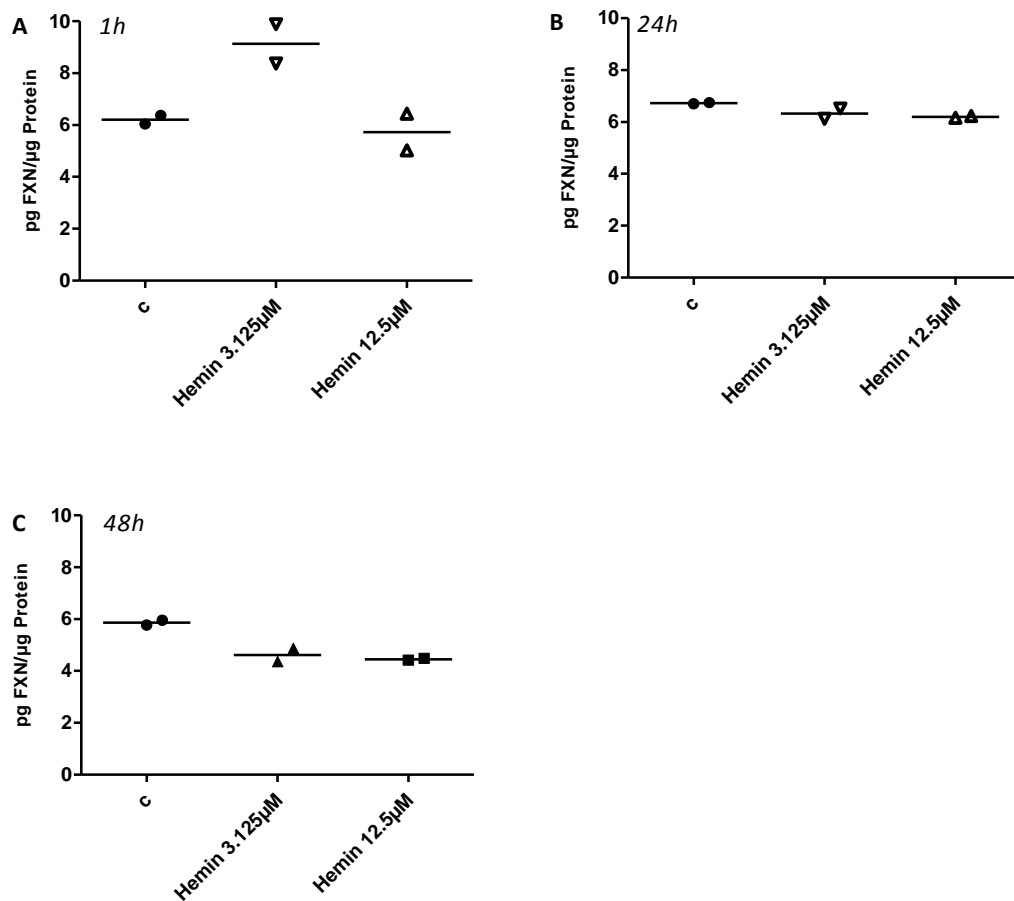


Figure 38: Influence of hemin on FXN expression in differentiated P19 neuronal cells.

P19 cells were differentiated to P19 neuronal cells by retinoic acid as described in Materials and Methods. The completely differentiated neuronal cells were seeded into 6-well microtiter plates according at a density of 8×10^4 cells per well and incubated with hemin concentrations of [3.125 μ M], [12.5 μ M] and [50.0 μ M] in modified α -MEM containing heat inactivated FCS and CS for (A) 1 hour, (B) 24 hours and (C) 48 hours at 37 °C and 5% CO₂ atmosphere. Controls (c) were incubated with modified α -MEM containing heat inactivated FCS and CS alone.

Frataxin content [pg FXN/ μ g Protein] was assessed by frataxin-ECLIA measurement as described in materials and methods. Shown are the means of two experiments.

4.2.3. Effect of other exogenous substances on frataxin expression

As described in the introduction, idebenone and erythropoietin are possible candidate drugs for the treatment of FRDA. It was therefore of interest to investigate effects of these substances alone or in combination on frataxin expression. This was tested again in differentiated Caco-2 cells as well as in P19 neuronal cells.

Effect of other compounds on frataxin expression in Caco-2 cells

Differentiated Caco-2 cells were incubated with idebenone and EPO alone or in combination for 24 hours. Afterwards frataxin expression in cell lysates was detected by frataxin-ECLIA.

In differentiated Caco-2 cells following idebenone alone or the combined incubation with Mg-CHL and idebenone a significant decrease in frataxin expression could be observed compared to the untreated control (**Figure 39**).

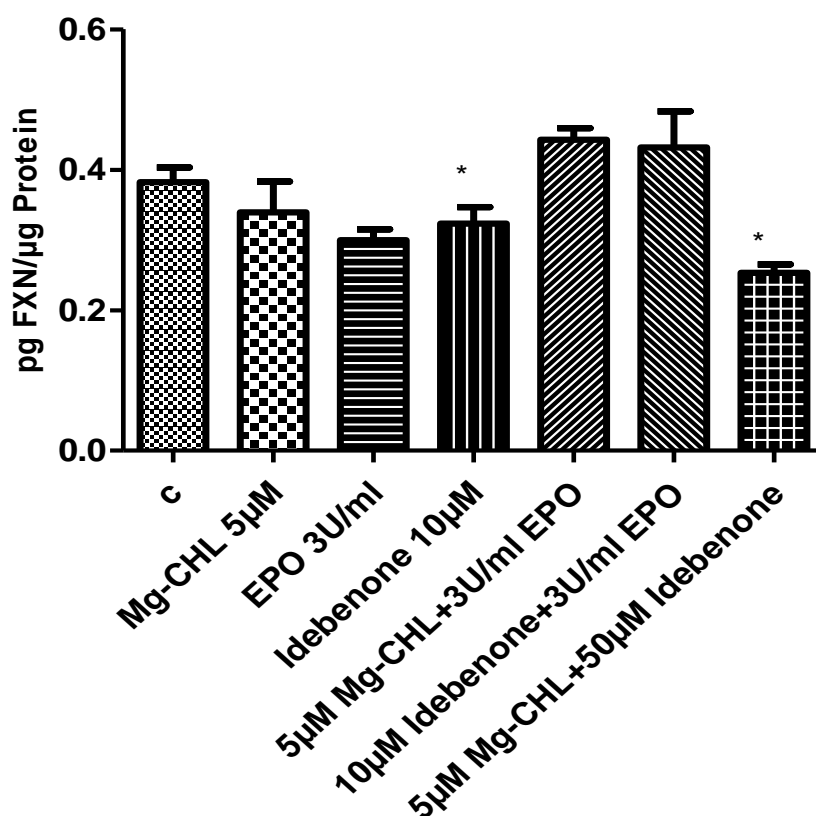


Figure 39: Influence of other substances on FXN content in differentiated Caco-2 cells.

Caco-2 cells were seeded into 6-well tissue culture plates at a density of 19.2×10^4 cells per well and cultivated for 21 days in modified DMEM culture medium; containing 1% L-glutamine, 0.1% gentamycin. Afterwards the cells were treated with different compounds alone and in combination for 24 hours at 37 °C and 5% CO₂ atmosphere. Controls (c) were incubated with modified DMEM containing heat inactivated FCS.

*Frataxin content [pg FXN/μg Protein] was assessed by ECLIA measurement as described in Materials and Methods. Shown are the means \pm SEM; (n=4). Significant differences vs. control are marked with * ($p < 0.5$), ** ($p < 0.01$) and *** ($p < 0.001$).*

Effect of other compounds on frataxin expression in P19 neuronal cells

In P19 neuronal cells treatment with Mg-CHL and EPO alone as well as the combination of Mg-CHL and idebenone increased levels of frataxin expression. Although incubation with EPO alone increases frataxin expression, the combinations of EPO with idebenone or Mg-CHL show a diminished impact on frataxin expression (**Figure 40**).

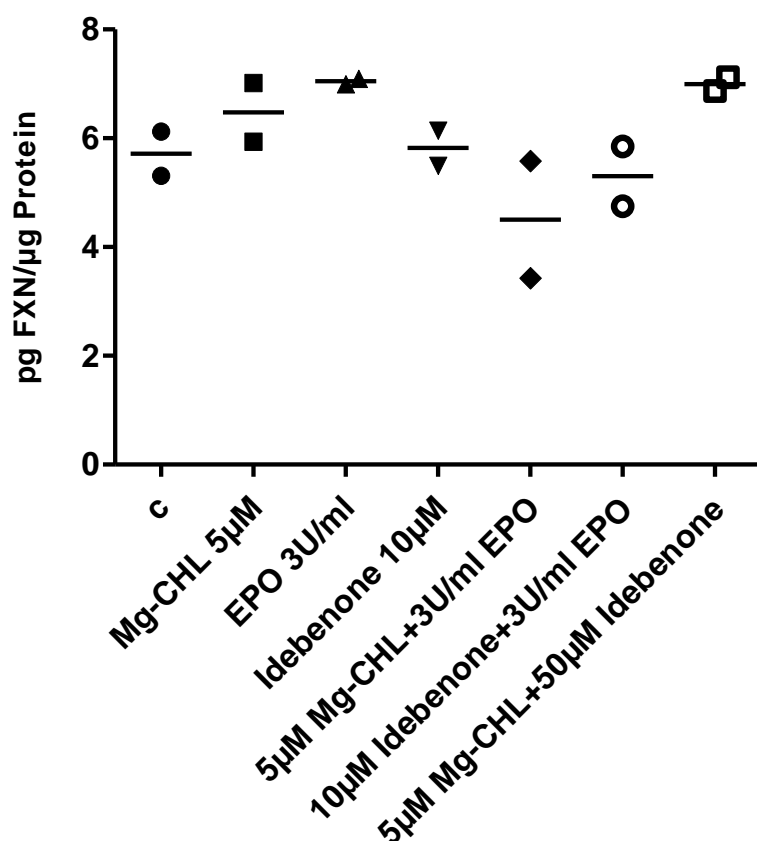


Figure 40: Influence of other substances on FXN content in differentiated P19 neuronal cells.

P19 cells were differentiated to P19 neuronal cells by retinoic acid as described in Materials and Methods. The completely differentiated neuronal cells were seeded into 6-well plates at a density of 8×10^4 cells per well and incubated with different compounds alone and in combination in modified α -MEM containing heat inactivated FCS and CS for 24 hours at 37 °C and 5% CO₂ atmosphere. Controls (c) were incubated with modified α -MEM containing heat inactivated FCS and CS alone.

Frataxin content [pg FXN/µg Protein] was assessed by ECLIA measurement as described in Materials and Methods. Shown are the means of two experiments.

4.3. Permeability measurement of Caco-2 cells

Bioavailability tests require a confluent Caco-2 monolayer, which is formed after about 3 weeks of cultivation [ZEMANN et al., 2011]. To ensure monolayer integrity non-invasive measurements of the TEER and Phenol Red Exclusion were performed, where Caco-2 cells were cultivated in hanging cell culture inserts to mimic the apical and basolateral conditions of enterocytes.

4.3.1. Phenol Red Exclusion

We could not find any difference between the empty control wells and wells containing Caco-2 cells in the hanging cell culture insert. Instead of a reduced diffusion of phenol red, depending on continuous cell growth, an increase of diffusion during cultivation time was observed (**Figure 41a**). Therefore it can be assumed that this method is not suitable for measuring the monolayer integrity of Caco-2 cells, despite Maznah I. showed conclusive results in performing this kind of permeability assay (**Figure 41b**). [MAZNAH, 1999] Therefore we decided to use a more established method to assess the integrity of the cell monolayer, the TEER measurement.

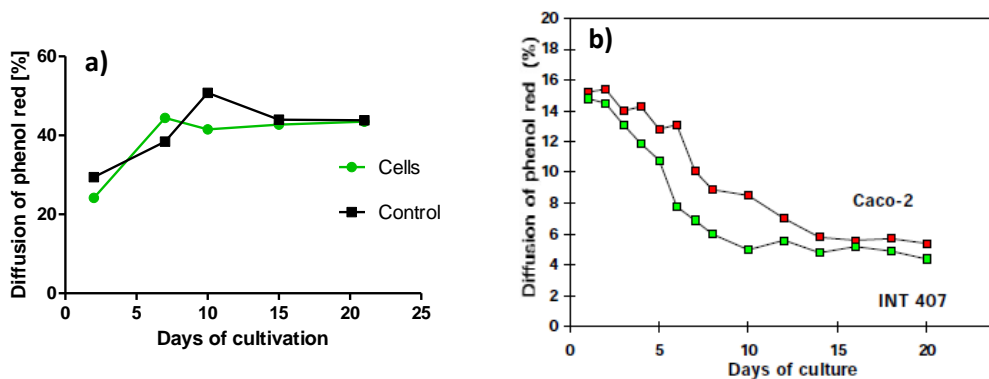


Figure 41: Testing the Caco-2 monolayer integrity by using phenol red exclusion. a) Results of our experiments. b) Results published by Maznah I. [MAZNAH, 1999]

Caco-2 cells were seeded into hanging cell culture inserts [membrane surface area = 4.5 cm²] in a 6-well tissue culture plate at a density of 9x10⁴ cells per well and cultivated in modified DMEM culture medium; containing 1% L-glutamine, 0.1% gentamycin at 37 °C and 5% CO₂ atmosphere. As controls (c) hanging cell culture insert without cells were used.

Phenol Red Exclusion was performed as described in Materials and Methods.

4.3.2. TEER-Measurement

Transepithelial electrical resistance (TEER) measurement provides a fast and easy way to assess the cell monolayer health and cell confluency.

Results of TEER measurement show a typical curve for Caco-2 cell cultivation with the slow progression of resistance at the beginning, followed by a steep increase between day 15. Based on literature, a TEER value of 300 [$\Omega \times \text{cm}^2$] demonstrate a confluent monolayer, which was reached at cultivation day 21. Obviously, permeability assays can not be performed before day 21 (**Figure 42**).

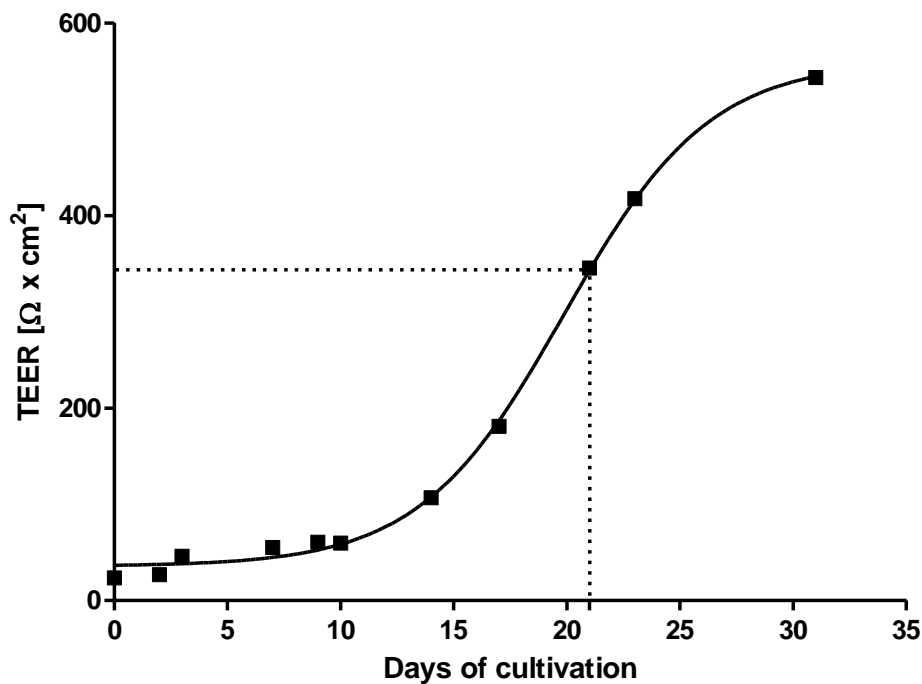


Figure 42: Testing the Caco-2 cell monolayer integrity by using TEER measurement.

Caco-2 cells were seeded into hanging cell culture inserts according to the conditions described in point 3.4. TEER values were assessed by using Millicell®-ERS as described in Materials and Methods at different time points.

4.3.3. Testing of bioactivity of CHL compounds in a Caco-2 cell/recipient cell co-culture model with P19 neuronal cells

Caco-2 cells were cultivated in hanging cell inserts and monolayer integrity was assessed by TEER measurement. At day 21 the hanging cell inserts with Caco-2 cells were transferred into 6-well tissue culture plates containing cultivated P19 neuronal cells. Culture medium containing chlorophyllin compounds was added to the apical side of the inserts (**Figure 43**). Effects on frataxin expression was assessed in the cell lysates of the basolateral cultured P19 neuronal cells, as well as of the differentiated Caco-2 cells on the apical side of the chamber by frataxin-ECLIA.

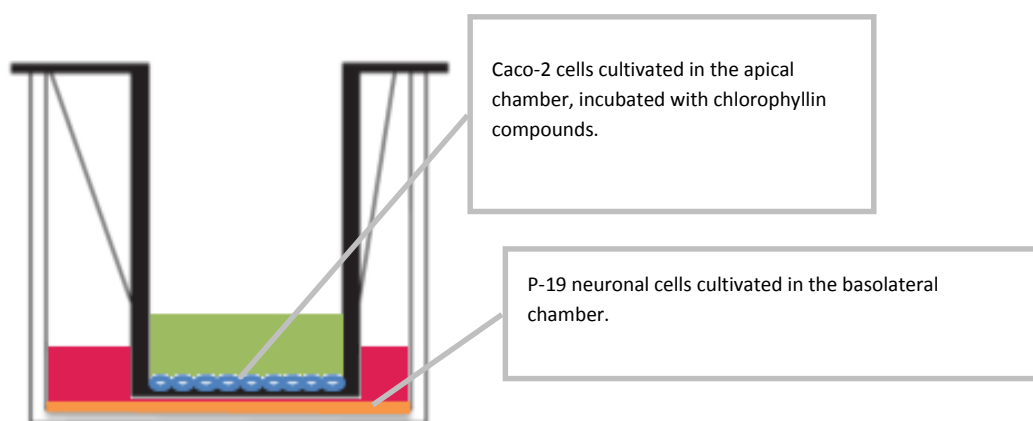


Figure 43: Caco-2/recipient co-culture model with P19 neuronal cells.

Differentiated Caco-2 cells

Comparable to our previous results (**Figures 35, 37 and 39**) of frataxin quantification by frataxin-ECLIA measurement, in differentiated Caco-2 cells the untreated control showed an increase in frataxin expression at 24h and 48h. At 1h both chlorophyllin compounds increased frataxin expression whereas at 24h and 48h no increase of frataxin expression could be observed (**Figure 44**).

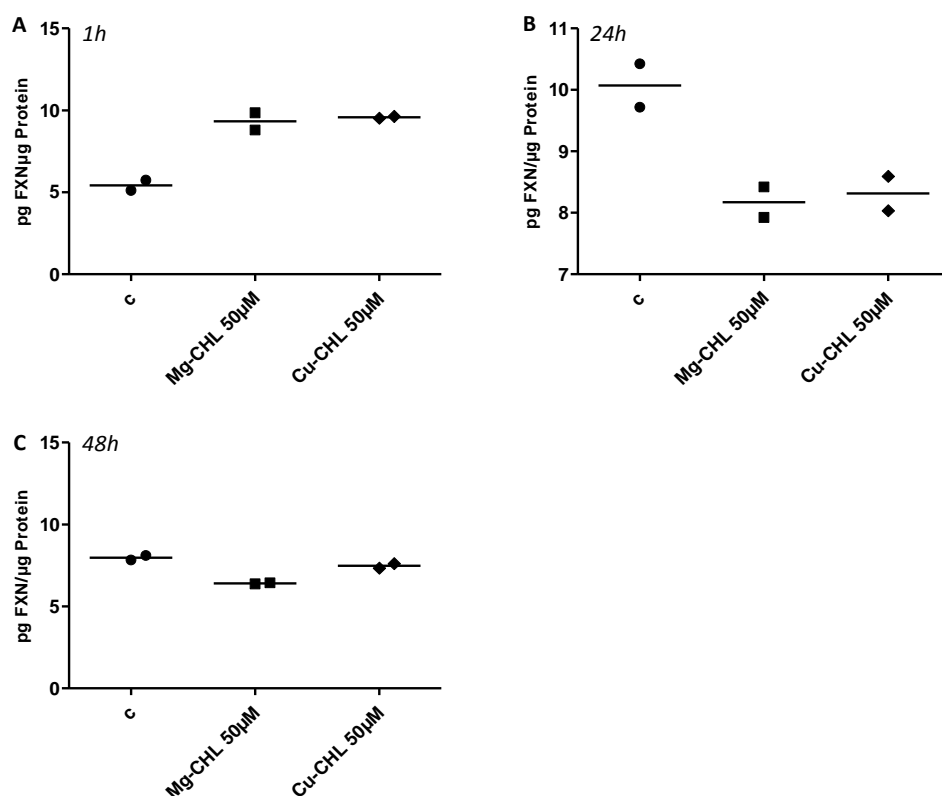


Figure 44: Effect of CHL compounds on FXN level in Caco-2 cells cultivated in hanging cell culture inserts.

Caco-2 cells were seeded into hanging cell culture inserts for 6-well culture plates at a density of 9×10^4 cells per insert and cultivated for 21 days in modified DMEM culture medium; containing 1% L-glutamine, 0.1% gentamycin.

*For the experiments the Caco-2 cells in the inserts were co-cultured with P19 neuronal cells in the 6-well plates as described in 4.3.3. The Caco-2 cells on the apical side were treated with Mg-CHL and Cu-CHL solutions at concentrations of $[50.0 \mu\text{M}]$ for **(A)** 1hour, **(B)** 24 hours and **(C)** 48 hours at 37 °C and 5% CO₂ atmosphere. Controls (c) were incubated with modified DMEM containing heat inactivated FCS alone.*

Frataxin content [pg FXN/μg Protein] of Caco-2 cells was assessed by frataxin-ECLIA measurement as described in Materials and Methods. Shown are the means of two experiments.

P19 neuronal cells

In P19 neuronal cells frataxin levels remained unchanged in the untreated control cells for 48h and no increase of frataxin expression could be observed following incubation with both chlorophyllin compounds. In addition frataxin levels remained unchanged in

P19 neuronal cells cultivated directly with chlorophyllin compounds in the absence of a Caco-2 cell monolayer in the hanging cell inserts (**Figure 45**). Unlike previous findings of our group where frataxin levels were assessed by Western blot or by the Frataxin Protein Quantity Dipstick Assay our results indicate that chlorophyllin has no effect on frataxin expression in P19 neuronal cells.

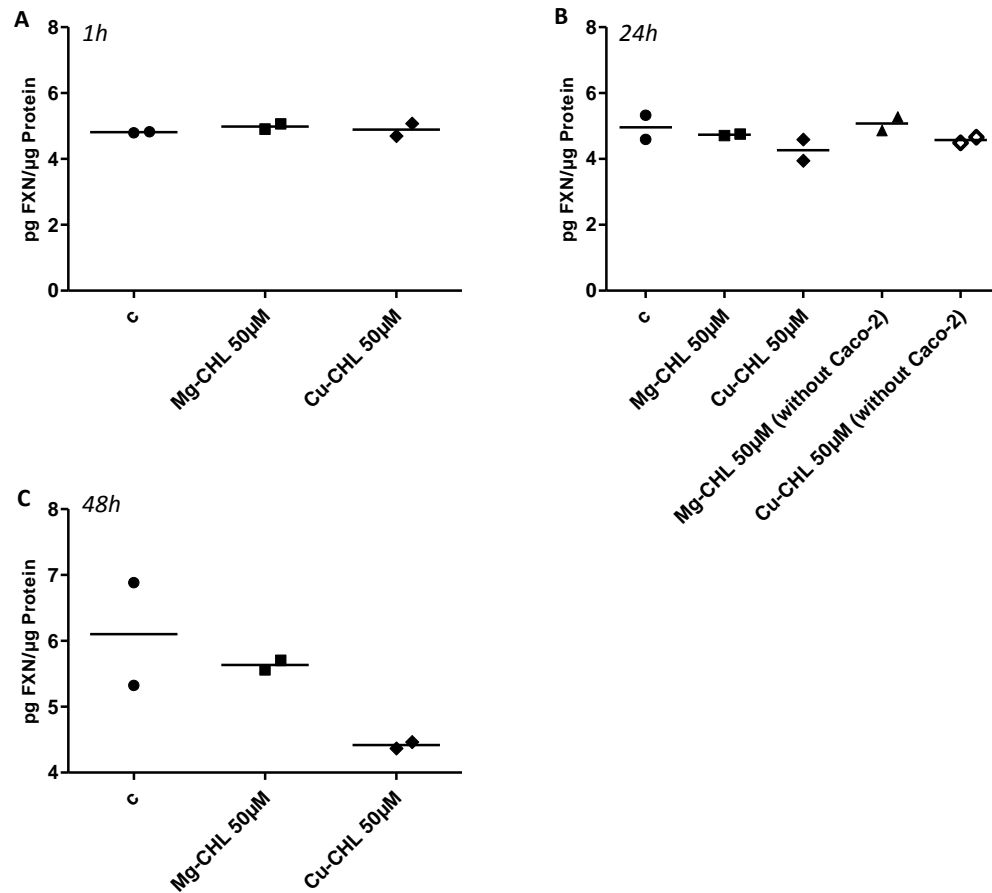


Figure 45: Effect of CHL compounds on FXN level in P19 neuronal cells after passaging a Caco-2 cell monolayer.

P19 cells were differentiated to P19 neuronal cells by retinoic acid as described in Materials and Methods. The completely differentiated neuronal cells were seeded into 6-well tissue culture plates at a density of 8×10^4 cells per well.

Experiments were performed as described in figure 44 and frataxin content [pg FXN/µg Protein] in P19 neuronal cells was assessed by frataxin-ECLIA measurement as described in Materials and Methods. Shown are the means of two experiments.

5. Conclusion

In 1863 the German pathologist and neurologist Nikolaus Friedreich was the first who described the elementary clinical and pathological features of Friedreich's ataxia (FRDA), also recognizing that this form of ataxia is hereditary. [FRIEDREICH, 1863 and 1867]

Friedreich's ataxia affects 1:50,000 Caucasians and is thereby the most common autosomal recessive ataxia in the white population. Due to the previous Migration Period it only affects peoples of European, North African, Middle Eastern and Indian origin. [KOEPPEN, 2011] [PANDOLFO, 2009]

Usually the mean age of onset is in the first half of puberty, by presenting the first typical symptoms of gait instability and generalized clumsiness. [KOEPPEN, 2011] These cardinal clinical features are followed by further neurological signs, like dysarthria or Babinski-signs and developing skeletal deformities. Beside these symptoms patients may also develop diabetes mellitus type II, ocular abnormalities and may lose their hearing ability. Additionally, in two thirds of patients cardiomyopathy is observed, which is the most frequent cause of death within FRDA patients. [SANTOS et al., 2010]

Although this multi systematic disease doesn't affect cognitive functions the patients are impaired in their academic, professional and personal development. [PANDOLFO, 2009]

The pathophysiology of FRDA is unique and displays significant differences to other hereditary ataxias by a typical combination of signs and symptoms of this disorder. [PANDOLFO, 2009] Neurodegeneration begins in the dorsal root ganglia (DRG), followed by affecting the spinal cord and the dentate nucleus in the cerebellum. [MARMOLINO, 2011]

The concerned gene in FRDA, the *FXN gene* is located on the proximal long arm of chromosome 9, encoding a 210 amino acids containing protein named frataxin (FXN).

FRDA patients represent a GAA-triplet repeat overexpression in the first intron of the gene, resulting in a reduced FXN expression of 5-30% compared to healthy people. [MARTELLI et al., 2012]

Responsible for the low FXN expression is the loss of transcriptional activity of the FXN gene due to the expanded GAA triplet repeats, which is described as the principal and critical step in developing FRDA. Several explanations for transcriptional silencing by GAA repeats exist, like forming a “sticky DNA”, or a persistent RNA•DNA hybrid formation, or the formation of heterochromatin. [WELLS, 2008]

Although there is still a controversial debate about the exact function of this mitochondrial protein, knockout experiments of multicellular organisms demonstrated that frataxin is essential to survive. [PANDOLFO, 2012] Available evidence provides the knowledge that frataxin is an important factor in iron homeostasis, the synthesis of Iron-Sulfur-Clusters (ISCs) and in the cellular defence of reactive oxygen species (ROS). [SCHMUCKER and PUCCIO, 2010]

Unfortunately FRDA is still an incurable illness without any sustainable therapeutically treatment. Beside palliative and symptomatic treatments, intense research work developed therapeutic strategies according to the pathological mechanisms. [RICHARDSON et al., 2013] [SCHMUCKER and PUCCIO, 2010]

Sarsero et al. demonstrated hemin as potent therapeutic agent by increasing the diminished frataxin gene expression. [SARSERO et al., 2003] Due to its reported neurotoxicity [DANG et al., 2011] our group investigated other non-toxic porphyrin compounds, more precisely the synthetic derivatives of the natural chlorophyll Mg-CHL and Cu-CHL.

Chlorophyllin compounds are normally used as colorant in food, drugs and cosmetics as well as for therapeutic treatment as internal deodorant or for accelerating wound healing. As several studies describe, CHL has an antimutagenic, anticarcinogenic and antioxidative efficacy. [TUMOLO and LANFER-MARQUEZ, 2012]

In our *in vitro* study we investigated the impact of a safe dose-dependent effect of chlorophyllin compounds on frataxin expression in differentiated Caco-2 cells and differentiated P19 neuronal cells.

Since the results of cytotoxicity measurements demonstrated no toxicological effect up to the maximum dose of 50µM in differentiated Caco-2 cells (cultivation day 21) and differentiated P19 neuronal cells, for further experiments the maximum dose can be used.

One critical point was the cultivation time of Caco-2 cells, whereas Markowska et al. provided an optimal stable state of Caco-2 cell monolayers in their study after 16–26 days. [MARKOWSKA et al., 2001] We identified a dose-dependent increase of toxicity after CHL incubation in Caco-2 cells cultivated for 17 days, assuming that cells are not fully differentiated and CHL compounds inhibit their metabolic activity.

Further in differentiated P19 neuronal cells Mg-CHL and Cu-CHL are able to enhance their metabolic activity assuming that CHL compounds may be a triggering factor of several metabolic pathways.

In addition the same cytotoxicity measurements were performed with cells following incubation with hemin, since studies indicated that hemin possesses neurotoxic potential. [DANG et al., 2011] Our results revealed only a slight reduction of metabolic activity of differentiated Caco-2 cells in the neutral red uptake. In P19 neuronal cells no cytotoxicity was observed, but in comparison with the results of CHL incubation, hemin induces only a modest increase in metabolic activity.

After establishing the safety of these porphyrin compounds, their effect on frataxin expression in differentiated Caco-2 cell and P19 neuronal cells could be assessed by frataxin-ECLIA measurement.

In differentiated Caco-2 cells only after one hour of incubation an increase of FXN content could be observed. Due to an unexpected increase of frataxin expression in untreated cells after 24h and less pronounced after 48h, the results of treated cells are comparable to the control cells.

Despite to previous data of our group, indicating a positive effect on frataxin expression in CHL treated P19 neuronal cells, we could not confirm these observations by frataxin-ECLIA measurement in our experiments. FXN expression remained stable during 48h of treatment and results are comparable to untreated cells.

Incubation with hemin, a compound with reported effect on frataxin expression was used as a positive control to increase frataxin expression in our model system. But again as with chlorophyllin, frataxin expression in differentiated Caco-2 cells was increased after 1 hour, compared to the untreated control, but showed the comparable frataxin level as the control during prolonged incubation up to 48hours.

Combination of Mg-CHL and idebenone showed a significant decrease in frataxin expression in differentiated Caco-2 cells, whereas in P19 neuronal cells this combination reaches the same increase of FXN expression as cells treated with EPO alone.

In permeability assays by using a Caco-2/recipient co-culture model with P19 neuronal cells there was no significant effect observed after CHL treatment, indicating that CHL compounds have no effect on frataxin expression.

In contrast to the previous findings of our group where other methods were used to assess frataxin expression, ensuring comparable results requires a simultaneous measurement of the cell lysates with all methods.

6. Summary

Friedreich ataxia is the most common autosomal-recessive inherited disease worldwide, affecting 1:50,000 Caucasians. Despite a lot of intense research work there is still no sustainable treatment option for FRDA patients. [RICHARDSON et al., 2013]

Sarsero et al. demonstrated hemin as potent inducer of frataxin gene expression, which is the mutated gene in FRDA. [SARSERO et al., 2003] Based on these findings our group investigated the effects of other non-toxic porphyrin compounds and found that chlorophyllin compounds significantly increased FXN expression in various cell types as well as in primary lymphocytes from FRDA patients (unpublished data).

Therefore the aim of this *in vitro* study was to identify a safe dose of chlorophyllin compounds effective to up-regulate frataxin expression providing a scientific basis for CHL-studies *in vivo*.

Cytotoxicity measurements demonstrate no toxicity up to the maximum dose of 50µM in differentiated Caco-2 cells and P19 neuronal cells. This indicates a safe use up to the maximum dose for further experiments.

In differentiated Caco-2 cells only after one hour of incubation an increase of FXN content could be observed. Due to an unexpected increase in frataxin expression in untreated cells after 24h which was less pronounced after 48h, the results of treated cells are comparable to the control cells.

Despite to previous data of our group, indicating a positive effect on frataxin expression in CHL treated P19 neuronal cells, we could not confirm these observations by frataxin-ECLIA measurement in our experiments. FXN expression remained stable during 48h of treatment and results are comparable to untreated cells.

Since the existing data were assessed by Western blot analysis and by the Frataxin Protein Quantity Dipstick Assay, analysis should be performed simultaneously with the same cell lysates.

7. Zusammenfassung

Friedreich's Ataxie ist mit einer Inzidenz von 1:50.000 die weltweit häufigste autosomal-rezessiv vererbte Erkrankung und tritt hauptsächlich in der europäisch abstammenden Bevölkerung auf. Trotz intensiver Forschungstätigkeit existiert noch keine nachhaltige Therapie für die Erkrankten. [RICHARDSON et al., 2013]

Als möglichen Therapieansatz wurde von Sarsero et al. die positive Wirkung von Hämin auf die FXN Genexpression publiziert [SARSERO et al., 2003]. Basierend auf diesen Resultaten gelang es unserer Forschungsgruppe, mit Chlorophyllin den Frataxinlevel sowohl in verschiedenen Zelltypen als auch in primären Lymphozyten von FRDA Patienten zu erhöhen (nicht publiziert).

Das Ziel dieser *in vitro* Studie war es daher, eine sichere Dosis für Mg- und Cu-CHL festzulegen, die gleichzeitig den FXN Gehalt in den Zellen erhöht. Toxizitätsmessungen der differenzierten Caco-2 und neuronalen P19 Zellen ergaben eine sichere Verwendung von Chlorophyllin bis zur maximal getesteten Dosis von 50µM.

Eine Steigerung des FXN Gehalts konnte in den Caco-2 Zellen nur nach einstündiger Inkubation beobachtet werden. Durch den unerwarteten Anstieg des FXN Gehalts in den Kontrollzellen nach 24h und 48h konnte in den mit CHL behandelten Zellen kein weiterer Anstieg erreicht werden.

Im Unterschied zu den bestehenden Ergebnissen unserer Forschungsgruppe, konnte mittels Frataxin-ECLIA kein signifikanter Anstieg des FXN Levels in den mit CHL behandelten neuronalen P19 Zellen verzeichnet werden, wodurch angenommen werden kann, dass Chlorophyllin keinen positiven Effekt auf die Frataxinexpression in neuronalen P19 Zellen bewirkt.

Da die früheren Daten mit anderen Methoden (Western blot, Frataxin Protein Quantity Dipstick Assay) erhoben wurden, sollten die Analysen mit den unterschiedlichen Methoden parallel mit den gleichen Zelllysaten durchgeführt werden, um vergleichbare Ergebnisse zu erzielen.

8. List of references

Amtsblatt der Europäischen Union, Verordnung (EU) Nr. 1129/2011 der Kommission vom 11. November 2011; L295–L295/177.

BENCZE K Z, KONDAPALLI K C, COOK J D, McMAHON S, MILLÁN-PACHECO C, STEMMLER T L. The Structure and Function of Frataxin. *Critical Reviews in Biochemistry and Molecular Biology* 2006; 41 (5): 269–291.

BOEHM T, SCHEIBER-MOJDEHKAR B, KLUGE B, GOLDENBERG H, LACCONE F, STURM B. Variations of frataxin protein levels in normal individuals. *Neurological Sciences* 2010; 32 (2): 327–330.

BOESCH S, STURM B, HERING S, GOLDENBERG H, POEWE W, SCHEIBER-MOJDEHKAR B. Friedreich's Ataxia: Clinical Pilot Trial with Recombinant Human Erythropoietin. *Annals of Neurology* 2007; 62 (5): 521–524.

BOESCH S, STURM B, HERING S, SCHEIBER-MOJDEHKAR B, STEINKELLNER H, GOLDENBERG H, POEWE W. Neurological effects of recombinant human erythropoietin in Friedreich's ataxia: A clinical pilot trial. *Movement Disorders* 2008; 23 (13): 1940–1944.

BRADFORD M M. A rapid and sensitive method for the quantitation of microgram quantities of protein utilizing the principle of protein-dye binding. *Analytical Biochemistry* 1976; 72: 248–254.

CAMPUZANO V, MONTERMINI L, MOLTÒ M D, PIANESE L, COSSEE M, CAVALCANTI F, MONROS E, RODIUS F, DUCLOS F, MONTICELLI A, ZARA F, CANIZARES J, KOUTNIKOVA H, BIDICHANDANI S I, GELLERA C, BRICE A, TROUILLAS P, DE MICHELE G, FILLA A, DE FRUTOS R, PALAU F, PATEL P I, DI DONATO S, MANDEL J L, COCOZZA S, KOENIG M, PANDOLFO M. Friedreich's ataxia: autosomal recessive disease caused by an intronic GAA triplet repeat expansion. *Science* 1996; 271: 1423–1427.

CAMPUZANO V, MONTERMINI L, LUTZ Y, COVA L, HINDELANG C, JIRALERSPONG S, TROTTIER Y, KISH S J, FAUCHEUX B, TROUILLA P, AUTHIER F J, DÜRR A, MANDEL J L, VESCOVI A, PANDOLFO M, KOENIG M. Frataxin is reduced in Friedreich ataxia patients and is associated with mitochondrial membranes. *Human Molecular Genetics* 1997; 6 (11): 1771–80.

CHAMBERLAIN S, SHAW J, ROWLAND A, WALLIS J, SOUTH S, NAKAMURA Y, VON GABAIN A, FARRALL M, WILLIAMSON R. Mapping of mutation causing Friedreich's ataxia to human chromosome 9. *Nature* 1988; 334: 248–250.

- CONDO I, VENTURA N, MALISAN F, RUFINI A, TOMASSINI B, TESTI R. *In vivo* maturation of human frataxin. *Human Molecular Genetics* 2007; 16 (13): 1534–1540.
- DANG T N, ROBINSON S R, DRINGEN R, BISHOP G M. Uptake, metabolism and toxicity of hemin in cultured neurons. *Neurochemistry International* 2011; 58: 804–811.
- DELATYCKI M B, WILLIAMSON R, FORREST S M. Friedreich ataxia: an overview. *Journal of Medical Genetics* 2000; 37: 1–8.
- DEUTSCH E C, SANTANI A B, PERLMAN S L, FARMER J M, STOLLE C A, MARUSICH M F, LYNCH D R. A rapid, noninvasive immunoassay for frataxin: utility in assessment of Friedreich ataxia. *Molecular Genetics and Metabolism* 2010; 101 (2-3): 238–45.
- DI PROSPERO N A, SUMNER C J, PENZAK S R, RAVINA B, FISCHBECK K H, TAYLOR J P. Safety, Tolerability, and Pharmacokinetics of High-Dose Idebenone in Patients With Friedreich Ataxia. *Archives of Neurology* 2007; 64: 803–808.
- DI PROSPERO N A, BAKER A, JEFFRIES N, FISCHBECK K H. Neurological effects of high-dose idebenone in patients with Friedreich's ataxia: a randomised, placebo-controlled trial. *The Lancet Neurology* 2007; 6: 878–886.
- DÜRR A, COSSE M, AGID Y, CAMPUZANO V, MIGNARD C, PENET C, MANDEL J L, BRICE A, KOENIG M. Clinical and genetic abnormalities in patients with Friedreich's Ataxia. *The New England Journal of Medicine* 1996; 335 (16): 1169–1175.
- FERRUZZI M G, BLAKESLEE J. Digestion, absorption, and cancer preventative activity of dietary chlorophyll derivatives. *Nutrition Research* 2007; 27: 1–12.
- FOGEL B L, PERLMAN S. Clinical features and molecular genetics of autosomal recessive cerebellar ataxias. *The Lancet Neurology* 2007; 6 (3): 245–257.
- FRIEDREICH N. Ueber degenerative Atrophie der spinalen Hinterstränge. *Archiv für pathologische Anatomie und Physiologie und für klinische Medizin* 1863; 26: 391–419.
- FRIEDREICH N. Ueber Ataxie mit besonderer Berücksichtigung der hereditären Formen. *Archiv für pathologische Anatomie und Physiologie und für klinische Medizin* 1867; 68: 145–245.
- GRABCZYK E, MANCUSO M, SAMMARCO M C. A persistent RNA·DNA hybrid formed by transcription of the Friedreich ataxia triplet repeat in live bacteria, and by T7 RNAP *in vitro*. *Nucleic Acids Research* 2007; 35 (6): 5351–5359.

HARDING A E. Friedreich's ataxia: a clinical and genetic study of 90 families with an analysis of early diagnostic criteria and intrafamilial clustering of clinical features. *Brain* 1981; 104 (3): 589–620.

HERBERT M D, WHITTON A A. Gene-based approaches toward Friedreich ataxia therapeutics. *Cellular and Molecular Life Sciences* 2007; 64: 3034–3043.

KOEPPEN A H, MORRAL J A, DAVIS A N, QIAN J, PETROCINE S V, KNUTSON M D, GIBSON W M, CUSACK M J, LI D. The dorsal root ganglion in Friedreich's ataxia. *Acta Neuropathologica* 2009; 118 (6): 763–776.

KOEPPEN A H. Friedreich's ataxia: Pathology, pathogenesis, and molecular genetics. *Journal of the Neurological Sciences* 2011; 303: 1–12.

LAGEDROST S J, SUTTON M S J, COHEN M S, SATOU G M, KAUFMAN B D, PERLMAN S L, RUMMEY C, MEIER T, LYNCH D R. Idebenone in Friedreich ataxia cardiomyopathy—results from a 6-month phase III study (IONIA). *American Heart Journal* 2011; 161: 639–645.

LYNCH D R, PERLMAN S L, MEIER T. A Phase 3, Double-blind, Placebo-Controlled Trial of Idebenone in Friedreich Ataxia. *Archives of Neurology* 2010; 67 (8): 941–947.

LYNCH D R, WILLI S M, WILSON R B, COTTICELLI M G, BRIGATTI K W, DEUTSCH E C, KUCHERUK O, SHRADER W, RIOUX P, MILLER G, HAWI A, SCIASCIA T. A0001 in Friedreich Ataxia: Biochemical Characterization and Effects in a Clinical Trial. *Movement Disorders* 2012; 27 (8): 1026–1033.

MARMOLINO D. Friedreich's ataxia: Past, present and future. *Brain research reviews* 2011; 67: 311–330.

MARTELLI A, NAPIERALA M, PUCCIO H. Understanding the genetic and molecular pathogenesis of Friedreich's ataxia through animal and cellular models. *Disease Models & Mechanisms* 2012; 5: 165–167.

MARKOWSKA M, OBERLE R, JUZWIN S, HSU C P, GRYSZKIEWICZ M, STREETER A J. Optimizing Caco-2 cell monolayers to increase throughput in drug intestinal absorption analysis. *Journal of Pharmacological and Toxicological Methods* 2001; 46: 51–55.

MAZNAH I. The use of Caco-2 cells as an *in vitro* method to study bioavailability of iron. *Malaysian Journal of Nutrition* 1999; 5: 31–45.

McBURNEY M W. P19 embryonal carcinoma cells. *The International Journal of Developmental Biology* 1993; 37 (1): 135–140.

- MEIER T, PERLMAN S L, RUMMEY C, COPPARD N J, LYNCH D R. Assessment of neurological efficacy of idebenone in pediatric patients with Friedreich's ataxia: data from a 6-month controlled study followed by a 12-month open-label extension study. *Journal of Neurology* 2012; 259: 284–291.
- MOTT F W. Case of Friedreich's disease, with autopsy and systematic microscopical examination of the nervous system. *Archive for Neurological Psychiatry* London 1907; 3: 180–200.
- MUSCO G, STIER G, KOLMERER B, ADINOLFI S, MARTIN S, FRENKIEL T, GIBSON T, PASTORE A. Towards a structural understanding of Friedreich's ataxia: the solution structure of frataxin. *Structure* 2000; 8 (7): 695–707.
- PANDOLFO M. Friedreich Ataxia. *Archives of Neurology* 2008; 65 (10): 1296–1303.
- PANDOLFO M, PASTORE A. The pathogenesis of Friedreich ataxia and the structure and function of frataxin. *Journal of Neurology* 2009; 256 [Suppl 1]: 9–17.
- PANDOLFO M. Friedreich ataxia: The clinical picture. *Journal of Neurology* 2009; 256 [Suppl 1]: 3–8.
- PANDOLFO M. Friedreich Ataxia: New Pathways. *Journal of Child Neurology* 2012; 27 (9): 1204–1211.
- PANDOLFO M. Treatment of Friedreich's ataxia. *Expert Opinion on Orphan Drugs* 2013; 1 (3): 221–234.
- PUCCIO H, KOENIG M. Recent advances in the molecular pathogenesis of Friedreich ataxia. *Human Molecular Genetics* 2000; 9 (6): 887–892.
- RICHARDSON T E, KELLY H N, YU A E, SIMPKINS J W. Therapeutic Strategies in Friedreich's Ataxia 2013; 1514: 91–97.
- ROUAULT T A, TONG W H. Iron-sulfur cluster biogenesis and human disease. *Trends in Genetics* 2008; 24 (8): 398–407.
- SANTOS R, LEFEVRE S, SLIWA D, SEGUIN A, CAMADRO J M, LESUISSE E. Friedreich Ataxia: Molecular Mechanisms, Redox Considerations, and Therapeutic Opportunities. *Antioxidants & Redox Signalling* 2010; 13 (5): 651–690.
- SACCÀ F, PIRO R, DE MICHELE G, ACQUAVIVA F, ANTENORA A, CARLOMAGNO G, COCOZZA S, DENARO A, GUACCI A, MARSILI A, PERROTTA G, PUORRO G, FILLA A. Epoetin alfa increases frataxin production in Friedreich's ataxia without affecting haematocrit. *Movement Disorders* 2011; 26 (4): 739–742.

SAKAMOTO N, CHASTAIN P D, PARNIEWSKI P, OHSHIMA K, PANDOLFO M, GRIFFITH J D, WELLS R D. Sticky DNA: Self-Association Properties of Long GAA•TTC Repeats in R•R•T Triplex Structures from Friedreich's Ataxia. *Molecular Cell* 1999; 3: 465–475.

SARSERO J P, LINGLI L, WARDAN H, SITTE K, WILLIAMSON R, IOANNOU P A. Upregulation of expression from the FRDA genomic locus for the therapy of Friedreich ataxia. *The Journal O Gene Medicine* 2003; 5: 72–81.

SAVELIEV A, EVERETT C, SHARPE T, WEBSTER Z, FESTENSTEIN R. DNA triplet repeats mediate heterochromatin-protein-1-sensitive variegated gene silencing. *Nature* 2003; 422: 909–913.

SCHMUCKER S, ARGENTINI M, CARELLE-CALMELS N, MARTELLI A, PUCCIO H. The *in vivo* mitochondrial two-step maturation of human frataxin. *Human Molecular Genetics* 2008; 17 (22): 3521–3531.

SCHMUCKER S, PUCCIO H. Understanding the molecular mechanisms of Friedreich's ataxia to develop therapeutic approaches. *Human Molecular Genetics* 2010; 19 (R1): R103–R110.

SÖDERBERG C A G, RAJAN S, SHKUMATOV A V, GAKH O, SCHAEFER S, AHLGREN E C, SVERGUN D I, ISAYA G, AL-KARADAGHI S. The molecular basis of iron-induced oligomerization of frataxin and the role of the ferroxidation reaction in oligomerization. *The Journal of Biological Chemistry* 2013; as manuscript in press.

STEINKELLNER H, SCHEIBER-MOJDEHKAR B, GOLDENBERG H, STURM B. A high throughput electrochemiluminescence assay for the quantification of frataxin protein levels. *Analytica Chimica Acta* 2010; 659 (1–2): 129–32.

STURM B, STUPPHANN D, KAUN C, BOESCH S, SCHRANZHOFER M, WOJTA J, GOLDENBERG H, SCHEIBER-MOJDEHKAR B. Recombinant human erythropoietin: effects on frataxin expression *in vitro*. *European Journal of Clinical Investigation* 2005; 35: 711–717.

STURM B, HELMINGER M, STEINKELLNER H, HEIDARI M M, GOLDENBERG H, SCHEIBER-MOJDEHKAR B. Carbamylated erythropoietin increases frataxin independent from the erythropoietin receptor. *European Journal of Clinical Investigation* 2010; 40 (6): 561–565.

TOMASSINI B, ARCURI G, FORTUNI S, SANDI C, EZZATIZADEH V, CASALI C, CONDÒ I, MALISAN F, AL-MAHDAWI S, POOK M, TESTI R. Interferon gamma upregulates frataxin and corrects the functional deficits in a Friedreich ataxia model. *Human Molecular Genetics* 2012; 21 (13): 2855–2861.

TUMOLO T, LANFER-MARQUEZ U M. Copper chlorophyllin: A food colorant with bioactive properties?. Food Research International 2012; 46: 451–459.

VYAS P M, TOMAMICHEL W J, PRIDE P M, BABBEY C M, WANG Q, MERCIER J, MARTIN E M, PAYNE R M. A TAT-Frataxin fusion protein increases lifespan and cardiac function in a conditional Friedreich's ataxia mouse model. Human Molecular Genetics 2012; 21 (6): 1230–1247.

WELLS R D. DNA triplexes and Friedreich ataxia. The FASEB Journal 2008; 22 (6): 1625–1634.

ZEMANN N, ZEMANN A, KLEIN P, ELMADFA I, HUETTINGER M. Differentiation- and polarization-dependent zinc tolerance in Caco-2 cells. European Journal of Nutrition 2011; 50: 379–386.

Internet sources

BabelFamily – The international project to defeat Friedreich's Ataxia: Letzte Nachrichten. Internet: <http://www.babelfamily.org/de> (accessed on: 27.05.2013).

Die Verbraucher Initiative e.V. (Bundesverband): E141 – Kupferkomplexe der Chlorophylle. Internet: <http://www.zusatzstoffe-online.de> (accessed on: 12.06.2013).

Friedreich's Ataxia Research Alliance (FARA): Research Pipeline. Internet: <http://www.curefa.org/pipeline.html> (accessed on: 26.05.2013).

Linus Pauling Institute – Oregon State University: Micronutrient Research for Optimum Health. Internet: <http://lpi.oregonstate.edu> (accessed on: 12.06.2013).

U.S. National Institutes of Health: ClinicalTrials.gov. Internet:

<http://www.clinicaltrials.gov/ct2/show/NCT01728064> (accessed on: 26.05.2013).

<http://www.clinicaltrials.gov/ct2/show/NCT00811681> (accessed on: 26.05.2013).

<http://www.clinicaltrials.gov/ct2/show/NCT01493973> (accessed on: 27.05.2013).

<http://www.clinicaltrials.gov/ct2/show/NCT01589809> (accessed on: 27.05.2013).

<http://www.clinicaltrials.gov/ct2/show/NCT01339884> (accessed on: 29.05.2013).

Internet figure sources

- [1] www.alzheimermed.com.br (accessed on: 23.06.2013)
- [2] <http://medicinexplained.blogspot.co.at> (accessed on: 23.06.2013)
- [3] <http://drugline.org/medic/term/pes-cavus/> (accessed on: 23.06.2013)
- [4] <http://en.wikipedia.org/wiki/Photosynthesis> (accessed on: 25.06.2013)
- [5] <http://en.wikipedia.org/wiki/Chlorophyll> (accessed on: 25.06.2013)
- [6] <http://lpi.oregonstate.edu/infocenter/phytochemicals/chlorophylls/chlorophyllins.html> (accessed on: 25.06.2013)
- [7] http://www.intechopen.com/books/understanding-alzheimer-s-disease/-secretase-regulated-signaling-and-alzheimer-s-disease_ (accessed on: 25.06.2013)
- [8] <http://www.baltic-analytics.de/index.php?id=39> (accessed on: 07.02.2012)
- [9] <http://www.sigmaaldrich.com/catalog/product/sial/n4638?lang=de®ion=AT>
(accessed on: 30.07.2013)
- [10] <http://de.wikipedia.org/wiki/Resazurin> (accessed on: 30.07.2013)
- [11] <http://www.wjgnet.com/1007-9327/full/v16/i31/WJG-16-3919-g003.htm#F2>
(accessed on: 25.06.2013)
- [12] <http://www.mesoscale.com> (accessed on: 10.01.2013)
- [13] <http://www.sigmaaldrich.com/catalog/product/sigma/h9039?lang=de®ion=AT>
(accessed on: 30.07.2013)

Curriculum vitae

Persönliche Angaben

Vor- und Zuname	Barbara Schwaiger, Bakk. rer. nat.
Geburtsort	Wolfsberg
Staatsangehörigkeit	Österreich

Ausbildung

WS 2010 - SS 2013	Masterstudium Ernährungswissenschaften, Universität Wien > Masterstudienzweig: „Molecular Nutrition“
WS 2006 – SS 2010	Bakkalaureatsstudium Ernährungswissenschaften, Universität Wien > Thema der Bakkalaureatsarbeit: „ <i>Das Melanocortinsystem als Schlüssel gegen Essstörungen</i> “
Sept. 2000 – Juni 2005	Handelsakademie Wolfsberg mit Matura erfolgreich abgeschlossen
Sept. 1996 – Juli 2000	Öffentliches Stiftsgymnasium St. Paul/Lavanttal
Sept. 1992 – Juli 1996	Volksschule St. Johann/Lavanttal

Berufserfahrung & Praktika

Nov. 2011 – Dez. 2011	Praktikum am Institut für med. Chemie und Pathobiochemie, 1090 Wien
Dez. 2010 – Feb. 2011	Praktikum am Department für Ernährungswissenschaften, 1090 Wien
Juli & August 2008 – 2011	Praktikum bei MONDI Frantschach GmbH, 9413 St. Gertraud/Lavanttal
Nov. 2005 – Sept. 2006	Sachbearbeiterin bei PAYLIFE GmbH, 1030 Wien